

# **Study of power fluctuation of DC motor in Chaotic and non-Chaotic drive system**

Thesis submitted in partial fulfillment of the requirement for the  
Award of the Degree of

**Master of Electrical Engineering**

Submitted By

**MRIGANKA ROY**

Registration number: **128896 of 2014-15**

Examination Roll number: **M4ELE1608**

Under the guidance of

**Prof. Dr. Samar Bhattacharya**

**Department of Electrical Engineering  
Faculty of Engineering and Technology**

**Jadavpur University  
Kolkata – 700 032  
YEAR-2016**

**Faculty Council of Engineering & Technology  
Jadavpur University  
Kolkata – 700032, India**

**Certificate of Recommendation**

This is to certify that **Mr. Mriganka Roy** (Examination Roll No.:**M4ELE1608**) has completed his dissertation entitled as “**Study of power fluctuation of DC motor in Chaotic and non-Chaotic drive system**”, under the guidance of Prof. Dr.Samar Bhattacharya, Department of Electrical Engineering, Jadavpur University, Department of Electrical Engineering, Jadavpur University. We are satisfied with the work, which is being presented for the partial fulfillment of the requirement for the Degree of **Master of Electrical Engineering** from the Department of Electrical Engineering of Jadavpur University.

-----  
**Prof. Dr. Samar Bhattacharya**

Professor, Department of Electrical Engineering  
Jadavpur University, Kolkata-700032

Countersigned by:

-----  
**Prof. Dr. Swapan Kumar Goswami**

Head ,Department of Electrical Engineering  
Jadavpur University, Kolkata-700032

-----  
Dean

Faculty Council of Engineering & Technology  
Jadavpur University, Kolkata-700032

**Faculty Council of Engineering & Technology  
Jadavpur University  
Kolkata – 700032, India**

**Certificate of Approval\***

The foregoing thesis, entitled as “**Study of power fluctuation of DC motor in Chaotic and non-Chaotic drive system**” is hereby approved by the committee of final examination for evaluation of thesis as a creditable study of an engineering subject carried out and presented by **Mriganka Roy** (Examination Roll No.: M4ELE1608, Registration No 128896 of 14-15) in a manner satisfactory to warrant it's acceptance as a prerequisite to the Degree of **Master of Electrical Engineering**. It is understood that by this approval, the undersigned do not necessarily endorse or approve any statement made, opinion expressed or conclusion drawn therein, but approve the thesis only for the purpose for which it is submitted.

**Committee of final examination**

**for evaluation of Thesis:**

-----  
-----

(Signature of Examiners)

\*Only in case the thesis is approved

## **Declaration of Originality and Compliance of Academic Ethics**

I hereby declare that this thesis contains literature survey and original research work by the undersigned candidate, as part of his **Master of Electrical Engineering**.

All information in this document has been obtained and presented in accordance with academic rules and ethical conduct.

I also declare that, as required by these rules and conduct, I have fully cited and referenced all material and results that are not original to this work.

Name (Block Letters) : MRIGANKA ROY

Examination Roll Number : **M4ELE1608**

Thesis Title : **Study of power fluctuation of DC motor in Chaotic and non-Chaotic drive system.**

Signature with date :

## Acknowledgements

I would like to express my deepest gratitude to my thesis supervisor, Prof. Dr. Samar Bhattacharya, professor and Mr. Partha Roy, Research Scholar, Dept. Of Electrical Engineering, Jadavpur University, for their valuable suggestions and advices during my thesis work. They have constantly given me support and encouragement without which it would not have been possible to complete my thesis successfully.

I would also like to take this opportunity to thank Prof. Dr. Swapan Kumar Goswami, Head, Dept. of Electrical Engineering, Jadavpur University and Dean, Faculty of Engineering & Technology, Jadavpur University. I am also very thankful to my classmates for their continuous encouragement. I would like to thank all the non-teaching staff, from the technicians to the librarians, who have done their bits in helping me to carry on with this work.

Lastly, I would like to thank my parents for their endless love and support that helped me to do my work sincerely.

Date:

Place: Jadavpur University

-----

Mriganka Roy

*Dedicated  
To  
My Parents*

*Who have always supported me in all my  
Endeavors.....*

# Contents

<b>ABSTRACT</b>	.....	I
<b>LIST OF FIGURES</b>	.....	II
<b>LIST OF TABLES</b>	.....	V
<b>LIST OF SYMBOLS AND ABBREVIATIONS</b>	.....	VI
<b>CHAPTER 1: INTRODUCTION</b>	.....	1
1.1 Introduction	.....	1
1.2 Motivation	.....	3
1.3 Objectives of the Realization of Chaos on Electrical Drives	.....	4
1.4 Thesis orientation	.....	4
<b>CHAPTER 2: LITERATURE SURVEY</b>	.....	6
2.1 Literature survey on nonlinear phenomena in power converters	.....	6
2.2 Literature survey on nonlinear phenomena in Electrical Drives	.....	9
2.3 Literature survey on nonlinear phenomena of PWM.....	.....	16
<b>CHAPTER 3: OVERVIEW OF CHAOS</b>	.....	18
3.1 Basic Ideas	.....	18
3.2 Classifications of dynamical systems	.....	18
3.2.1 Deterministic and Non-Deterministic Systems	.....	19
3.2.2 Continuous Time and Discrete Time Systems	.....	19
3.2.3 Linear and Nonlinear Systems	.....	19
3.3 Definition of Chaos	.....	21
3.4 History of Chaos	.....	21
3.5 What is chaos theory?	.....	22
3.6 A typical example of a chaotic system	.....	23
3.7 Features of Chaos	.....	24
3.8 Examples of chaotic systems	.....	24
3.9 Tools for detecting Chaos	.....	25

<b>CHAPTER 4: ELECTRICAL DRIVES FUNDAMENTALS</b>	29
4.1 Introduction	29
4.2 Elements of an Electrical Drive System	29
4.2.1 Components of a DC Motor Drive System	31
4.2.1.1 DC Motors	32
4.2.1.2 Power Converters	32
4.2.1.3 Control Electronics	33
4.2.1.4 Mechanical Loads	33
4.3 Permanent Magnet DC Drives	33
4.3.1 System Overview	34
4.3.2 PMDC Drive Operation	35

**CHAPTER 5: Problem formulation and Mathematical Modelling of PMDC motor Drives**

5.1 Problem Formulation	38
5.2 Mathematical Model of Open Loop PMDC Drive	39
5.3. Mathematical Model of Closed Loop PMDC Drive	43
5.4 Simulation Model	47

**CHAPTER 6: OBSERVATION AND ANALYSIS OF CHAOTIC PHENOMENA IN DC CHOPPER FED PERMANENT MAGNET DC DRIVES:**

6.1 Introduction	48
6.2 Observation and Analysis of DC Chopper -fed PMDC Drives Employing the Proportional Controller (error amplifier gain)	49
6.3 Observation and Analysis of DC Chopper Fed PMDC Drives Employing Variation of Load Torque	56
6.4 Observation of different Chaotic behavior of the DC Chopper Fed PMDC Drives for different switching frequencies ( $f_s$ )	63
6.5. Observation of switching signal (PWM) during route to Chaos	70
6.6. Special Observation on impact of Chaos in PMDC motor Drives	76
6.7 Summery	79



<b>CHAPTER 7: CONCLUSION AND FUTURE SCOPE OF WORK</b>	.....80
7.1 Conclusion	.....80
7.2 Future scope on this Work	.....81
<b>REFERENCES:</b>	.....82

## ABSTRACT

The present thesis work focuses on the observation and analysis of Chaotic behavior in a DC chopper fed PMDC motor Drive system. Chaotic behavior in a voltage mode controlled DC chopper fed PMDC motor drive system is presented with employing the Proportional Controller. Time series (Observe the state variables) and Phase portraits method are used to detect the chaos.

At constant load torque( $T_L$ ) and switching frequency ( $f_s$ ) the PMDC motor Drives become Chaotic while the speed error amplifier gain( $g$ ) is varying. The PMDC Drive system also becomes Chaotic for variation of load torque( $T_L$ ) at constant error amplifier gain ( $g$ ) and switching frequency ( $f_s$ ). The PMDC motor drive shows different chaotic behavior when different switching frequency( $f_s$ ) is introduced. The chaotic and non-chaotic region is separated by the boundary which is obtained at error amplifier gain( $g$ ) against switching frequency( $f_s$ ) and a mathematical relationship is built. The interaction of the control signal( $V_c$ ) and ramp signal( $V_r$ ) exhibit different switching signal (PWM) during route to Chaos is reported.

A special observation is reported that the average value and the standard deviation of the power wave fluctuations become less when the system is in Chaotic zone. This phenomenon has been investigated at different switching frequency( $f_s$ ) to justify the realization and it indicates that Chaos can be worthy for Electrical Drives.

In this work, the analysis and experimental results are carried out in MATLAB environment. This study is helpful in selecting the range and combination of parameters to run the motor as per requirement.

# LIST OF FIGURES

Figure 3.1: Bifurcation diagram of logistic equation	24
Figure 3.2 (a) Bifurcation diagram (b) Phase portrait	28
Figure 4.1: Parts of an electrical Drives system	30
Figure 4.2: Parts of a DC Drive system	31
Figure 4.3: Open loop PMDC drive's equivalent circuit	34
Figure 4.4: Switch ON circuit topology of a PMDC drive	36
Figure 4.5: Switch OFF circuit topology of a PMDC drive	36
Figure 5.1: Block diagram of a DC Chopper fed DC Drive	38
Figure 5.2: Open loop (a) Switch ON and (b) Switch OFF circuit topology of a PMDC drive	39
Figure 5.3: Open loop speed response ( $f_s=100\text{Hz}$ , $T_L=0.3 \text{ Nm}$ )	42
Figure 5.4: Open loop current response ( $f_s=100\text{Hz}$ , $T_L=0.3 \text{ Nm}$ )	43
Figure 5.5: Block diagram of closed loop PMDC drive	44
Figure 6.1: Time series plot of motor armature current at $g=0.20$ (Period-1)	50
Figure 6.2: Time series plot of motor speed at $g=0.20$ (Period-1)	50
Figure 6.3: Phase portrait of motor speed and armature current at $g=0.20$ (period1)	50
Figure 6.4: Time series plot of armature current at $g=0.30$ (Period-2)	51
Figure 6.5: Time series plot of motor speed at $g=0.30$ (Period-2)	51
Figure 6.6: Phase portrait of motor speed and armature current at $g=0.30$ (period2)	51
Figure 6.7: Time series plot of armature current at $g=0.90$	52
Figure 6.8: Time series plot of motor speed at $g=0.90$	52
Figure 6.9 Phase portrait of motor speed and armature current at $g=0.90$	52
Figure 6.10: Time series plot of armature current at $g=1$ (Period-1)	53
Figure 6.11 Time series plot of motor speed at $g=1$ (Period-1)	53
Figure 6.12: Phase portrait of motor speed and armature current at $g=1$ (period1)	53
Figure 6.13: Chaotic time series plot of armature current at $g=1.2$	54

Figure 6.14: Chaotic time series plot of motor speed at $g=1.2$	54
Figure 6.15: Phase portrait of motor speed and armature current at $g=1.2$ (Chaotic trajectory)	54
Figure 6.16. Non chaotic and chaotic armature current waveforms. Where A is non chaotic wave and B is chaotic wave	55
Figure 6.17. Non chaotic and chaotic speed waveform. Where C is non chaotic wave and D is chaotic wave	55
Figure 6.18: Time series plot of armature current at $(\tau_L)=0.09$ (Period-1)	57
Figure 6.19: Time series plot of motor speed at $\tau_L=0.09$ (Period-1)	57
Figure 6.20: Phase portrait of motor speed and armature current at $\tau_L=0.090$	57
Figure 6.21: Time series plot of armature current at $\tau_L=0.10$ (Period-2)	58
Figure 6.22: Time series plot of motor speed at $\tau_L=0.10$ (Period-2)	58
Figure 6.23: Phase portrait of motor speed and armature current $\tau_L=0.10$ (Period-2)	58
Figure 6.24: Time series plot of armature current at $\tau_L=0.12$	59
Figure 6.25: Time series plot of motor speed at $\tau_L=0.12$	59
Figure 6.26:Phase portrait of motor speed and armature current $\tau_L=0.12$	59
Figure 6.27:Time series plot of armature current at $\tau_L=0.20$	60
Figure 6.28: Time series plot of motor speed at $\tau_L=0.20$	60
Figure 6.29: Phase portrait of motor speed and armature current at $\tau_L=0.20$	60
Figure 6.30: Time series plot of armature current at $\tau_L=0.25$	61
Figure 6.31:Time series plot of motor speed at $\tau_L=0.25$	61
Figure 6.32: Phase portrait of motor speed and armature current $\tau_L=0.25$	61
Figure 6.33: Chaotic time series plot of armature current at $\tau_L=0.30$	62
Figure 6.34 :Chaotic time series plot of motor speed at $\tau_L=0.30$	62
Figure 6.35: Phase portrait of motor speed and armature current (Chaotic trajectory)	62
Figure 6.36: Phase portrait of motor speed and armature current (Chaotic trajectory) at $f_s=100\text{Hz}$	65

Figure 6.37: Phase portrait of motor speed and armature current (Chaotic trajectory) at $f_s=150\text{Hz}$ .....	65
Figure 6.38: Phase portrait of motor speed and armature current (Chaotic trajectory) at $f_s=200\text{Hz}$ .....	66
Figure 6.39: Phase portrait of motor speed and armature current (period-2) at $f_s=250\text{Hz}$ .....	66
Figure 6.40: Phase portrait of motor speed and armature current (period-2) at $f_s=300\text{Hz}$ .....	67
Figure 6.41: Phase portrait of motor speed and armature current (period-2) at $f_s=350\text{Hz}$ .....	67
Figure 6.42: Phase portrait of motor speed and armature current (period-2) at $f_s=400\text{Hz}$ .....	68
Figure 6.43: Phase portrait of motor speed and armature current (period-2) at $f_s=450\text{Hz}$ .....	68
Figure 6.44: Phase portrait of motor speed and armature current (period-1) at $f_s=500\text{Hz}$ .....	69
Figure 6.45: Error amplifier gain( $g$ ) against Switching frequency( $f_s$ ) to identify Chaotic and Non-Chaotic region .....	69
Figure 6.46. Interaction of the control and ramp signal at 100 Hz, $T_L=0.3\text{Nm}$ , $g=0.2$ .....	72
Figure 6.47. Interaction of the control and ramp signal at 100 Hz, $T_L=0.3\text{Nm}$ , $g=0.3$ .....	73
Figure 6.48. Interaction of the control and ramp signal at 100 Hz, $T_L=0.3\text{Nm}$ , $g=0.9$ .....	74
Figure 6.49. Interaction of the control and ramp signal at 100 Hz, $T_L=0.3\text{Nm}$ , $g=1.0$ .....	75
Figure 6.50. Control and ramp signal at 100 Hz, $T_L=0.3\text{Nm}$ , $g=1.2$ .....	76

Figure 6.51: Non chaotic and chaotic power waveforms. Where A is chaotic wave and B is non-chaotic wave	.....77
Figure 6.52: Non chaotic and chaotic power waveforms. Where A is chaotic wave and B is non-chaotic wave	.....78
Figure 6.53: Non chaotic and chaotic power waveforms. Where A is chaotic wave and B is non-chaotic wave	.....78
Figure 6.54: Non chaotic and chaotic power waveforms. Where A is chaotic wave and B is non-chaotic wave	.....79
Figure 6.55: Standard deviation of power wave in Chaotic and non-Chaotic conditions	.....79

## LIST OF TABLES

Table 3.1 the results with different initial conditions	.....23
Table.3.2 Solutions of dynamic systems (Poincare Maps)	.....26
Table 6.1: Solutions of dynamic systems (Phase Portrait)	.....48
Table 6.2: Condition of system at different switching frequency(fs)	.....63
Table 6.3: Occurrence of Chaos at different switching frequency(fs) and error amplifier gain(g)	.....64

## LIST OF SYMBOLS AND ABBREVIATIONS

Symbols	Description
$A$	State matrix
$A_{ON}$	State matrix when the power switch is closed
$A_{OFF}$	State matrix when the power switch is opened
$B$	Input matrix
$D$	Diode
$d$	Duty cycle (fraction of time the power switch is closed in one period)
$E_b$	Back emf induced at the armature coil terminals (V)
$I_a$	Armature current (A)
$J$	Moment of inertia (Nm.rad-1.sec2.)
$K_e$	Back emf constant (V. rad-1.sec)
$g$	error amplifier gain
$K_t$	Torque constant (Nm/A)
$L$	Inductance of the armature coil (H)
$R_a$	Resistance of the armature coil ( $\Omega$ )
$T$	Period of the PWM cycle (s)
$T_L$	Load torque (Nm)
$T_e$	Electrical torque (Nm)
$T_{on}$	The time interval when the power switch is ON (s)
$T_{off}$	The time interval when the power switch is OFF(s)
$V_{avg}$	The average voltage applied at the armature coil terminals (V)
$V_{in}$	The supply voltage (V)
$V_c$	Control signal (V)
$V_l$	Lower voltage limit of the ramp signal (V)
$V_{OFF}$	Product of the input matrix ( <b>B</b> ) and the input vector ( <b>U</b> ) when the switch is OFF





# Chapter 1

## Introduction

## 1.1 Introduction:

Electrical motors can be found in steel rolling mills, drilling machines, railway traction, industrial robots, and in most household items and office equipment. They convert electrical energy into mechanical energy by exploiting the 19th century discovery by Michael Faraday that a current carrying coil within a magnetic field will experience a force. Today, there are several variants of electric motors whose operation depend on this simple principle.

There is a necessity for both speed and torque control in order to ensure more diverse application of electric motors. This was realized in the past with DC motors by controlling the motor current with connecting a rheostat in series with armature or field winding or through the use of an external dc generator. These old control techniques were costly, incompetent and complex. The heat dissipation factor in the rheostat was also a massive problem to deal with. With the recent progresses in power electronics, digital electronics and microprocessors, speed and torque control of electric motors can now be efficiently accomplished through a process known as pulse width modulation (PWM). The PWM signals are used to turn ON and turn OFF the power electronic switches so as to control the average voltage applied at the motor terminals and thus speed control purpose is served. The access of power electronic switches in the drives has also led to gradual switch over from brushed DC motors to brushless DC and AC motors since speed control of the later can now be achieved through variable frequency inverters. The electric motor along with the speed and current transducers, the power converter circuit and control electronics are referred to as an electric drive.

There are the huge benefits that could be achieved by the implementation of power electronic switches for both speed and torque control of electric motors, but the PWM switching action makes the entire drive system to be time varying and nonlinear. The features of such systems during the switch ON states are often different from those during the switch OFF states. Also due to the switching action, the trajectories of the state variables of the system will converge to a periodic orbit or limit cycle at the steady state instead of converging to an equilibrium point thus adding to the complexity of the system. A power electronic (PE) converter is sensitively dependent on system parameter. Hence, a complete knowledge about the domains of nonlinear

performance and chaos in the parameter space is very important for the design engineer who must choose the system parameter values depending on the required output behavior.

As some drive parameters such as the supply voltage, Error amplifier gain ( $g$ ), Load Torque( $T_L$ ) and Switching frequency( $f_s$ ) are being varied by the operators, this nominal orbit (period-1) leading to the birth of new attracting orbit that is periodic (period- $nT$ ) or chaotic in nature. This change in qualitative behavior of the system is referred to as a bifurcation [44]. If the period of the new attracting orbit is double the period of the nominal orbit, the bifurcation will be referred to as period doubling bifurcation. The period doubling route to chaos has been observed in virtually the PMDC drives operating with simple proportional control.

The switching operation of power electronic systems, the corresponding system dynamics are generally nonlinear. A dc drive system based on pulse width modulation (PWM) technique often exhibit different types of nonlinear and chaotic phenomena. An investigation into chaos in power electronic circuits was launched in the late 1980s. In 1988, Hamill and Jefferies reported a one-dimensional mapping successfully that employed to derive the chaotic region of switching DC to DC converters. Most of the investigations have focused on the derivation of period-1 and period-2 orbits only by Chakrabarty *et al.* (1996), Fossas and Olivar (1996) and Hamill *et al.* (1992).

Nagy *et al.* (1995) have investigated the chaos in industrial drive systems by ignoring the switching effect. A pulse width modulation (PWM) inverter-fed induction motor drive system is considered for the study with numerical analysis, whereas Hemati (1994) has examined the chaos in a brushless DC drive system by ignoring the switching effect and approximately transforming into the Lorenz system. The switching effect has been ignored due to the complexity of analytical formulation. The nonlinearity caused by the switching effect is considered by Chau *et al.* in 1997.

A simple DC chopper-fed permanent-magnet (PM) DC drive system is selected to demonstrate its complex behavior without ignoring the switching effect nor accepting rough assumptions.

A generalized two-dimensional iterative mapping that describes the nonlinear dynamics of a second-order DC drive system operating in the continuous conduction mode is derived. The derivation considers all possible solutions in order to handle different system parameters and conditions. To check the stability of the system an analytical modelling of the period-1 and period- $p$  is presented. In 2010 Chau *et al.* published a study based on the derived iterative mapping, chaotic behavior through computer simulations and as well as tested experimentally

with a practical DC drive system. Many researchers have made a significant contribution to this study that makes the topic an important one, is thoroughly discussed in next chapter. The necessity of investigation to find out the system parameter's range where the system meets the nonlinear dynamical phenomena or chaos is the key of interest to researchers. Thus the overall goal of the project is to observe the Chaotic phenomena in some common electrical drive systems (namely permanent magnet dc (PMDC) drives) and find out the impact of Chaos on that particular system.

It is the purpose of this paper to investigate the nonlinear dynamics and chaotic behavior of industrial drive systems and find out the impact of Chaos in it.

## **1.2 Motivation:**

Chaos plays very important role in our everyday life. It is avoided due to its complexity. The complexity would no longer exist if the ultimate knowledge of chaos is developed. That's why to observe Chaos in an Electrical system is an interesting study for an electrical engineer.

Since the need of most electrical engineers is to maintain the system within the nominal period-1 behavior, there is a requirement for thorough understanding of the mechanism through which this nominal orbit changes to chaotic behavior. The thorough understanding of the mechanism through which the engineer can detect the desired range of the system parameter is important. Large number of power electronic circuits belongs to the adjustable structure piecewise-linear systems. They change their structure after each switching. The overall systems are nonlinear because of feedback controlled switching, hence the dependence of the switching instants on state and input variables, or in some other cases because of saturations or other nonlinearities. Hence, it is necessary to investigate the nonlinearity and chaotic behavior and to realize the impact of Chaos on a PMDC motor Drives.

There is a vast scope of research in the area of Chaos. A new idea regarding Chaos and its applications are expected.

### **1.3 Objectives of the Realization of Chaos on Electrical Drives:**

The qualitative behavior of all nonlinear systems including electrical drives often changes when some of the system parameters are being varied. Some of the needs for a thorough nonlinear analysis of drives are:

- To predict the dynamic behavior of an Electrical Drives (such as PMDC Motor Drives) as the system parameters are being varied and bring it to the designers.
- To provide knowledge in setting the operational parameter limits of the drives. For instance, at some range of the system parameters the steady state behavior will be the nominal Period-1 orbit, while at some other ranges the steady state trajectory will be either of quasi Periodic or chaotic.
- To find out the impact of chaos on Electrical Drives whether it is worthy or not.

### **1.4 Thesis orientation:**

This thesis is structured as follows:

Chapter 2 gives the literature survey on the study regarding the Chaotic behavior in electrical systems and its control and its applications.

Chapter 3 gives background knowledge and basic idea of Chaos and the tools by which it is detected.

Chapter 4 gives an overview of electrical drives and their control techniques. A brief discussion of the various components of electrical drives is given.

Chapter 5 presents the problem formulation and mathematical modelling of the selected DC chopper fed PMDC motor Drives. The simulation model in MATLAB environment is given in this chapter.

Chapter 6 presents simulation results of in a selected DC chopper-fed PMDC Drive system in MATLAB environment. This chapter includes the observation and analysis of the nonlinear phenomena (route to Chaos).

In Chapter 7 gives the conclusion of this study and suggestions for future work.

# Chapter 2

## Literature survey

## Literature survey

The basic belief is that a simple systems exhibit simple behavior. Though, an investigation of some simple switching power converters, electrical Drives and Switched Mode Power Electronic Systems has revealed remarkably complex behavior, namely chaos.

### 2.1 Literature survey on nonlinear phenomena in power converters:

An investigation into chaos in power electronic circuits was launched in the late 1980s. Since linear system theory is ill-suited to investigate the subharmonics and chaotic phenomena occurred in power electronic circuits, the most attractive approach has been that of iterative nonlinear mapping.

In 1984, *Brockett et al.* [1] reported that a DC-DC buck converter can exhibit nonlinear bifurcations and chaotic phenomena. In 1988 the first detailed study of One-dimensional mapping is successfully employed to derive the chaotic region of switching DC to DC converters in which the load voltage has been assumed to be a constant-voltage sink in of these nonlinear phenomena in DC-DC converter by *Hamill et al.* [2]. In 1990, *Deane et al.* [3], validated experimentally the initial analysis and simulation report of bifurcation and chaos in DC-DC converter using both first-order and second-order buck converters as example systems. Later, in 1992, *Hamill et al.* [4] carried out further investigations on the nonlinear phenomena in a DC-DC buck converter by using both iterative maps and Lyapunov exponent computations, and the results are also experimentally validated. In order to investigate the chaos of the practical switching DC to DC converters, again the corresponding two-dimensional mapping has been manipulated in 1996 by *Hamill et al.* 1992[4], *K.Chakrabarty et al.*[5], *Fossas et al.* 1996 [6]. Nevertheless, most of these investigations have focused on the derivation of period-1 and period-2 orbits only, while the corresponding characteristic multipliers need to be numerically computed. In [7] the strange behavior of a Colpitts-Like oscillator is generated by using a suitable connection of three SC-CNN cells. Another example of SC-CNN based nonlinear dynamic generation is presented. These facts lead to guessing how the Chua's CNN paradigm can be considered as a general scheme for nonlinear circuit dynamic generation. The conclusion is that the reported implementation approach does not require the use of any inductors. In 1997, the observation of coexisting attractors with fractal basin



boundaries in the voltage mode controlled buck converter has been made an important contribution to the study by *S. Banerjee* [8]. The long chaotic transients resulting from chaotic saddles are observed for a large range of parameter values on a power electronic circuits like converters. This paper reported the first observation of simultaneously existing stable orbits in a power electronic circuit. Rather long bursts of erratic behavior can be observed in systems with coexisting attractors and chaotic saddles in presence of occasional random disturbances. The study may have serious technological implications for the engineers. In this paper [9], the analysis of nonlinear phenomena in dc/dc converters is introduced through a new kind of nonlinear map, which is applied to all the fundamental topologies and state feedback control strategies. Nonlinear phenomena in closed-loop pulse-width modulated (PWM) dc/dc converters are analyzed. A new discrete time nonlinear map is introduced for asynchronous switching. This map is compared with the stroboscopic map, which is typically used in the study of dc/dc converters. Analytical conditions for the occurrence of periodic orbits and flip bifurcations are obtained in this work. Furthermore, necessary conditions for infinite local stretching on the phase space are derived. In conclusion, a possible explanation of the sudden jump to chaos exhibits by dc/dc converters is proposed.

A method of continuation of periodic orbits (stable or not) in non-smooth dynamical systems is developed for bilinear dynamical systems by *G. Olival et al.*[10]. An adding orbit process is detected, probable ending in a chaotic saddle. A specific method for computing the characteristic multipliers of periodic orbits is reported in this work. This method can be applied to find period-doubling and saddle-node bifurcations as well as the jump discontinuities in border-collision non-smooth bifurcations. In conclusion, a specific method for continuation of unstable periodic orbits in a model of a PWM Buck converter is proposed in this work.

In the study by *J. H. B. Deane et al.*[11], is done with some different observation with different motivation. A possibility of a novel application of chaos in DC-DC converter is investigated. A briefly discussion is reported for EMC (electromagnetic compatibility) improvement by chaos in the used system. The electromagnetic interference requirements for switch-mode power supplies are, in essence, that the input current PDS (power density spectrum) should be less than a specified frequency dependent level. The demonstration suggested that use of chaos may reduce the spectral peaks, significantly in some cases. A simple mapping is derived, which describes the behavior of a peak current-mode controlled boost converter operating chaotically. The invariant density of this mapping is calculated iteratively and, from this, the power density

spectrum of the input current at the clock frequency and its harmonics is deduced. The calculation is presented, along with experimental verification.

The experimental investigation of the nonlinear phenomena in the current mode controlled buck-boost converter is done by *A.Gupta et al.*[12]. Power converters exhibit a means of nonlinear phenomena. The prime source of nonlinearity is found that the switching element present in all power electronics circuits. Nonlinear components (e.g. power diodes) and control methods (e.g. pulse width modulation) are further sources of nonlinearity. They reported that the buck-boost converter operates in period one, period two, higher periods and chaotic mode and represent an overview of the bifurcation phenomena with the help of bifurcation diagrams with supply voltage as the variable parameter, and for different values of the resistor, inductor and capacitor.

Intermittent subharmonic and chaotic operations are often observed in switching converters. Noise and bad hardware construction are the usual blame. In this work by *S. C. Wong et al* [13], a circuit model is used to study the phenomenon incorporates in a coupling process through which a spurious signal is coupled to the current sensing and ramp compensation circuitry, resulting in a modulation of the compensation slope which turns the system unstable intermittently. They rationalize this phenomenon by an appropriate circuit model that is taken into consideration the effect of coupling of spurious signals. In particular, it is reported in a simple but popular current-mode controlled boost converter. It is found that the key process that leads to intermittent operations in the vicinity of stability boundary is due to modulation of a crucial parameter. In that case, it is identified that the slope of the compensation ramp is become the crucial parameter. Simulation and analysis is performed to illustrate the process through which that crucial parameter can be unintentionally modulated by spurious signals, leading to intermittent subharmonic and chaotic operations. It is concluded that the coupling of spurious signals into the compensation ramp may cause intermittent chaotic or subharmonic operations.

In this paper by *B.Cheng Bao et al* [14], an inductor current samples feedback control is used to control the chaos in the current-mode boost converter and focus on the quantitative analysis of control mechanism. A simple discrete map of the controlled system is established. The stability criterion, feedback gain, and corresponding critical duty ratio are deriving from eigenvalue analysis. The simulation is also performed to verify the results. The theoretical analysis and numerical simulation results is indicated that the inductor current sampled

feedback control method can be able to effectively control the current-mode boost converter to avoid chaos. This control strategy can also be easily applied to the control of other power converters.

## **2.2 Literature survey on nonlinear phenomena in Electrical Drives:**

The success of the initial research on nonlinear phenomena in simple DC-DC buck converters stimulated research in other SMPE systems especially the electrical drives. Research on nonlinear bifurcation and chaotic phenomena in electrical drives started with AC drives in the pioneering work conducted in 1989 by *Kuroe et. al.* [14] in inverter-fed induction motor drive systems. Using the Poincare map approach, they analyze the period doubling bifurcation in a three-phase inverter-fed induction drive system employing V/F control. In 1994, *Nagy* [15] studied the bifurcation and chaotic phenomena in tolerance-band based current controlled induction motor drives. Also in 1994 *Hemati* [45] reports the strange attractors in a permanent magnet brushless DC drive system by transforming the drives mathematical model into a Lorenz system.

Remarkably complex behavior, namely chaotic behavior, in a simple dc chopper-fed dc motor drive system is investigated by *Chau et al* [17] in 1997. The paper is to investigate, both numerically and analytically, the nonlinear dynamics and chaotic behavior of industrial motor drives without ignoring the switching effect or accepting rough assumptions. A simple dc chopper-fed permanent-magnet (PM) dc motor drive is selected for investigation which forms the basis for investigating other industrial motor drives. A generalized two-dimensional iterative map is established to describe the nonlinear dynamics of a second-order dc drive system operating in the continuous condition mode. That derivation covered all possible solutions, such as real and complex roots, to handle different system parameters and conditions. The analytical modeling of the period-1 and then the generalized period-p orbits as well as their stability analysis is presented. It is based on the derived iterative map and computer simulations is carried out to study the chaotic behavior and possible route to chaos. Also in 1997, *Chau et al.* [18] investigated the subharmonics and chaotic phenomena in both voltage mode and current mode controlled DC drives. The paper contains the nonlinear dynamics of both voltage-mode and current-mode controlled dc motor. The investigation is based on the derivation of

the discrete mappings that describe their system subharmonics and chaos in the continuous conduction mode of operation.

It reveals that the different bifurcation diagrams can be obtained by using different modes of control while varying the same system parameters. A unified modeling approach for the period-1 and hence the period-p orbits as well as their stability analysis during both voltage-mode and current-mode of control is proposed and verified in this study. The theoretical results are verified by comparing with the bifurcation points occurred during simulation. The identification of the desired stable operating ranges with different system parameters and conditions is the main purpose of this work. The another paper was published by *K.T. Chau et al* [19] in 1997, regarding dynamic bifurcation as well as chaotic behavior in a fixed-frequency current-mode controlled dc chopper-fed dc motor drive system. The theme of the study is to derive an iterative map that describes the nonlinear dynamics of the system operating in the continuous conduction mode. It is found that the different bifurcation diagrams can be obtained by varying different system parameters. Analytical modeling of period-1 and hence period-p orbits as well as their stability analysis using the characteristic multipliers are also presented. The stable ranges of various system parameters are determined. Moreover, chaotic behavior is quantified by evaluating the Lyapunov exponents in that study. The proposed approach is so generalized that it can readily be applied to other current-mode dc drives.

In 1999, *Chau et al.* [20] extended the nonlinear analysis to switched reluctance motor drives. Later in 2000, *Suto et al.* [21] reported the period adding route to chaos in a hysteresis current controlled AC drive. In 2000 *J. H. Chen et al.* [22] published a work on analysis of chaos in current-mode-controlled dc drive systems. The chaotic behavior in current-mode-controlled dc drive systems is analyzed in this work. The main purpose of the study is to derive an iterative map that describes the nonlinear system dynamics. An analytical modeling of fundamental and subharmonic oscillations as well as their stability analysis has been presented. The results show that the current-mode-controlled dc drive systems generally exhibit chaotic behavior. To avoid the occurrence of chaos, the stable ranges of various system parameters are determined. Both computer simulation and experimental measurement are used to verify the theoretical analysis.

In 2002, *Li et al.* [23] investigated the chaotic behavior in a permanent magnet synchronous motor (PMSM) by reducing the system model to a Lorentz system. The paper states at three different cases in which the trajectories of the state variables of the PMSM can approach an equilibrium point, a limit cycle or a chaotic attractor at steady state.

Some new phenomena are investigated in the DC motor drive system with PWM full-bridge converter by *T. Tang et al.* [24] in 2006. The paper works on a remarkably simple system to find rich and interesting chaotic and bifurcation behaviors at certain system parameters and operation conditions. To find out the area coverage of parameter of system fallen into chaos or bifurcation, an improved small-data algorithm is presented for system testes. The simulation results show that different bifurcation diagrams can be obtained at different system parameter conditions. This is a new discovery in the domain of chaotic analysis. The deferent data can be obtained and analyzed by the observation of time series with the variation of the system parameters. And an improved small-data algorithm is adopted to calculate the maximal Lyapunov exponent. The explicit and implicit analysis from the simulation results is convinced the occurrence of chaos in this remarkably simple system. The system structure and circuit topology are introduced and chaos and bifurcation diagram are displayed through the simulation.

In 2009 another study has been introduced by *B. Basak et al.* [25]. The paper simulates a current mode controlled separately excited dc motor in both continuous conduction mode as well as in discontinuous conduction mode. The bifurcation phenomena are explored with input voltage and speed error amplifier gain as bifurcation parameter. The study is helpful in selecting the range and combination of parameters if the mode of operation of the motor needs to be restricted in a particular operating mode. The study is conducted with three different sets of motor data so that the system can be engineered to achieve desired system performance. The knowledge of the operation of the industrial drives in discontinuous conduction mode and the phenomena that take place during CCM to DCM transition are important. The paper develops the map of a current mode controlled dc drive and explored the bifurcation and chaos in CCM as well as in DCM.

The phenomena of Hopf bifurcation and chaos from torus breakdown in a voltage-mode controlled DC drive system has also been reported in 2009 by *D. Dai et al* [26]. It is shown through the work that Hopf bifurcation may occur when the DC drive system adopts a more practical proportional-integral control. The phenomena of period-adding and phase locking is also observed after the Hopf bifurcation. It is shown that the stable torus can breakdown and chaos emerges afterwards. The work presents in paper provide more complete information about the dynamical behaviors of DC drive systems. Comparing to the previous work, this is identified a totally different type of bifurcation behavior and route to chaos in the DC motor

drive system, which is controlled by a practical proportional-integral control. This specific control scheme is shown to be an important factor that determines DC motor drive system. Remarkably complex behavior, namely chaos, in voltage-mode controlled DC drive systems has been again investigated in 2010 by *J. H. Chen et al* [27]. This work consists with the second-order generalized Poincare map that describes the nonlinear dynamics of a DC drive system operating in the continuous conduction mode is derived. Based on the derived map, computer simulation reveals that the drive system exhibits a typical period-doubling route to chaos. Focused on the normal situation that the orbits cross the voltage ramp once per cycle, the second order Poincare map and hence the analytical modelling of the period-1 and period- $p$  orbits is also derived. With the use of these models and the evaluation of characteristic multipliers, stability analysis is employed to identify the desired stable operating ranges during different system parameters and conditions. The theoretical results are varied experimentally. Although the experiment is focused on a particular DC drive system with only a speed feedback control loop, the proposed approach and derivation can readily be applied or extended to other DC drive systems with more complicated control schemes. It is noted that the aim of this paper is to illustrate the occurrence of chaos even in a simple DC drive system and to analyze the corresponding stable operating region. The use of duty-cycle limitation, current limitation or inner current control loop, further work is being considered to control the onset of chaos, either avoiding the occurrence of chaos for stable steady-state operation or even temporarily forcing the system to chaos for some special applications.

The existence of period-doubling bifurcation cascades and chaos in DC drives with full-bridge converter is well known. The paper reported for the first time the occurrence of coexisting attractors with a fractal basin of attraction in this relatively simple deterministic system in 2010 by *N. Okafor et al* [28]. It is reported that at some parameter values the trajectories converge on either a period-1 or a period-3 attracting set depending on the initial state of the system. There is an attempt to separate the basins of attractions of each attracting set revealed the existence of a riddled basin of attraction. That phenomenon is a practical consequence in that it might render future prediction of the system's steady state behavior almost impossible. Using Filippov's method, it shows analytically that the co-existing period-3 attractor is born due to a saddle node bifurcation that occurs at some critical parameter value, and thus it co-exists with the stable period-1 attractor. The analysis can be used to prevent the occurrence of this phenomenon by designing an effective controller capable of extending the parameter range for safe period-1 operation.

DC shunt and series drives are extensively used in the industry. The occurrence of bifurcation and chaos in dc shunt and permanent magnet drives are well known. It is observed that the behavior of the drives not only depends on the value of system parameters but also on the value of initial conditions in 2013 by *S Kundu et al* [29]. It is reported that the multiple attractors are existing for same parameter value. A different choice of initial conditions has been revealed a different periodic behavior of that chose system. The drive is intended to operate in a parameter range to give period-1 behavior. The existence of sub- harmonic oscillations in the period-1 region of the bifurcation diagram along with co-existing attractor with fractal basin boundaries in PWM controlled dc series drives is investigated. The experiment is also done in the series drive. This dc voltage can be derived from a DC source or an AC source with a rectifier and then it shows the different bifurcation behavior when different types of input voltage and switching elements are used. The existence of period-1, period-2 and period-4 orbits are observed with different initial conditions in the desired period-1 region of the bifurcation diagram. The dependence of system's behavior on initial condition may render the system's behavior unpredictable. This unpredictable behavior is the main outcome of that research work. The paper by *P. Stumpf et al.*[30] , deals with the stability analysis and the ramp compensation of a permanent magnet dc drive system operated in two and four-quadrant that is a different approach. The stability analysis is based on the eigenvalues of the Jacobian matrix of the Poincare Map Function (PMF) with the help of the auxiliary state vector. The Jacobian matrix can be determined without the derivation of the PMF. A compensating saw-tooth signal is used to avoid bifurcation and improve the performance of the DC drive. The slope of the ramp signal is also determined by the auxiliary state vector. The results are verified by computer simulations in the time domain.

*C. Kratochvil et al.* [31] evaluates the properties and behavior of dynamic system that is useful to define the parameters of models, which can influence the occurrence of parasitic motion including chaotic one (fluctuation of initial conditions, links gaps, control parameters).It is observed that the evolution of responses in phase planes based on changes of selected parameters .To identify typical chaos effects the Fourier spectrum is used. The purpose of this article is to provide an elementary introduction to the subject of chaos in the electromechanical drive systems. In this article, the chaotic solutions of maps are in continuous time domain. These solutions are also bounded like equilibrium, periodic and quasiperiodic solutions.

In 2004 *Chau et al.* [32], proposed a work from that the impact of Chaos is changed. It showed that the Chaos can be utilized for betterment of the industry. An Industrial mixers are among the most expensive and ineffective equipment in food, drug, chemical and semiconductor industries, chosen for the experiment. Instead of using complicated mechanical means, this paper presented a new way that can electrically produce the desired chaotic motion for industrial mixing processes. The work proposes and implements Chaoization of the DC motor using time-delay feedback control. Theoretical derivation and computer simulation are provided to illustrate the controllable chaotic motion. Experimental results are demonstrating that chaotic mixing prevents the formation of segregated regions, thus leading to efficient mixing compared with normal constant speed mixing. Another analysis on the use of Chaotic motion is made by *S. Ye et al.*[33] in 2007. In that an effective mixing approach is proposed and implemented by using an electrical chaoization. A permanent-magnet dc motor, which acts as the agitator, has been electrically chaoized by time-delay feedback control. It is identified that three adjustable control parameters like, the torque parameter which induces chaotic motion, the speed parameter which adjusts the motion boundary, and the time-delay parameter which tunes the refreshing rate. Both computer simulation and experimental results are given to verify the proposed chaoization.

The Chaos is also realized in Induction Motor Drives by *K. Chakrabarty et al.* [34]. The dynamical behavior of an indirect field oriented control (IFOC) induction motor drive in the light of bifurcation theory is reported. The speed of high performance induction motor drive is controlled by IFOC method. The identification of qualitative change of the behavior of the motor such as equilibrium points, limit cycles and chaos with the change of motor parameters and load torque are made for proper control of the motor. This paper provided a numerical approach to understand better the dynamical behavior of an indirect field oriented control of a current-fed induction motor. The emphasis is on bifurcation analysis of the IFOC motor, with a particular importance on the change that affects the dynamics and stability under small variations of Proportional Integral controller (PI) parameters, load torque and  $k$ , the ratio of the rotor time constant. Bifurcation diagrams are computed in this work and also attempted to discuss various types of the transition to chaos in the induction motor. The results of the obtained bifurcation simulations give useful guidelines for adjusting both motor model and PI controller parameters. It is also important to ensure desired operation of the motor when the motor shows chaotic behavior. Infinite numbers of unstable periodic orbits are embedded in a chaotic attractor. The unstable periodic orbit is stabilized by proper control algorithm in this



paper. Proper implementation of the delayed feedback control method to control chaos in the system is the main purpose this work.

A work regarding Control of Chaos in synchronous reluctance motor is reported by *M. Babaei et al.* [35]. In this paper, chaotic behavior is realized in a synchronous reluctance motor drive system. It stated that the chaotic behavior is observed when the d-axis component of stator voltage of the synchronous reluctance motor drive loses its control. The objective of that work is to stabilize the chaotic drive systems to imply a stable point. The nonlinear feedback control method is proposed there to control the Chaos via control of d and q-axis component of stator voltage and that strategy applies through computer simulation to verify the desired result.

*J. H. Chen et al.* [36] presented the investigation of the nonlinear dynamics of an adjustable-speed switched reluctance motor (SRM) drive with voltage pulse width modulation (PWM) regulation.

Nonlinear iterative mappings are based on both nonlinear and approximately linear flux linkage models that are derived to analyze the subharmonic and chaotic behaviors of that particular system. The nonlinear method offers a more computational time but the merit of accuracy is better. The bifurcation diagrams show that the system generally exhibits a period-doubling route to chaos. The theoretical analysis based on a practical SRM drive system is carried out to study the subharmonic and chaotic behaviors and to apply it on the other SRM drives practically.

The chaotic behavior in the permanent magnet synchronous generator for wind turbine system is investigated by *R. Lina et al.* [37]. In this work the Active Disturbance Rejection Control(ADRC) strategy is proposed to suppress chaotic behavior of the desired system and make operating it stably. The permanent magnet synchronous generator of wind power system is transformed into a model which is similar to Lorenz through a series of transforms, and is demonstrated existing chaotic phenomena when its parameters falling into a certain range of values. The ADRC controller is proposed to suppress chaos and to drive it to desire value for obtaining maximum wind power, meanwhile to solve problems of existing uncertainty parameters in wind turbine system by taking full use of ADRC's not relying on accurate mathematical model. The proposed strategy is proved valid by the simulation illustration.

### **2.3 Literature survey on nonlinear phenomena in PULSE WIDTH MODULATION (PWM) Electronic Systems:**

With the introduction of pulse width modulation (PWM), switching power converters have received a great attraction for application in electric drive systems, because of the advantages of flexible power control, compact size, and high efficiency.

A simple PWM current-mode single phase inverters are known to exhibit bifurcations and chaos when parameters vary. In a paper by *M. Feki et al.* [38], presents a control method for chaos control in the selected PWM and to extend the stability range of a commonly used linear controller. To achieve this objective, an extended time-delayed feedback controller (ETDFC) is used in conjunction with the proportional controller. An obvious advantage of this method is the robustness and simplicity of implementation because it does not require the knowledge of an accurate model but only the period of the target unstable periodic orbit (UPO). The effect of the ETDFC on the bifurcation diagram is thoroughly presented in this work and two-dimensional bifurcation diagrams are used to represent qualitative changes of the dynamics with respect to two system parameters.

Another work is done by *B. Robert et al.* [39], with a time-delayed feedback controller (TDFC) to control the chaotic behavior in a PWM. The range of the stable  $T$ -periodic mode of the PWM inverter is widened and the dynamical performances are improved. Results on tracking sinusoidal reference have been presented with the perspective of an experimental realization of the presented control methods. It is observed that the TDFC as well as (extended form) ETDFC induces longer settling time if parameters are not appropriately chosen. To avoid this problem, an adaptive TDFC is proposed in this study and numerical analysis of ETDFC has been presented to give the optimal parameters that lead to minimum settling time.

The switching operation of power electronic systems, the corresponding system dynamics are generally nonlinear. A dc drive system based on pulse width modulation (PWM) technique often exhibit different types of bifurcation and chaotic phenomena. A study by *K. Chakrabarty et al.* [40], describes bifurcation phenomena of a PWM controlled dc shunt drive. Bifurcation behavior of the system is observed by varying system parameters. The route of transition from periodic behavior to chaos is analyzed. The stability of the system is found out using the state

transition matrix over one switching cycle (the monodromy matrix) including the state transition matrices during each switching (the saltation matrices). The parameter values at which the nominal period-1 orbit loses stability is determined. A new controller is proposed in this study, that can significantly cover the parameter range for nominal period-1 operation.

The PWM H-Bridge is an industrial converter widely used in motor drives. Usually corrector parameters are tuned to avoid non-periodic running modes but non-periodic behaviors may take place under unexpected situations. In this paper by *B. robert* [41], shows a detailed model of the modulation function that may lead to important differences in chaotic running mode. The shape of the saturation threshold of electronic amplifier may lead to self-similarity property in the Feigenbaum's diagram of current whereas digital saturation eliminates most of bifurcations. This study shows that non-linear dynamics of an industrial converter depend greatly on details related to modulator technology but not really depending on details of the reality of components. It also shows that special bifurcation diagrams based on mean values or variance can add insightful information on intimate details of original bifurcation diagram. Particularly, the variance spikes can detect synchronization modes of the inverter inside the chaotic zone.

The possibility of diagnosing bifurcation phenomena in the dynamics of a PWM converter by the symbolic and the spectral methods is reported by *Y. Kolokolov et al.* [42]. The investigation is done using an experimental DC PWM drive setup. A different approach is made to analysis of the first bifurcation that leads to the loss of stability in operation of the PECs. The symbolical diagnostic method is proposed and compares with the geometrical interpretation of the time series invariants and analyzed. The main advantage of the symbolical method is that it allows unambiguous recognition of qualitative changes in the evolution of the dynamics that are related to the intermittency phenomenon in the vicinity of the bifurcation boundary. In addition, execution of this method involves a smaller amount of sampling, does not need any periodic resetting of the parameters of the sampling "window," and uses simpler algorithms.

In this chapter the studies regarding Chaos in Electrical systems following the literatures has been discussed. In the next chapter the overview of Chaos is highlighted.

# Chapter 3

## OVERVIEW OF CHAOS

## OVERVIEW OF CHAOS

### 3.1 Basic Ideas

The dynamical system refers to any physical or abstract entity whose configuration at any given time can be specified by some set of numbers, called **system variables**, and whose configuration at a later time is uniquely determined by its present and past configurations through a set of rules for the transformation of the system variables.

A dynamical system can be represented in following two ways:

- Differential equations: time is continuous

$$\frac{dx}{dt} = F(x, t) \dots\dots\dots (3.1)$$

- Difference equations (iterated maps): time is discrete

$$\begin{aligned} X(t + \Delta t) &= F(x(t)) \\ X_{n+1} &= F(X_n) \dots\dots\dots (3.2) \end{aligned}$$

### 3.2 Classifications of dynamical systems

Dynamical systems can be classified using several criteria as discussed below:

#### 3.2.1 *Deterministic and Non-Deterministic Systems:*

Dynamical systems can be broadly classified as either deterministic or non-deterministic. A system is said to be deterministic if the future value of the state variables can be completely predicted once the initial or past states and other system parameters are known. For instance, if the angular position ( $\theta(t_0)$ ) of a simple pendulum at  $t=t_0$  is known, then the position at any other time in the future ( $\theta(t)$ ) should be predictable. Deterministic systems can be modelled using either ordinary differential equation or iterative maps depending on whether the state variables evolve in a continuous or discrete manner.

Similarly, systems whose behaviors are random in nature and cannot be easily predicted are referred to as non-deterministic or stochastic systems. A typical example of a non-deterministic system is the price of stocks in the stock market. Even if the price yesterday is known, the price today could be difficult to predict.

### 3.2.2 Continuous Time and Discrete Time Systems:

Continuous time systems (CTS) are dynamical systems whose state variables evolve continuously with time. Continuous time systems are often modelled using ordinary differential equations of the form below.

$$\frac{d\mathbf{X}(t)}{dt} = \mathbf{f}(\mathbf{X}(t), t) \quad \dots\dots\dots (3.3)$$

Where  $[\mathbf{x}_1, \mathbf{x}_2, \mathbf{x}_3, \dots, \mathbf{x}_n]^T \in \mathbb{R}^n$  is the state vector,  $\mathbf{x}_1, \mathbf{x}_2, \mathbf{x}_3, \dots, \mathbf{x}_n$  are the state variables and the function  $\mathbf{f}(\mathbf{X}(t), t)$  is the vector field. There are different possible solutions for a system of the form (3.3) depending on the initial values of the state variables. Such solutions (also referred to as the *flow* or *trajectory*) are used to predict future values of the state variables as  $t \rightarrow \infty$ . Assuming  $\mathbf{X}(t_0) = \mathbf{X}_0$  is the initial state vector for system (3.1), the flow or solution will be expressed as  $\mathbf{X}(t)$ . Such a solution can be evaluated analytically or numerically depending on whether the system is linear or nonlinear as discussed in section 3.2.3. Systems of the form (3.3) can be referred to as *autonomous* if the vector field does not depend on time and *non-autonomous* otherwise.

There are also dynamical systems where the state variables evolve in a discrete manner. Such systems are referred to as discrete time systems (DTS) and are often modelled using an *iterative map* or *difference equation* of the form below.

$$\mathbf{X}_{n+1} = \mathbf{f}(\mathbf{X}_n) \quad \dots\dots\dots (3.4)$$

where  $n$  is an integer,  $\mathbf{X}_n$  denotes the present state of the system,  $\mathbf{X}_{n+1}$  denotes the state of the system at the next observation instant (hour, minute, second, etc.), and  $\mathbf{f}(\mathbf{X})$  is the evolution rule that relates the present state to the next state.

### 3.2.3 Linear and Nonlinear Systems:

Linear systems are dynamical systems in which the time evolution rules for the state variables are expressed as linear differential equations [47]. Such systems obey the principle of superposition and a change in any of the system parameters causes only quantitative, but not qualitative change in the nature of the flow. Linear systems usually have only one equilibrium

point whose stability does not depend on the system parameter and they can be modelled using the *state equation* of the form (3.5) and *output equation* of the form (3.6) [47]

$$\frac{dX(t)}{dt} = AX(t) + BU(t) \quad \dots\dots\dots (3.5)$$

$$Y(t) = CX(t) + DU(t) \quad \dots\dots\dots (3.6)$$

Where  $[x_1, x_2, x_3, \dots, x_n]^T \in R^n$  is the state vector,  $U = [u_1, u_2, u_3, \dots, u_n]^T$  is the input vector,  $Y = [y_1, y_2, y_3, \dots, y_n]^T$  is the output vector, **A** is an  $(n \times n)$  state matrix, **B** is an  $(n \times m)$  input matrix, **C** is an  $(p \times n)$  output matrix and **D** is an  $(p \times m)$  feed forward matrix which is often zero in most systems.

Linear systems can be further classified as *linear time invariant* (LTI) and *linear time varying* (LTV) systems. If the parameters in the state matrix (**A**) vary with time, then the system will be referred to as LTV, but if the parameters in the state matrix remain constant over time, the system will be referred to as LTI. Also, if the input or external forcing function to the system is zero ( $U(t) = 0$ ), the system will be referred to as *homogenous*, and if ( $U(t) \neq 0$ ), the system will be referred to as *non-homogenous*. Linear systems usually have analytical solutions.

Systems whose state equations cannot be expressed in the form (3.5) are considered as *nonlinear*. Precisely without exceptions, all systems in the real world are nonlinear at least to some extent. The evolution rule for the state variables in such systems are usually expressed as nonlinear differential equations. Unlike linear systems, nonlinear systems can only be solved using numerical techniques and are characterized by multiple equilibrium points. A small change in any of the system parameters can lead to sudden and dramatic changes in both the qualitative and quantitative behavior of the system [47].

### 3.3 Definition of Chaos

According to Poincaré: (1880)

“It so happens that small differences in the initial state of the system can lead to very large differences in its final state. A small error in the former could then produce an enormous one in the latter. Prediction becomes impossible, and the system appears to behave randomly.”

*Chaos means disorder, but in our engineering science the chaos defines orderly disorder* [49].

### 3.4 History of Chaos

In the year **1890** King Oscar II of Sweden announced a prize for the first person who could solve the n-body problem to determine the orbits of celestial bodies and thus prove the stability of the solar system. Henri Poincare won the first prize in that contest discovering that the orbit of three or more interacting celestial bodies can exhibit unstable and unpredictable behavior [49].

**Year 1963** Edward Lorenz introduced first modern concept of chaos theory, all though he did not use the term chaos.

**Year 1975** Tien-Yien Li and James A. Yorke in paper “Period three implies chaos” introduced the term chaos theory.

**Year 1976** Robert M may, in the application of logistic equation to ecology developed the chaotic population behavior.

**Year 1978** Mitchell Feigenbaum introduced universal number associated with the chaos and strange attractors.

**Year 1980** Benoit mandelbort developed the concept of fractal geometry which can be considered as the modified field of applications of chaos theory.

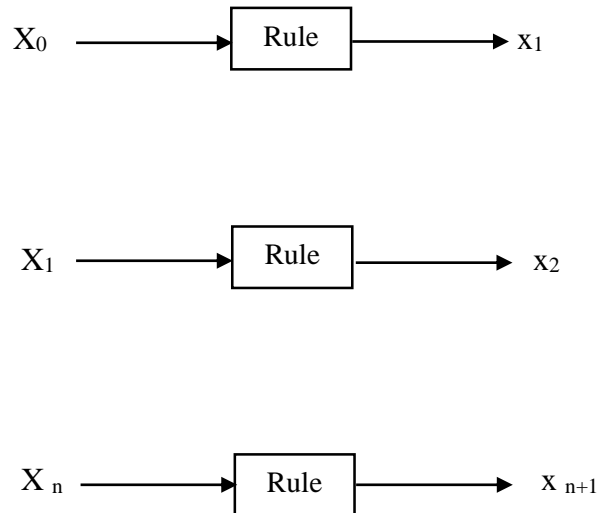
**Year 1990** Ed Ott, Celso Grebogi and James Yorke introduced the chaos control theory, which is known as OGY method, since then the chaos theory is versatile used in engineering practice, especially in control engineering.



### 3.5 What chaos theory?

Chaos theory is based on the observation that simple rules when iterated can give rise to apparently complex behavior.

example:



The basic observation is that if in the implementation of the above rule is changed by a small amount, the resulting sequence will be very different. After some iterations mathematicians have still not agreed on a definition of chaos that is acceptable to all. However, an operational (meaning one that captures most essential features) definition of a chaotic system is:

- 1) The solution must be aperiodic.
- 2) The solution must be bounded.
- 3) The solution must be exponentially sensitive to initial conditions.

The rule that governs a chaotic system must satisfy certain properties as:

- 1) The rule must be nonlinear.
- 2) In the case of maps, it must be Non-invertible if it is one dimensional.
- 3) In the case of ordinary differential equations it must be at least three dimensional.

### 3.6 A typical example of a chaotic system:

The mathematical model of the logistic equation can be defined as [Robert May, 1976]:

$$X_{n+1} = r X_n (1 - X_n) \quad 0 \leq X_n \leq 1$$

To show chaos in action in this system;

Consider that:

$$X_0 = 0.1123456 \dots$$

$$X_0^1 = 0.1123598 \dots$$

Then we see

$$X_1 = 0.1123456 \dots$$

$$X_1^1 = 0.1123598 \dots$$

And

$$X_2 = 0.23456 \dots$$

$$X_2^1 = 0.23598 \dots$$

It is seen that the iterates diverge very rapidly.

Table 3.1

Initial value of $x_n$	$r$	After sufficient number of iterations the final values converges to
$x_0$		
0.8	0.9	After 30 or more iterations it is observed that the series converges to 0.
0.6	1.4	After 30 or more iterations it is observed that the series converges to 0.2861
0.6	2.3	After 30 or more iterations it is observed that the series converges to 0.2861
0.2	3.2	After 30 or more iterations it is observed that despite of the converging of the series it oscillates between 0.7995 and 0.5130
0.2	3.520	After 30 or more iterations it is observed that despite of the converging of the series it oscillates between four values as 0.8233 0.5121 0.8795 0.3731
0.2	3.62	After 30 or more iterations it is observed that despite of the converging of the series it oscillates between 0.7995 and 0.5130

It is realized from the table3.1, the results with different initial conditions are very much bounded in a certain range and the values oscillate with some hidden rules.

The indication of hidden rules can easily be authenticated following in next discussion.

The bifurcation diagram of logistic equation is shown in the Fig-3.1.[49] It is basically a plot of the final values of  $x_n$  with sufficient number of iterations varying  $r$  from 0 to 4.

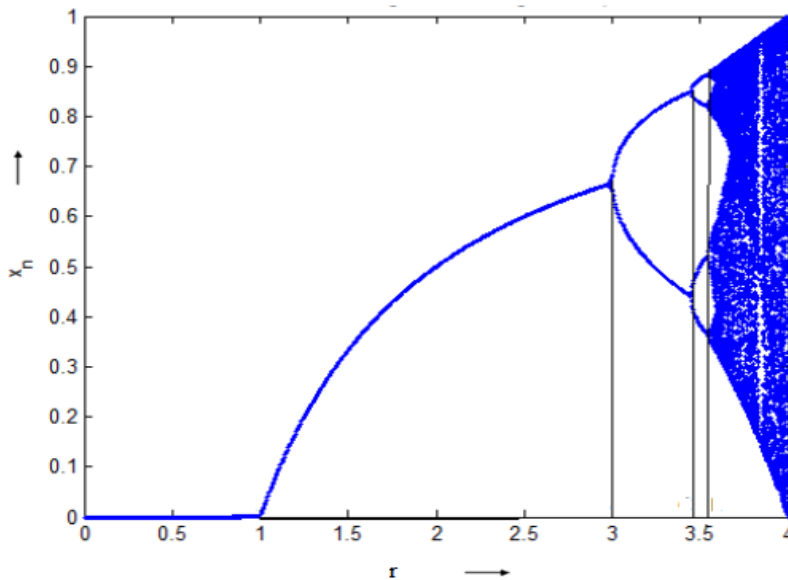


Figure 3.1: Bifurcation diagram of logistic equation

*Chaos is aperiodic long-term behaviour in a deterministic system that exhibits sensitive dependence to the initial condition [49]*

### 3.7 Features of Chaos:

- **Nonlinearity:** Chaos cannot occur in a linear system. Nonlinearity is a necessary, but not sufficient condition for the occurrence of chaos. Essentially, all realistic systems exhibit certain degree of nonlinearity.
- **Determinism:** Chaos must follow one or more deterministic equations that do not contain any random factors. The system states of past, present and future are controlled by deterministic, rather than probabilistic, underlying rules. Practically, the boundary between deterministic and probabilistic systems may not be so clear since a seemingly random process might involve deterministic underlying rules yet to be found.

- Sensitive dependence on initial conditions: A small change in the initial state of the system can lead to extremely different behavior in its final state. Thus, the long-term prediction of system behavior is impossible, even though it is governed by deterministic underlying rules.
- Aperiodicity: Chaotic orbits are aperiodic, but not all aperiodic orbits are chaotic. Almost-periodic and quasi-periodic orbits are aperiodic, but not chaotic.

### **3.8 Examples of chaotic systems:**

- The solar system (Poincare)
- The weather (Lorenz)
- Turbulence in fluids (Libchaber)
- Solar activity (Parker)
- Population growth (May)
- lots and lots of other systems

### **3.9 Tools for detecting Chaos:**

There are various methods for detecting chaos. The most useful methods are:

- A. Time series (Observe the state variables),
- B. Phase portraits,
- C. Poincare maps,
- D. Power spectrum,
- E. Lyapunov exponents,
- F. Bifurcation diagram.

### A. Time Series (Trajectory Plot)

This method is easiest one and it is a visual method. In this method, the state variables of the system are observed and if they exhibit irregular or unpredictable behavior, then it is called chaotic. Otherwise (fixed point, periodic and quasi periodic) it is called non chaotic.

### B. Phase Portraits

Phase portrait is a two-dimensional projection of the phase-space. It represents each of the state variable's instantaneous state to each other.

### C. Poincare Maps

Another method is the Poincare map. The basic is that  $n^{\text{th}}$  order continuous time system is replaced with  $(n-1)^{\text{th}}$  order map. It is constructed by sampling the phase portrait stroboscopically. Its aim is to simplify the complicated systems, and it is useful for stability analysis [5]. Chaotic and other motions can be distinguished visually from each other according to the Table3.2.

**Table.3.2** Solutions of dynamic systems (Poincare Maps)

Solution	Fixed	Periodic	Quasi Periodic	Chaos
Poincare Maps	-	Point	Closed Curve	Distinct points

#### **D. Power Spectrum**

Chaotic signals are wideband signals, so they can be easily distinguished from periodic signals by looking at their frequency spectra. If the behavior is chaotic, then power spectra of system is expressed in terms of oscillations with a continuum of frequencies.

#### **E. Lyapunov Exponents**

The Lyapunov exponents ( $\lambda_i, i=1,2,..n$ ) are the numbers that measure the exponential attraction or separation in time of two adjacent orbits in the phase space with close initial conditions. n dimensional system has n Lyapunov exponents. If original system is non autonomous one Lyapunov exponent is zero. If the system has at least one positive Lyapunov exponent, it indicates the chaos. If the largest Lyapunov exponent is negative, then the orbits converge in time and system is insensitive to initial conditions. If it is positive, then the distance between adjacent orbits grows exponentially and system exhibits sensitive dependence on initial conditions, so it is chaotic.

#### **F. Bifurcation Diagram**

In differential equations, if a change in the number of solution is depending on parameter variation, it is called bifurcation [43]. The dynamics may also be viewed more globally over a range of parameter values, thereby allowing simultaneous comparison of periodic and chaotic behavior.

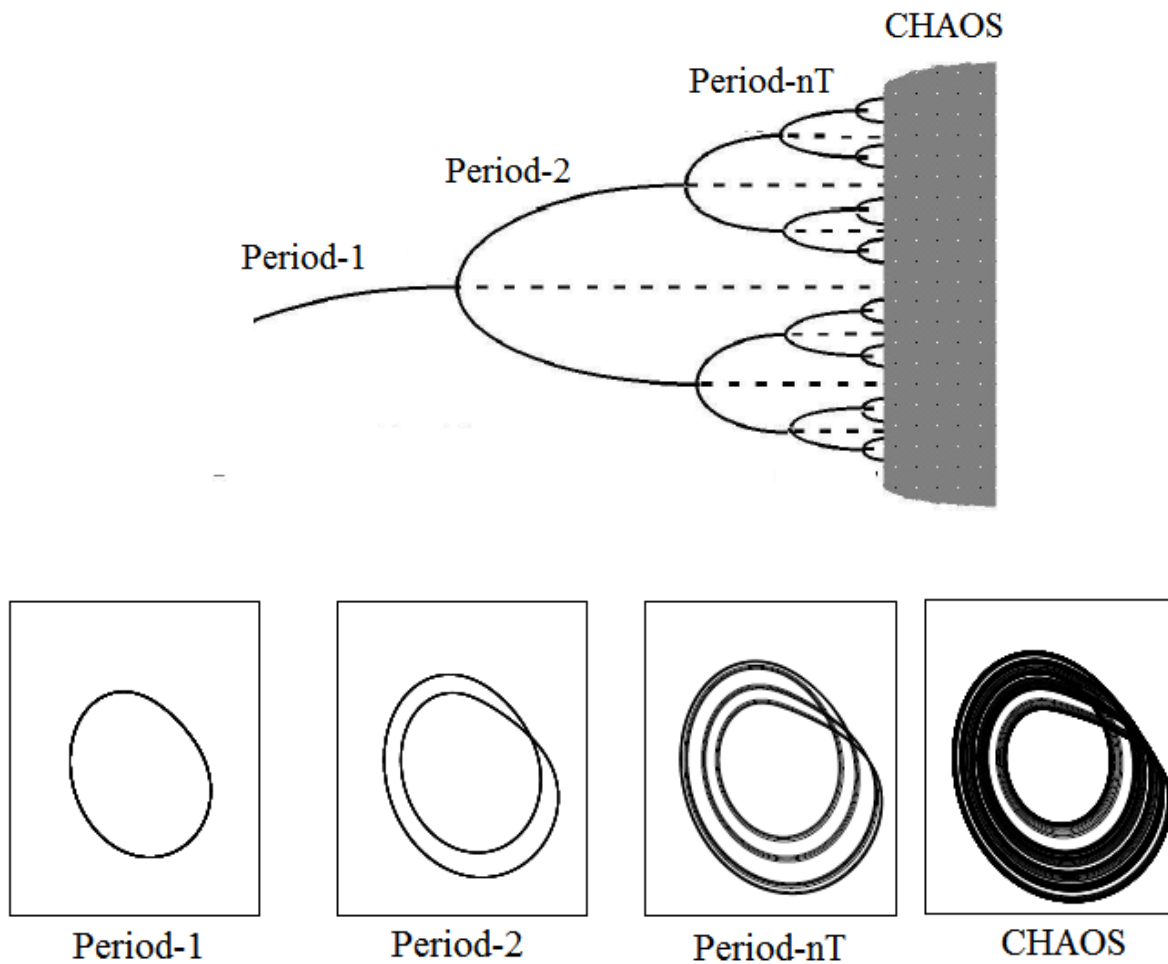


Figure 3.2 (a) Bifurcation diagram (b) Phase portrait

In this chapter the complex phenomena (Chaos) associated with nonlinear dynamical systems and tools are used to detect the Chaos are discussed. In the next chapter the fundamentals of electrical drives will be discussed and in Chapter-6 the nonlinear analysis (Chaos) of the PMDC drives will be discussed.

# Chapter 4

## ELECTRICAL DRIVES FUNDAMENTALS



## ELECTRICAL DRIVES FUNDAMENTALS

### 4.1 Introduction:

Electrical drives are found in homes, industry, automobiles, aircrafts, space crafts, etc. Most modern home appliances often have several electrical drives hidden in devices such as vacuum cleaners, dishwashers, washing machines, refrigerators, air conditioning units, etc. Such electrical drives are controlled through its rotational speed and torque by the changing ON and OFF of power electronic switches via pulse width modulated (PWM) signals. The “switch ON” equivalent circuit topology is often different from the “switch OFF” circuit topology. The electrical drives are inherently nonlinear in nature due to the switching of the power electronic devices, and are susceptible to complex nonlinear phenomena, namely *bifurcation* and *chaos*. In this chapter, the fundamentals of electrical drives with highlighting on DC drives.

### 4.2 Elements of an Electrical Drive System:

DRIVES can be defined as a system or systems that are employed for motion control, and may employ any of prime movers such as diesel or petrol engines, gas or steam turbines, steam engines, hydraulic motors and electric motors, for supplying mechanical energy for motion control. ELECTRICAL DRIVES are made of electric motors.

An ELECTRIC DRIVE can be defined as an electromechanical device for converting electrical energy into mechanical energy to impart motion to different machines and mechanisms for various kinds of process control.

A typical modern electrical drive (Fig.4.1) [46] contain an electric motor, a power converter, control electronics and a sensing unit working together to move a mechanical load. An input power supply that delivers the energy needed by the drive and sensors for closed-loop control, are also needed as integral parts of the system.

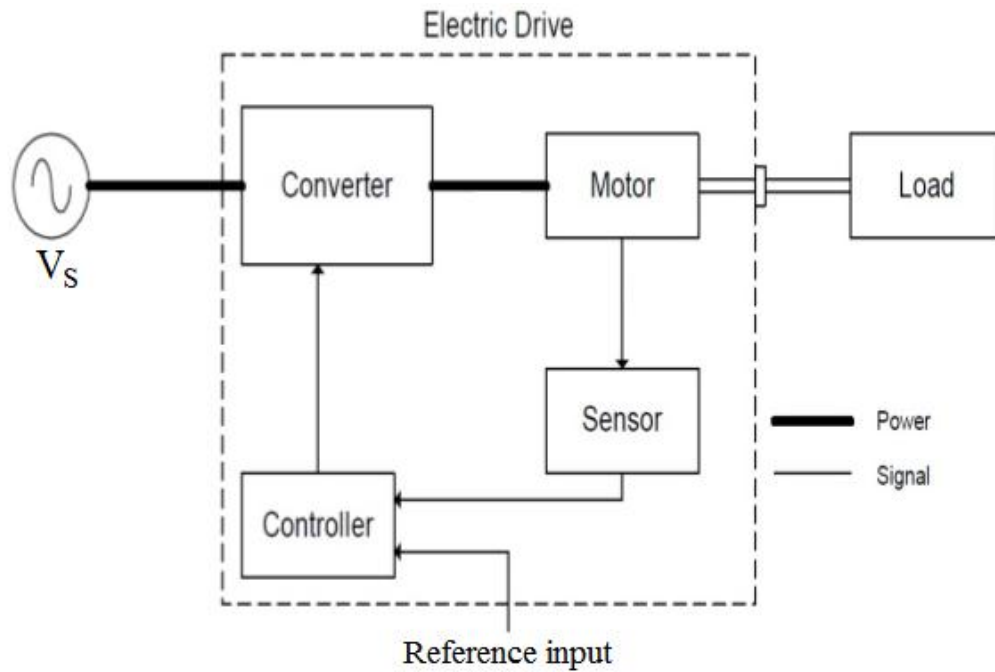


Figure 4.1: Parts of an electrical Drives system

A modern variable speed electrical drive system has the following components

- A. Electrical machines and loads
- B. Power Modulator
- C. Sources
- D. Control unit
- E. Sensing unit

Classification of Electrical Drives:

Another main classification of electric drive is

- DC drive
- AC drive

#### 4.2.1 Components of a DC Motor Drive System:

DC drive was used as the most common drive system for the variable speed application in the industry before the advances in field of power electronics and microprocessor technology is taken place.

DC drives are relatively easy to analyze and control and are commonly used in several domestic and industrial applications (children toys, robots, paper mills, steel rolling mills etc.). Typically, PMDC drives consist of a permanent magnet DC motor, the DC chopper, sensing unit and control electronics. The DC chopper can be (for first quadrant motoring operation) a full-bridge converter (for two quadrant operation) or even an active front end full-bridge converter (for four quadrant operation). The permanent magnet provides the field excitation, but since the permanent magnet flux is fixed, PMDC drives are widely used in low power applications [45]. In this section, the fundamentals of DC chopper fed PMDC drives will be discussed.

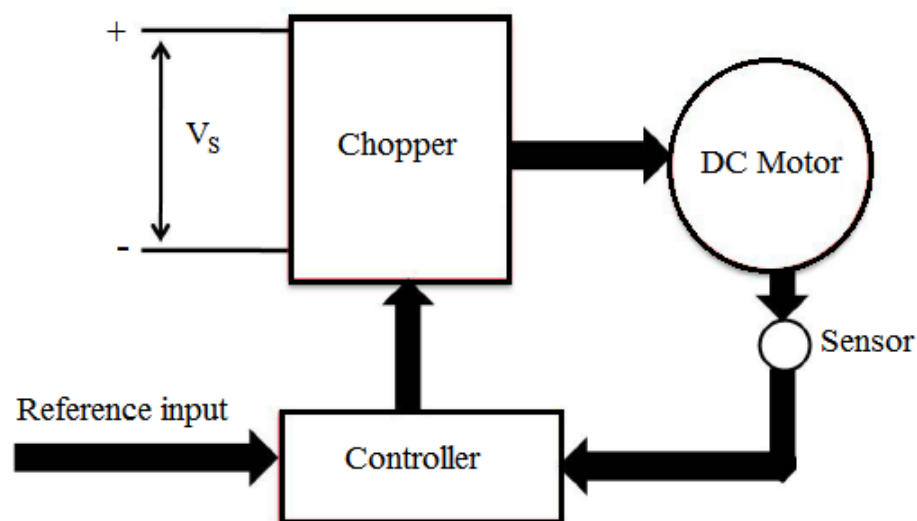


Figure 4.2: Parts of a DC Drive system

#### 4.2.1.1 *DC Motors :*

Electric motors are a basic component of electric drive systems and they convert the input electrical energy into mechanical energy [46]. There are several types of electrical motors in use today and possible classification criteria include the commutation strategy, the input power source and the type of torque being produced. In terms of the commutation strategy, there are mainly two variations as mechanical commutation and electronic commutation. An example of an electrical motor employing mechanical commutation is the conventional brushed DC motor (BDCM) which comes in four variants: separately excited (SE), series connected (SC), shunt connected (SHC), and compound motors (CM). Separately excited DC motors can also be subdivided into permanent magnet DC (PMDC) motors and field excited DC (FEDC) motors. The commutation strategy in those motors involves the use of mechanical commutators and carbon brushes. As the commutators and brushes wear out due to friction, conventional dc motors need routine maintenance. But, the ease at which the speed of conventional dc motors can be controlled makes them appealing for variable speed application and many industrial drives today still rely on brushed DC motors.

To overcome the problems caused by the wear and tear in mechanical commutators, electronic commutation is employed. Electronic commutation (brushless schemes) is based on the idea that a rotating magnetic field is produced by balanced three phase AC currents flowing in the stator coils [46]. Typical examples of electrical motors employing electronic commutation are brushless DC motors (BLDCM), inverter-fed induction motors (IM) & permanent magnet synchronous motors (PMSM), and synchronous reluctance motors (SR). Other variants of electronically commutated motors include switched reluctance motors (SRM) and stepper motors (SM) that rely on the principle of reluctance torque.

#### 4.2.1.2 *Power Converters:*

Power converters are used to adjust the voltage, current and frequency of the input electrical power for the purposes of motor speed and torque control. They receive electrical energy from the mains at constant voltage and frequency and then supply electrical energy to the motor at

variable voltage and frequency [46]. The power conversion process could be DC-DC (chopper), DC-AC (inverter), or AC-DC-AC (rectifier + inverter).

#### 4.2.1.3 *Control Electronics:*

In general, the state variables of an electrical drive system can be controlled either in open loop or closed loop. In closed loop control, the controller compares the actual state of the system measured by sensors with the reference state to produce an error signal. Based on the error signal a pulse width modulated (PWM) signal of appropriate duty ratio will be produced to turn ON or OFF the power switches in the power converter and thus achieve the required speed or current control [46]. Control electronics can be implemented in analog form using operational amplifiers and comparators or in digital form using microprocessors. Most modern drives make use of the later.

#### 4.2.1.4 *Mechanical Loads:*

Electrical motors are designed to carry mechanical loads of one form or the other. The mechanical load imposes an opposing torque to the electrical torque produced by the motor. The load can be a constant load or may vary with the shaft speed. The load can also introduce nonlinearity in the drive's dynamic model. For example, the load torque imposed on the shaft by a fan or pump type load is proportional to the square of the speed ( $T_L \propto \omega^2$ ) thus making the system nonlinear.

### **4.3 Permanent Magnet DC Drives:**

There is a negligible difference in between a DC Drives and a Permanent Magnet DC Drives. Both the system has same working principle but in case of Permanent Magnet DC (PMDC) Drives, there is no scope for field flux control, as a PMDC motor has a permanent magnet field coil.

### 4.3.1 System Overview:

The schematic diagram and equivalent circuit of DC-chopper fed PMDC drives (operating under open loop control) are shown in Fig. 4.3 [50]. The drive consists of the PMDC motor, an electronic switch (S) and free-wheeling diode (D). The switch (BJT, MOSFET, IGBT) is controlled by a PWM signal fed through a suitable device driver. The PMDC motor consists of a field circuit (a permanent magnet), and an armature circuit containing the armature coils, mechanical commutators (not shown) and brushes. The coils and the commutator are mounted on the rotor shaft and rotate with the rotor while the brushes are mounted on the stator and are stationary.

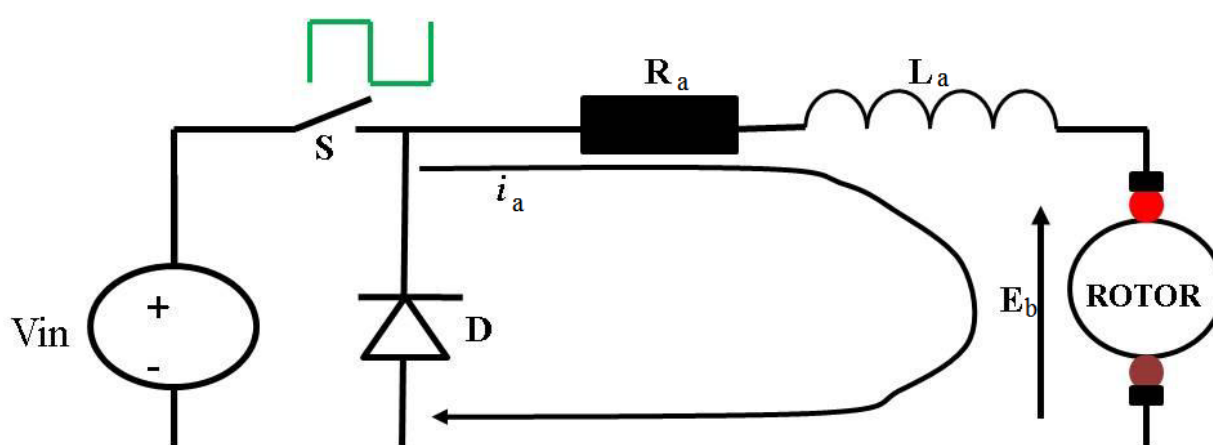


Figure 4.3: Open loop PMDC drive's equivalent circuit.

The speed of the motor depends on the average voltage applied at the armature terminals which depends on the duty cycle ( $d$ ) of the PWM signal.

$$V_{avg} = V_{in} \times d \quad \dots\dots\dots (4.1)$$

where  $d$  is the ratio of the switch ON time ( $T_{ON}$ ) to the period of the switching cycle ( $T$ )

$$d = \frac{T_{ON}}{T_{ON} + T_{OFF}} \quad \dots\dots\dots (4.2)$$

$$\text{Where } T = T_{ON} + T_{OFF} \quad \dots\dots\dots (4.3)$$

Since  $d \in [0,1]$ , the average voltage applied at the armature terminals using the DC Chopper will be between 0 and  $v_{in}$ , thus making it possible to achieve a speed range from zero to full speed.

#### 4.3.2 PMDC Drive Operation:

The operation of the open loop PMDC drive can be described through Fig.4.2. When the PWM signal is High, the switch (S) is closed and  $+v_{in}$  is applied at the terminals of the armature coil of the permanent magnet (PM) thus causing current  $i(t)$  to flow in the coil via the brushes. The interaction of the permanent magnet flux and the armature current produces a force  $F$  (also known as Lorentz force) at both ends of the winding. The force produces an electrical torque ( $T_e$ ) that causes anti-clockwise rotation of the shaft. When the PWM signal is Low, the switch opens and the diode (D) conducts thus causing zero volts to be applied at the armature coil terminals. The armature current thus decays via the diode. The switch ON and switch OFF circuit topologies are shown in Fig.4.4 and Fig.4.5, respectively [50].

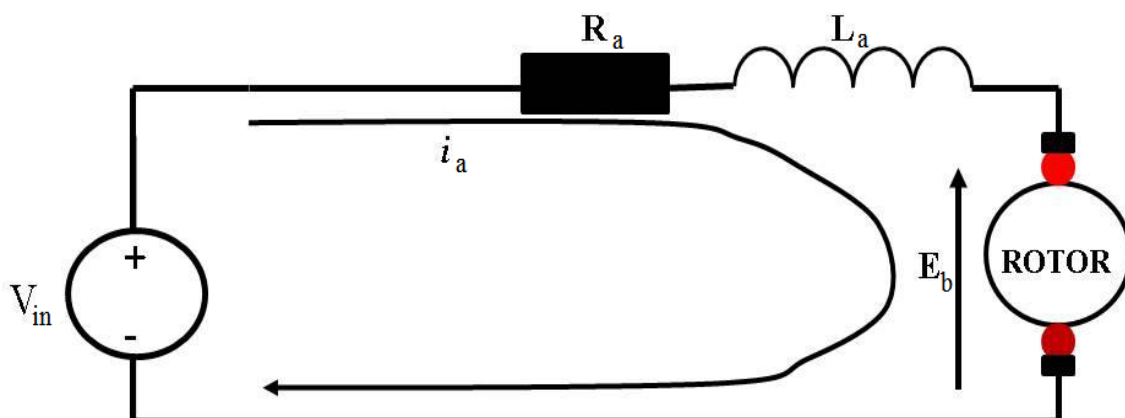


Figure 4.4: Switch ON circuit topology of a PMDC drive

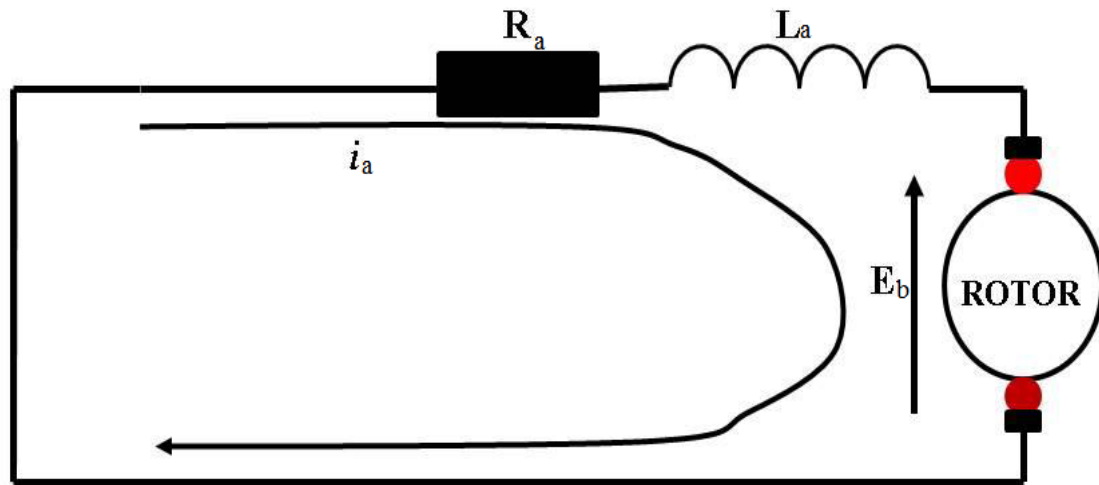


Figure 4.5: Switch OFF circuit topology of a PMDC drive

If the armature current decays to zero during the switch OFF interval, the operational mode will be referred to as discontinuous conduction mode (DCM), otherwise it will be referred to as continuous conduction mode (CCM). In order for the drive to operate in CCM, the inductance of the motor winding must be high enough to ensure that the current does not drop to zero during the switch OFF interval.

The force ( $F$ ) and the electrical torque ( $T_e$ ) produced are functions of the armature current and field flux as shown below:

$$F = B \times i_a \times l \quad \dots\dots\dots (4.4)$$

$$T_e = K_t \times \phi \times i_a \quad \dots\dots\dots (4.5)$$



Where  $\phi$  is the field flux,  $i_a$  is the armature current,  $B$  is the field flux density,  $l$  is the length of the armature coil being linked by the field flux and  $k_t$  is the torque constant.  $\phi$  is constant in PMDC motor and consequently the electrical torque produced will depend only on the armature current as expressed below:

$$T_e = K_t \times i_a \dots\dots\dots(4.6)$$

As the rotor rotates, an emf ( $E_b$ ) will be induced at the terminals of the armature coil as it is being linked by the field flux. This emf is commonly referred to as back emf and is proportional to the field flux and the shaft angular velocity ( $w(t)$ )

$$E_b = K_e \times \phi \times w(t) \dots\dots\dots (4.7)$$

Since  $\phi$  is constant for the PMDC motor and the back emf  $E_b$  can also be expressed as

$$E_b = K_e \times w(t) \dots\dots\dots (4.8)$$

In this chapter the fundamentals of Electrical Drives operation with emphasis on DC drives are discussed. In the next chapter problem formulation and mathematical modelling of PMDC drive system will be analyzed in detail.

# Chapter 5

## Problem formulation and Mathematical Modelling of PMDC motor Drives

## Problem formulation and Mathematical Modelling of PMDC motor Drives

### 5.1 Problem Formulation:

A DC chopper-fed PMDC motor drive operates under the proportional controller is a very simple method of speed control for a DC motor. But the simple closed loop control method become interesting when a special phenomenon (Chaos) is observed for the variation of the Drive's parameters. It is rather interesting to observe how the armature current ( $i_a$ ) and motor speed ( $\omega(t)$ ) loses its nominal orbit (period-1) and become Chaotic. In view of a design engineer it is rather important to find out the range of a DC motor drives where it can operate in its required zone.

To investigate a Period-doubling and its route to chaos in voltage-mode controlled DC motor drives under simple proportional control and to find out the range and combination of parameters (error amplifier gain( $g$ ), Load Torque( $T_L$ ) and switching frequency( $f_s$ )), if the mode of operation of the motor needs to be restricted in a particular operating mode. Also to investigate if the Chaos makes a worthy impact on the selected system or not.

In order to observe the Chaotic phenomena in MATLAB using simulation, the parameters of the DC chopper-fed PMDC DC drive used in this thesis are the same as those used in [25] :  $K_e=0.05\text{Vs/rad}$ ,  $K_r=0.05\text{ Nm/A}$ ,  $R_a=0.5\ \Omega$ ,  $L=1.5\text{ mH}$ ,  $B=0.0001\text{ Nm.rad}^{-1}.\text{sec}$ ,  $V_{in}=12\text{ V}$ ,  $T=10\text{ ms}$ ,  $J=0.00025\text{ N.m.rad}^{-1}.\text{sec}^2$ .

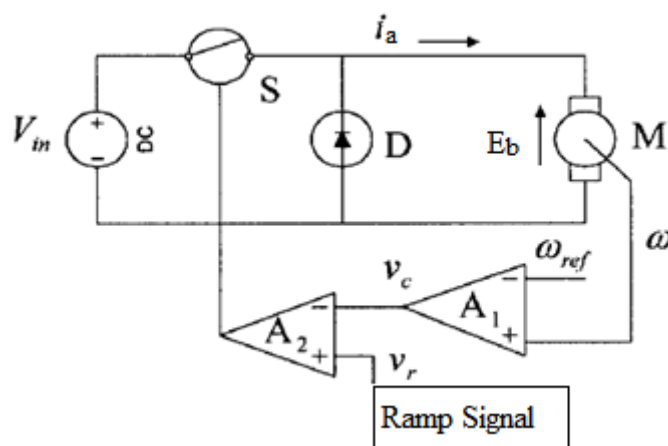


Figure 5.1: Block diagram of a DC Chopper fed DC Drive

## 5.2 Mathematical Model of Open Loop PMDC Drive

Under CCM operation, the system will alternate between two different topological states as the switch is turned ON and OFF.

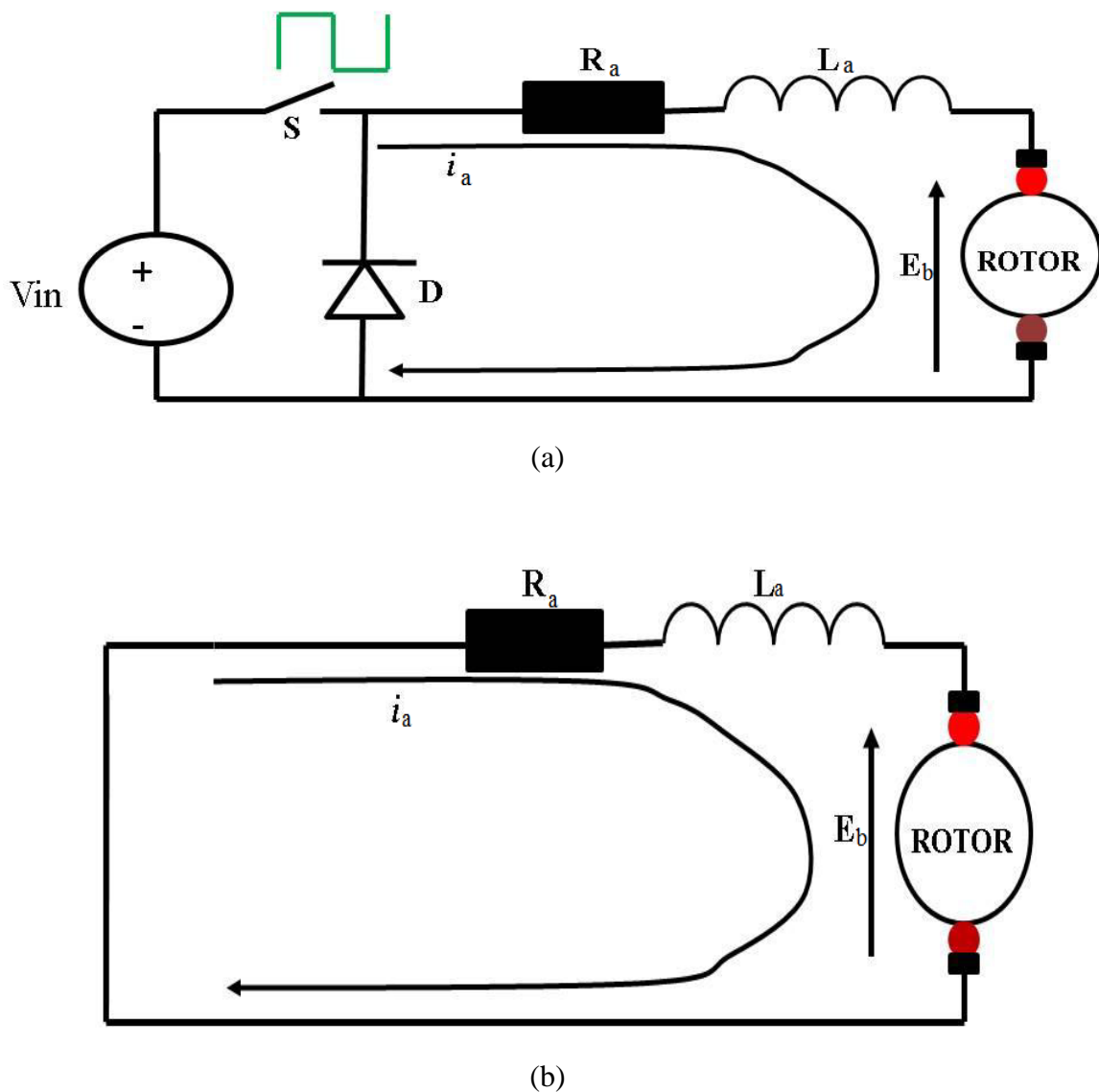


Figure 5.2: Open loop (a) Switch ON and (b) Switch OFF circuit topology of a PMDC drive

The mathematical model depicting the switch ON state will be different from the mathematical model for the switch OFF state.

When the switch is ON and the diode is OFF (Fig.5.2(a)) [50] the mathematical model will be expressed as:

$$T_e = J \frac{d\omega(t)}{dt} + B\omega(t) - T_L \dots\dots\dots(5.1)$$

$$T_e = K_t \times i_a(t) \dots\dots\dots(5.2)$$

By comparing both the equation (5.1) and (5.2) we get

$$K_t \times i_a = J \frac{d\omega(t)}{dt} + B\omega(t) - T_L \dots\dots\dots(5.3)$$

$$\frac{d\omega(t)}{dt} = \frac{(K_t \times i_a) - T_L - B\omega(t)}{J} \dots\dots\dots(5.4)$$

Again

$$V_{in} = i_a(t)R + L \frac{di_a(t)}{dt} + E_b \dots\dots\dots(5.5)$$

$$E_b = K_e \times \omega(t) \dots\dots\dots(5.6)$$

$$V_{in} = i_a(t)R + L \frac{di_a(t)}{dt} + K_e \times \omega(t) \dots\dots\dots(5.7)$$

$$\frac{di_a(t)}{dt} = \frac{V_{in} - i_a(t)R - K_e \times \omega(t)}{L} \dots\dots\dots(5.8)$$

where  $i_a$  is the armature current,  $\omega(t)$  is the shaft speed,  $L$  is the armature inductance,  $R$  is the armature resistance,  $K_e$  and  $K_t$  are the back emf and the torque constants, respectively,  $B$  is the viscous damping factor,  $T_L$  is the load torque,  $J$  is the moment of inertia, and  $V_{in}$  is the supply voltage.

But when the switch is OFF and the diode conducts (Fig.5.2(b)), the mathematical model will be expressed as:

$$\frac{d\omega(t)}{dt} = \frac{K_t}{J} \times i_a(t) - \frac{B}{J} \times \omega(t) - \frac{T_L}{J} \dots\dots\dots(5.9)$$

$$\frac{di_a(t)}{dt} = \left( -\frac{R}{L} \right) \times i_a(t) - \left( \frac{K_e}{L} \right) \times \omega(t) + \frac{V_{in}}{L} \dots\dots(5.10)$$

The switch ON model equation (5.7) and (5.8) and the switch OFF model equation (5.9) and (5.10) can be edited in state space form as shown below:

$$\dot{X}(t) = A_{ON} X(t) + V_{ON} \dots\dots\dots(5.11)$$

$$\dot{X}(t) = A_{OFF} X(t) + V_{OFF} \dots\dots\dots(5.12)$$

$$X(t) = \begin{bmatrix} x_1(t) \\ x_2(t) \end{bmatrix} = \begin{bmatrix} \omega(t) \\ i_a(t) \end{bmatrix} \dots\dots\dots(5.13)$$

$$A_{ON} = A_{OFF} = A = \begin{bmatrix} \frac{-B}{J} & \frac{K_T}{J} \\ \frac{-K_E}{L} & \frac{-R}{L} \end{bmatrix} \dots\dots\dots(5.14)$$

$$V_{ON} = \begin{bmatrix} \frac{-T_L}{J} \\ \frac{V_{in}}{L} \end{bmatrix} \dots\dots\dots(5.15)$$

$$V_{OFF} = \begin{bmatrix} -T_L \\ J \\ 0 \end{bmatrix} \dots\dots\dots(5.16)$$

The steady state speed and current when the switching frequency ( $f_s=100$  Hz), ramp signal ( $V_r= 2.2$  volt) and Load torque ( $T_L=0.3$  Nm) are as shown in Fig.5.3 and Fig.5.4. From the Figures, it could be seen that the steady state behavior of the state variables is a periodic ripple of the same period as the external clock signal. This is referred to as a period-1 orbit. In chapter 6 it will be shown that as some system parameters (such as the Error amplifier controller gain( $g$ ), Load Torque ( $T_L$ ) of the closed loop PMDC drive) are being varied, the nominal period-1 orbit changes to a Chaotic behavior may appear. The study of the mechanism through which such Chaotic behavior occurs is a main objective of this thesis.

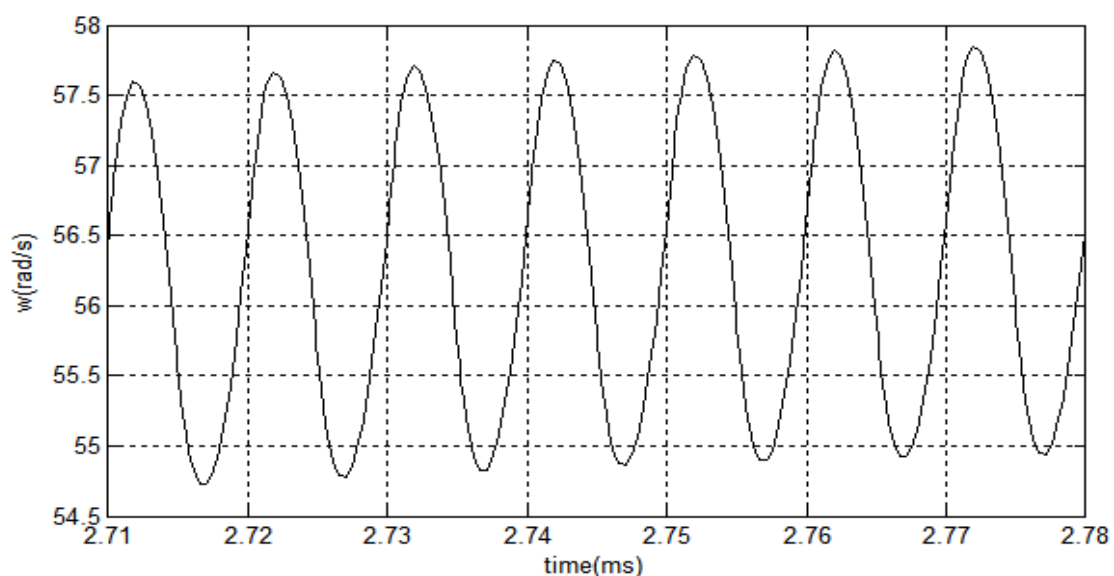


Figure 5.3: Open loop speed response ( $f_s=100$ Hz,  $T_L=0.3$  Nm )

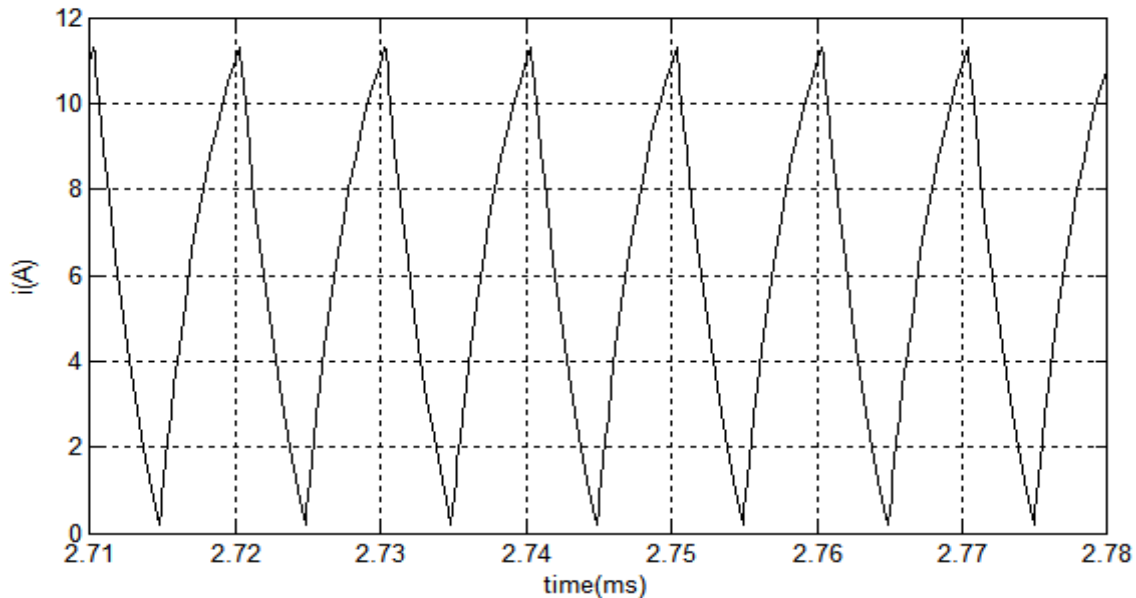


Figure 5.4: Open loop current response ( $f_s=100\text{Hz}$ ,  $T_L=0.3\text{ Nm}$ )

### 5.3. Mathematical Model of Closed Loop PMDC Drive:

The schematic diagram of DC-chopper fed voltage mode controlled PMDC drive employing the proportional controller is shown in Fig. 5.5. The system consists of three main components namely the PMDC motor, the power converter (a dc chopper) and the control electronics. The shaft speed  $\omega(t)$  is controlled by control of the average voltage at the armature terminals via pulse width modulation (PWM). Under CCM, the system will alternate between two circuit topologies (in figure 5.2) at steady state, depending on the relative magnitudes of the control signal  $V_c(t)$  and the ramp signal  $V_r(t)$ .

A Low side switching has been done to avoid energy losses using a MOSFET in the chopper. The MOSFET is switched on by a voltage at the gate and switched off with no voltage at the gate. IGBT or GTO may also use as another switching element.



The speed of the motor  $\omega(t)$  is sensed by the speed sensor and compared with a reference speed ( $\omega_{ref}$ ).  $g$  is the speed error amplifier gain and the proportional controller signal can be expressed as

$$V_c = g (\omega(t) - \omega_{ref}) \dots\dots(5.17)$$

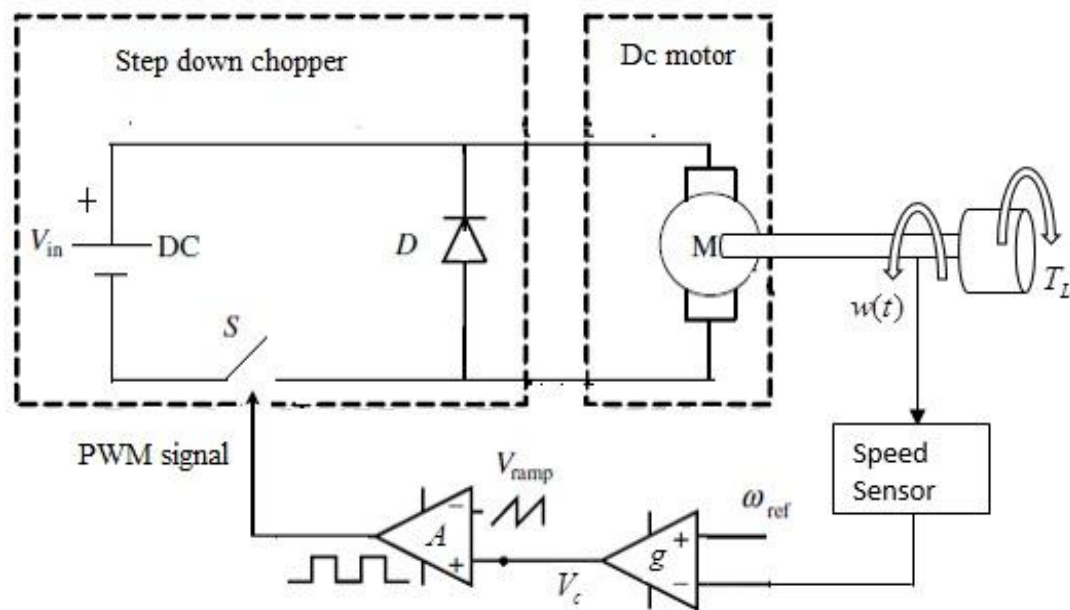


Figure 5.5: Block diagram of closed loop PMDC drive

The ramp generator voltage can be expressed as

$$V_r = v_l + \frac{(v_u - v_l)}{T} t \dots\dots(5.18)$$

Where  $v_u$  and  $v_l$  are the upper and lower voltages of the ramp signal respectively and  $T$  is the time period. Then both  $V_r$  and  $V_c$  fed to the comparator.

Whose output signal goes to power switch (S). The switch S will be in “ON” and the diode D is “OFF” until  $V_c$  exceeds  $V_r$  otherwise S is “OFF” and the diode is “ON”. Thus the system operated in two stages.

State 1: When  $V_c \geq V_r$  Switch (S) is OFF hence diode (D) becomes ON

$$\begin{bmatrix} \frac{d\omega(t)}{dt} \\ \frac{di(t)}{dt} \end{bmatrix} = \begin{bmatrix} \frac{-B}{J} & \frac{K_T}{J} \\ \frac{-K_E}{L} & \frac{-R}{L} \end{bmatrix} \begin{bmatrix} \omega(t) \\ i(t) \end{bmatrix} + \begin{bmatrix} \frac{T_L}{J} \\ 0 \end{bmatrix} \dots\dots\dots(5.19)$$

State 2: When  $V_c < V_r$  Switch (S) is ON hence diode (D) becomes OFF

$$\begin{bmatrix} \frac{d\omega(t)}{dt} \\ \frac{di(t)}{dt} \end{bmatrix} = \begin{bmatrix} \frac{-B}{J} & \frac{K_T}{J} \\ \frac{-K_E}{L} & \frac{-R}{L} \end{bmatrix} \begin{bmatrix} \omega(t) \\ i(t) \end{bmatrix} + \begin{bmatrix} \frac{T_L}{J} \\ \frac{V_{in}}{L} \end{bmatrix} \dots\dots\dots(5.20)$$

Where  $i_a$  is armature current,  $R_a$  armature resistance,  $L_a$  armature inductance, DC supply voltage,  $K_e$  back-EMF constant,  $K_T$  torque constant,  $B$  viscous damping,  $J$  load inertia, and  $T_L$  load torque .So the system equation can be written by the following sequence of state equations

$$\bullet$$

$$\dot{X}(t) = A_1 X(t) + B_1 E \quad \text{for } V_c \geq V_r \dots\dots\dots(5.21)$$

$$\bullet$$

$$\dot{X}(t) = A_2 X(t) + B_2 E \quad \text{for } V_c < V_r \dots\dots\dots(5.22)$$

the system equation given by (5.21) and (5.22) can be rewritten as

$$\dot{X}(t) = A_K X(t) + B_K E \quad (\text{where } K=1,2) \dots \dots \dots (5.23)$$

The switching condition at  $V_c = V_r$  can be expressed from the equation (5.17) and (5.18)

$$B_3 (X(t) - B_4) = V_r(t) \dots \dots \dots (5.24)$$

$$\text{Where, } B_3 = [g \quad 0], B_4 = \begin{bmatrix} \omega_{ref} \\ 0 \end{bmatrix}$$

the system equation given by (5.23) is a time-varying state equation. Thus this drive system is a second-order non-autonomous dynamical system. We simulate this model using MATLAB.

From the first order equations,  $i_a$  during on and off (CCM) can be expressed as:

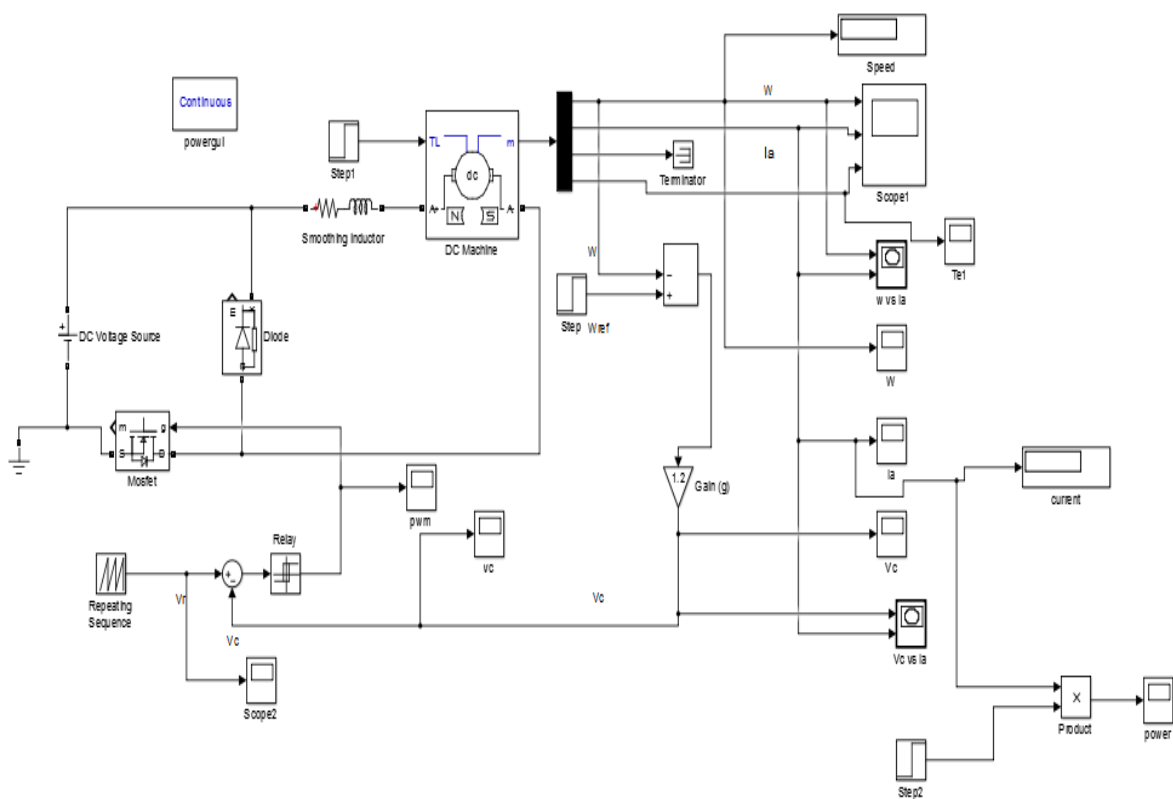
$$P \frac{d^2 i(t)}{dt^2} + Q \frac{di(t)}{dt} + R i_a(t) = Z \dots \dots \dots (5.25)$$

Where,

$$P = \frac{L}{K_E}, Q = \left( \frac{R}{K_E} + \frac{BL}{JK_E} \right), R = \left( \frac{K_T}{J} + \frac{BR}{JK_E} \right), Z = \left( \frac{T_L}{J} + \frac{BSV_{in}}{JK_E} \right)$$

and  $S = 1$  when the switch is on,  $S = 0$  when the switch is off.

### 5.4 Simulation Model:



In this chapter problem formulation of this study and detailed mathematical modelling of a PMDC motor drives are discussed. In the next chapter the nonlinear phenomena(Chaos) that occur in a PMDC drive system will be analyzed in detail.

# Chapter 6

## OBSERVATION AND ANALYSIS OF CHAOTIC PHENOMENA IN DC CHOPPER FED PERMANENT MAGNET DC DRIVES

## OBSERVATION AND ANALYSIS OF CHAOTIC PHENOMENA IN DC CHOPPER FED PERMANENT MAGNET DC DRIVES

### 6.1 Introduction:

There are various methods for detecting chaos. In this thesis work two of them are used. These are:

- Time series (Observe the state variables),
- Phase portraits.

#### a. Time Series (Trajectory Plot)

This method is easiest one and it is a visual method. In this method, the state variables of the systems are observed and if they exhibit irregular or unpredictable behavior, then it is called chaotic. Otherwise (fixed point, periodic and quasi periodic) it is called non-chaotic.

#### b. Phase Portraits

Phase portrait is a two-dimensional projection of the phase-space. It represents each of the state variables instantaneous state to each other. Chaotic and other motions can be distinguished visually from each other according to the Table.1. A fixed point solution is a point in a phase portrait. A periodic solution is a closed curve in phase portrait. Chaotic solutions are distinct curves in phase portrait.

Table 6.1: Solutions of dynamic systems (Phase Portrait)

<b>Solution</b>	Fixed	Periodic	Quasi Periodic	Chaos
<b>Phase portrait</b>	Point	Closed curve	Torus	Distinct shapes

## 6.2 Observation and Analysis of DC Chopper -fed PMDC

### Drives Employing the Proportional Controller (error amplifier gain)

Time series and Phase portrait methods are used to detect the chaos in a DC Chopper fed PMDC Drives. The switching frequency( $f_s$ ) and Load Torque ( $\tau_L$ ) are kept constant and error amplifier gain( $g$ ) is varied to observed the chaotic phenomena. Figure 5.1.-Figure 5.10 exhibit route to chaos of armature current and speed of the motor with  $\tau_L = 0.30\text{Nm}$  at switching frequency 100 Hz.

In the previous chapter, simulation results of the open loop control are observed of the selected DC chopper fed PMDC Drive. It is found that in open loop condition for same system parameters (switching frequency ( $f_s=100$  Hz), ramp signal ( $v_r=2.2$  volt) and Load Torque ( $T_L=0.3\text{Nm}$ )) the selected system operates in nominal orbit (period-1). The behavior changes when it operates in closed loop as well as parameters are changing. This is the main purpose of this study to realize the Chaos in DC Chopper fed DC Drives.

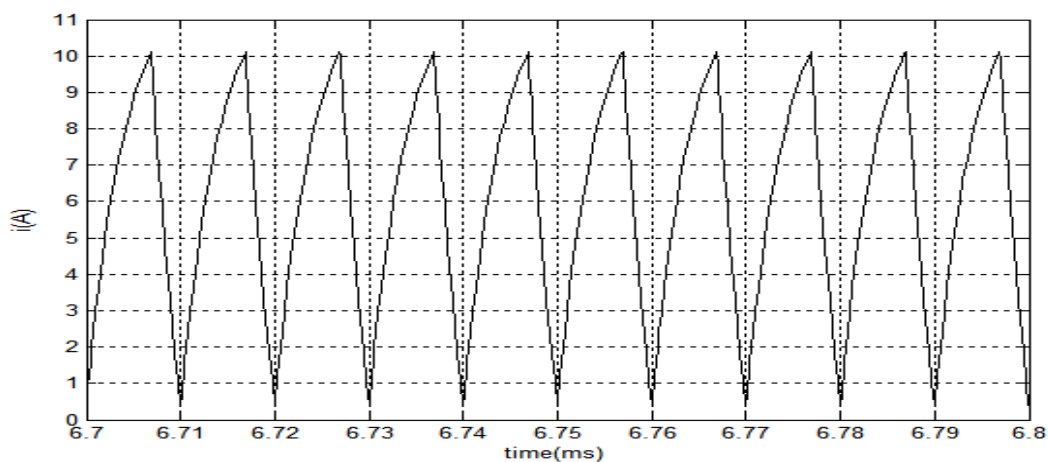


Figure 6.1: Time series plot of motor armature current at  $g=0.20$  (Period-1)

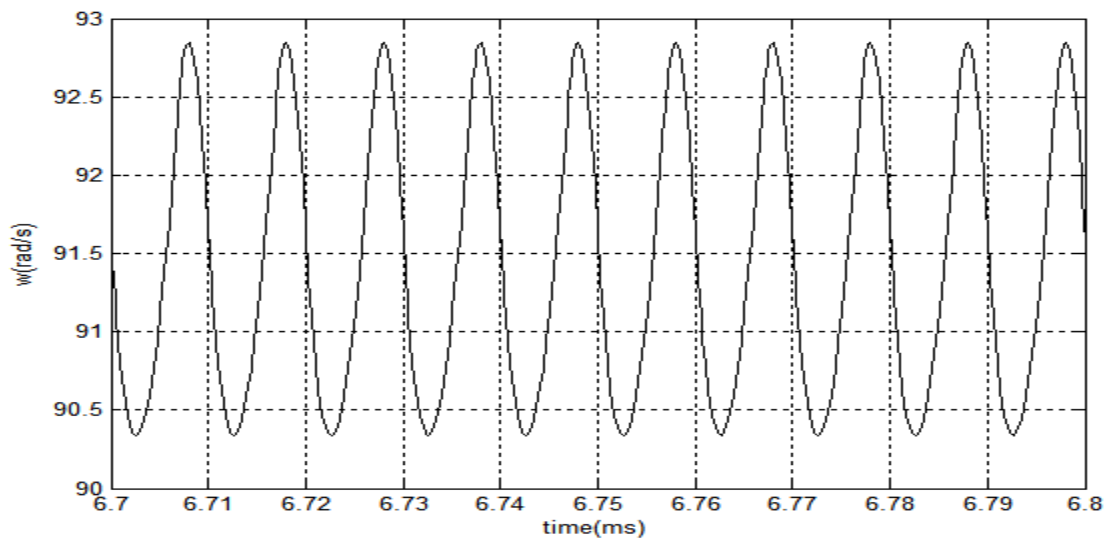


Figure 6.2: Time series plot of motor speed at  $g=0.20$  (**Period-1**)

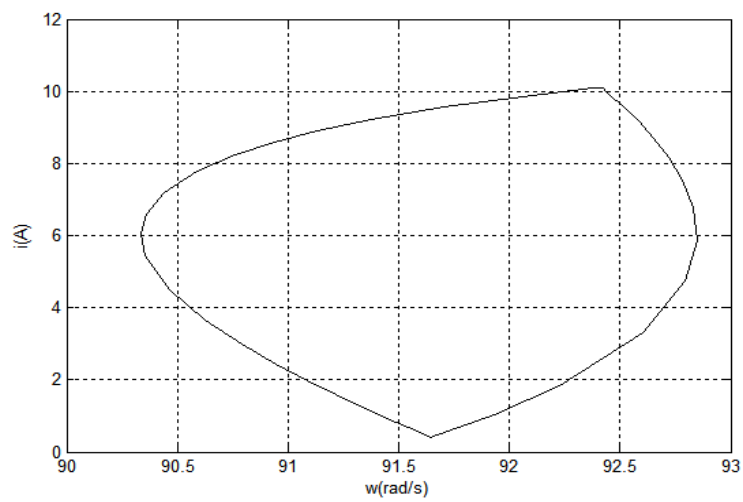


Figure 6.3: Phase portrait of motor speed and armature current at  $g=0.20$  (period1)



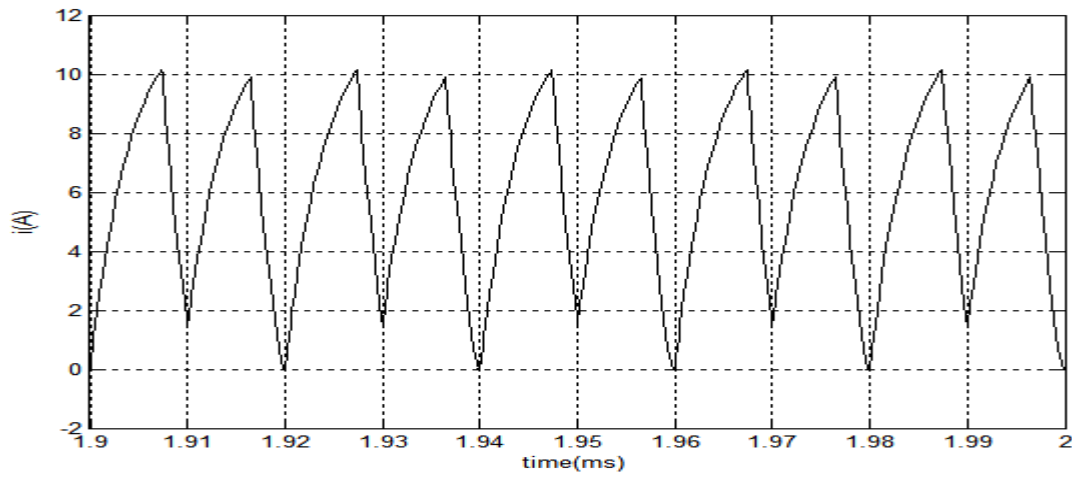


Figure 6.4: Time series plot of armature current at  $g=0.30$  (**Period-2**)

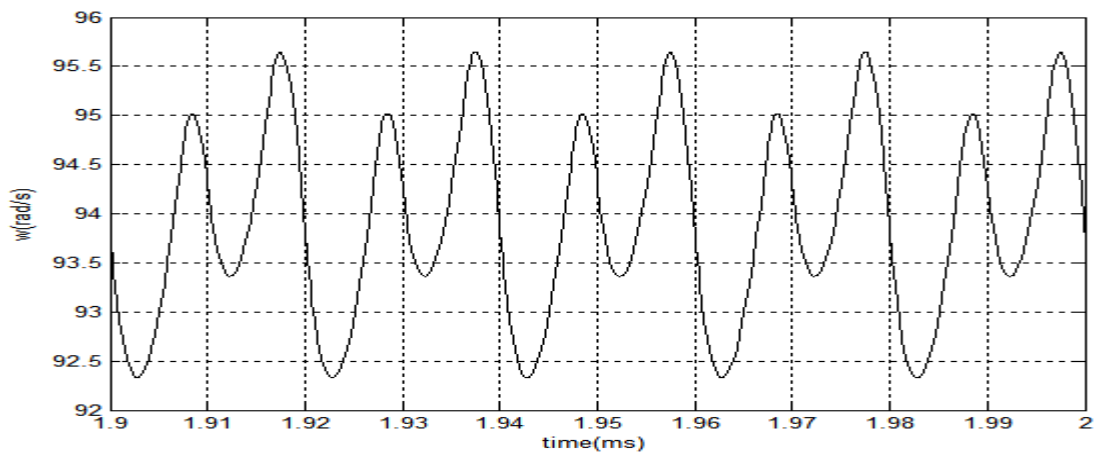


Figure 6.5: Time series plot of motor speed at  $g=0.30$  (**Period-2**)

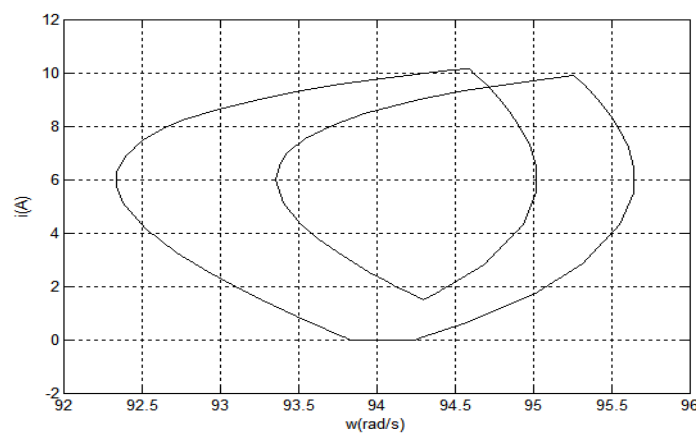


Figure 6.6: Phase portrait of motor speed and armature current at  $g=0.30$  (period2)

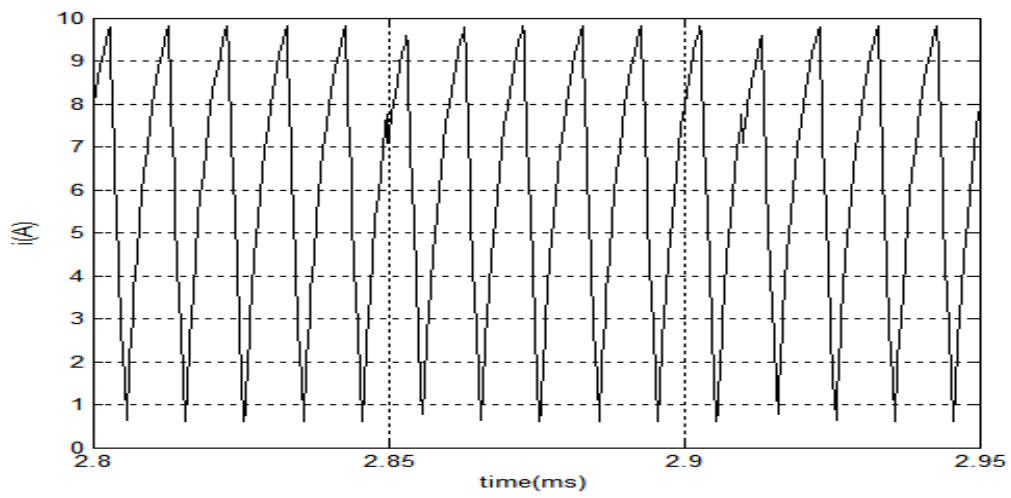


Figure 6.7: Time series plot of armature current at  $g=0.90$

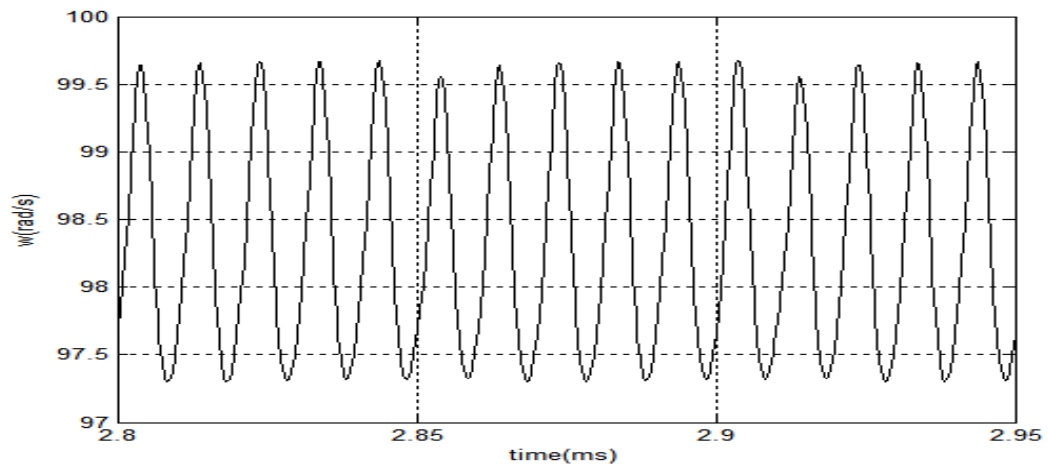


Figure 6.8: Time series plot of motor speed at  $g=0.90$

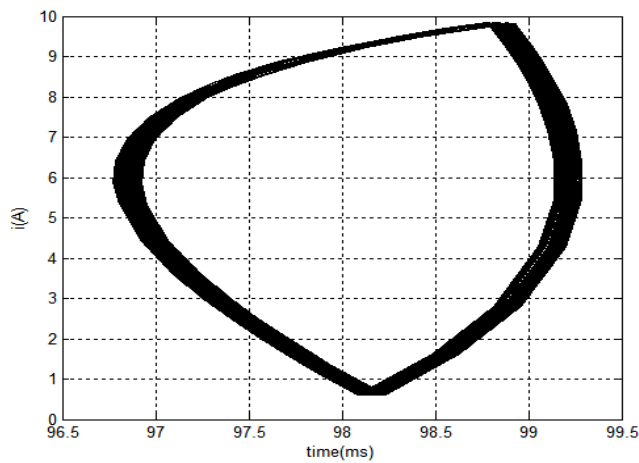


Figure 6.9 Phase portrait of motor speed and armature current at  $g=0.90$

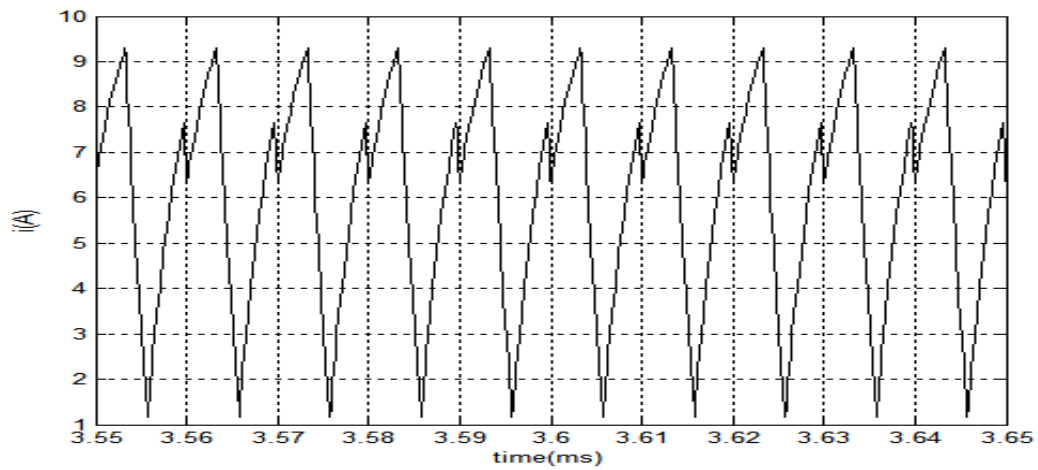


Figure 6.10: Time series plot of armature current at  $g=1$  (**Period-1**)

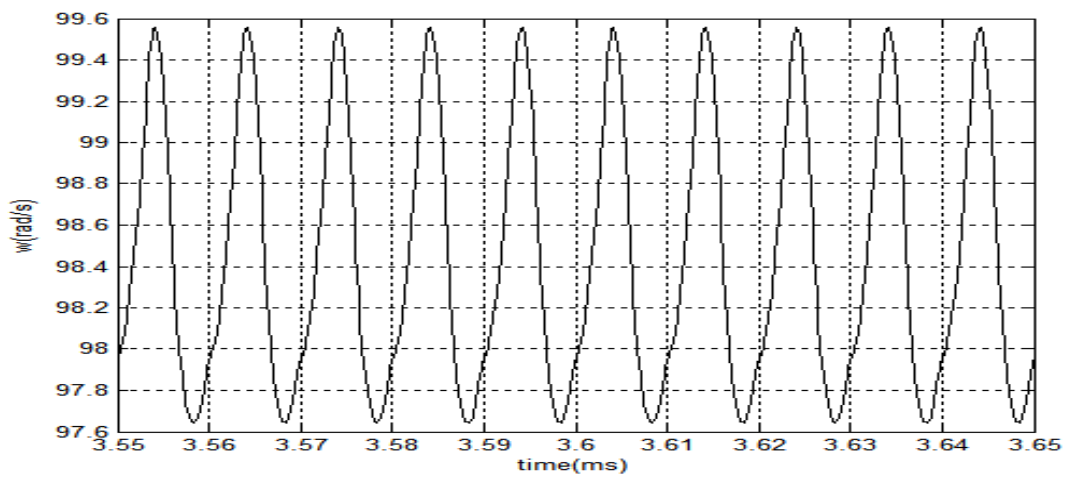


Figure 6.11 Time series plot of motor speed at  $g=1$  (**Period-1**)

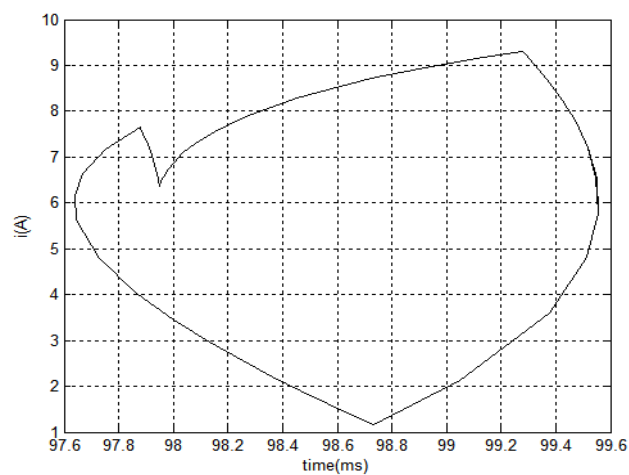


Figure 6.12: Phase portrait of motor speed and armature current at  $g=1$  (period1)

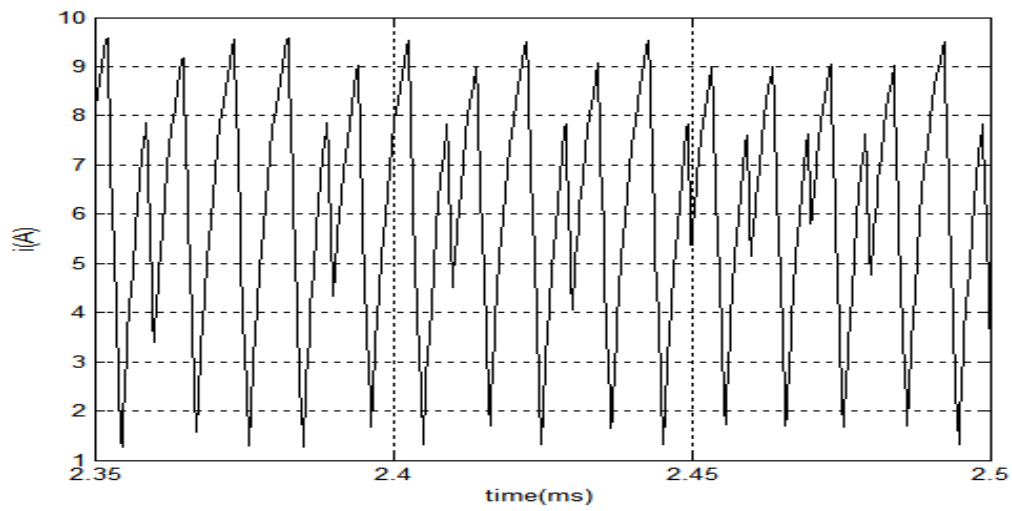


Figure 6.13: Chaotic time series plot of armature current at  $g=1.2$

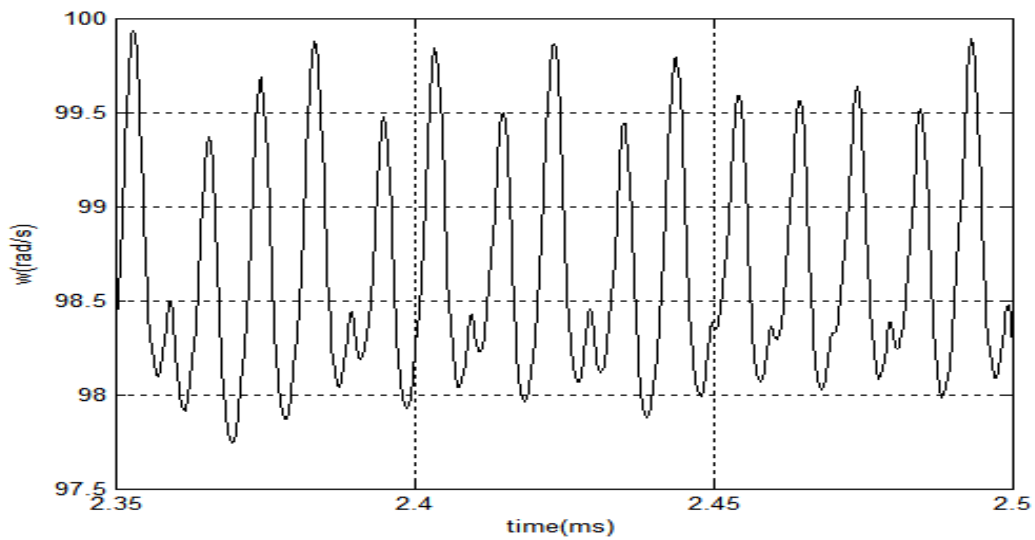


Figure 6.14: Chaotic time series plot of motor speed at  $g=1.2$

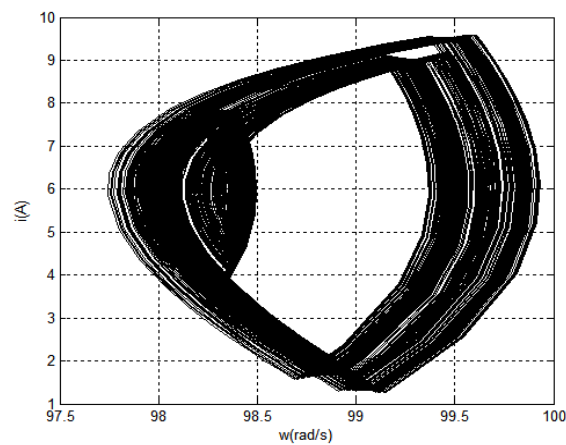


Figure 6.15: Phase portrait of motor speed and armature current at  $g=1.2$  (Chaotic trajectory)

Figure 6.1 and Figure 6.2 exhibit period-1 orbit of armature current and speed at  $g=0.20$  in Time Series plot and Figure 6.3 shows period-1 orbit in phase portrait. A new orbit whose period is double (period-2) is observed at  $g=0.30$  from Figure 6.4 to Figure 6.6. Further variation of error amplifier gain ( $g$ ) at 0.90 leads to a new pattern in Figure 6.7 and Figure 6.9. Again the system undergoes nominal period (period-1) at  $g=1$  from Figure 6.10 to Figure 6.12. The dynamic behavior of the state variables of this system lead to chaotic when  $g$  is changed to 1.2 from Figure 6.13 and Figure 6.15.

A chaotic and non-chaotic time series plot of armature current and motor speed is shown respectively in Figure 5.16 and Figure 5.17.

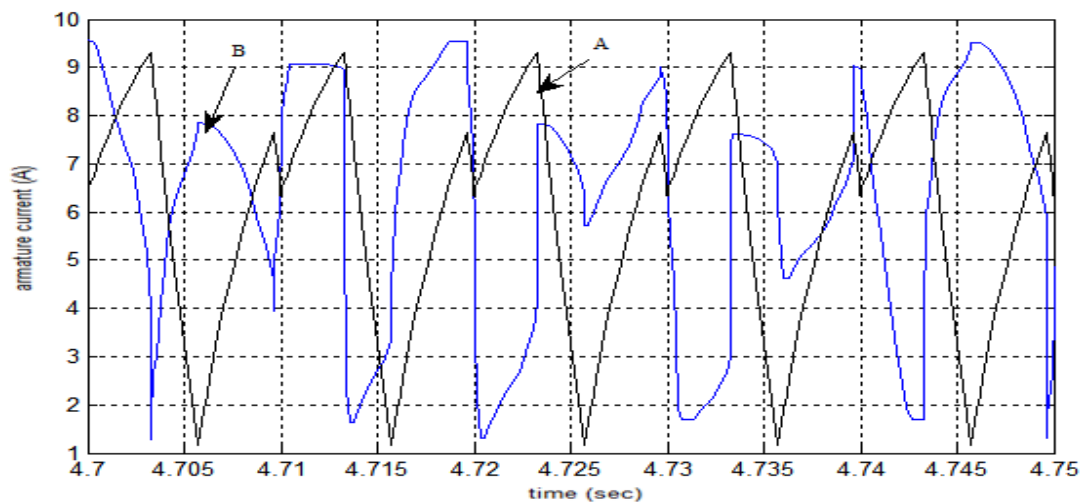


Figure 6.16. Non chaotic and chaotic armature current waveforms. Where A is non chaotic wave and B is chaotic wave.

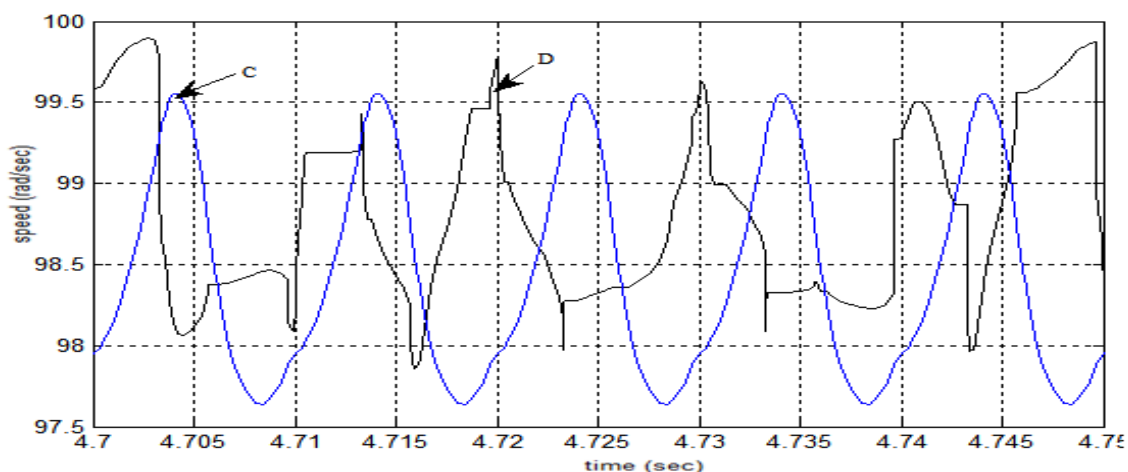


Figure 6.17. Non chaotic and chaotic speed waveform. Where C is non chaotic wave and D is chaotic wave.

Phase portrait method is used as another method of detecting chaos. In this case armature current and speed of the motor graph is a phase portrait. In this case switching frequency( $f_s$ ) and Load Torque ( $T_L$ ) are kept constant and error amplifier gain( $g$ ) is varied to observed the chaotic phenomena. Figure 6.13.-Figure 6.17 exhibit route to chaos of armature current and speed of the motor with  $\tau_L=0.30\text{Nm}$  at switching frequency 100 Hz.

Figure 6.13 exhibit period-1 orbit of armature current and speed at  $g=0.20$ . A new orbit whose period is double(period-2) is observed at  $g=0.30$  in Figure 6.14. Further variation of error amplifier gain( $g$ ) at 0.90 leads to a new pattern in Figure 6.15. Again the system undergoes period doubling (period-2) at  $g=1$  in Figure 6.16. The dynamic behavior of the state variables of this system lead to chaotic when  $g$  is changed to 1.2 in Figure 6.17.

### **6.3 Observation and Analysis of DC Chopper Fed PMDC Drives Employing Variation of Load Torque.**

Nonlinear phenomena or chaotic behavior is also observed during the variation of the Load Torque ( $T_L$ ) of a voltage-mode controlled PMDC motor drive system. In this case switching frequency( $f_s$ ) and error amplifier gain( $g$ ) are kept constant and Load Torque ( $T_L$ ) is varied to observe the chaotic phenomena through Time Series and Phase Portrait method. Figure 5.1.- Figure 5.10 exhibit route to chaos of armature current and speed of the motor with error amplifier gain( $g$ ) at switching frequency 100 Hz.

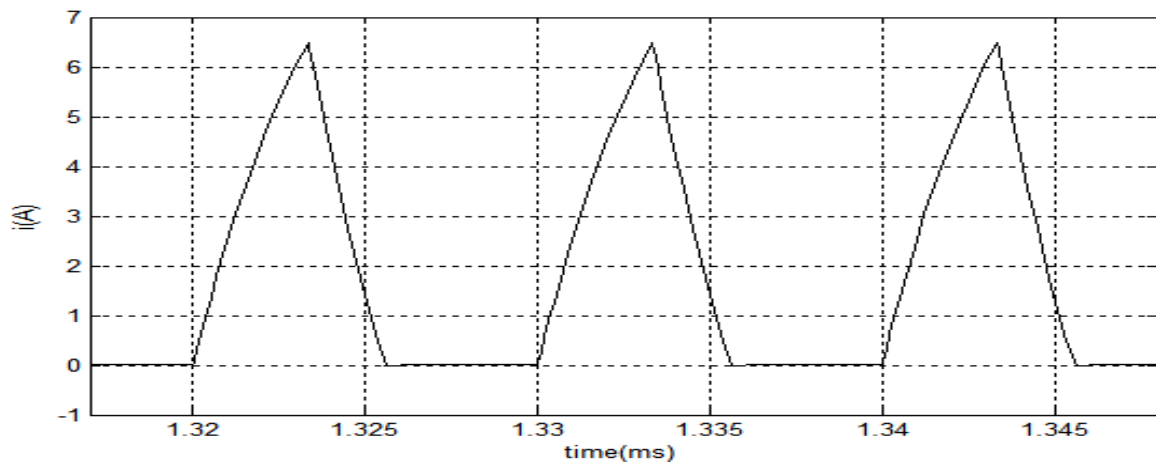


Figure 6.18: Time series plot of armature current at  $(T_L)=0.09$  (Period-1)

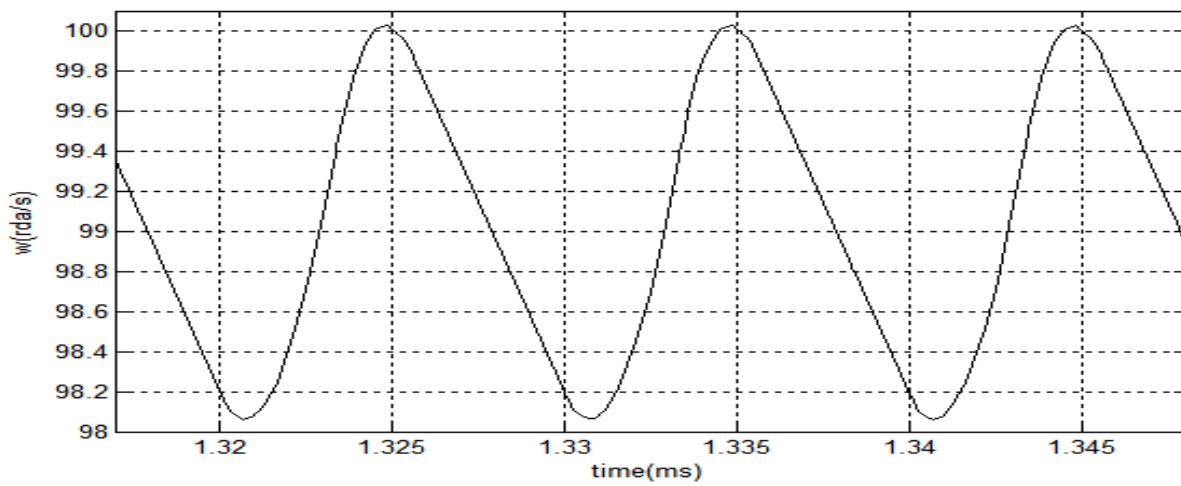


Figure 6.19: Time series plot of motor speed at  $T_L=0.09$  (Period-1)

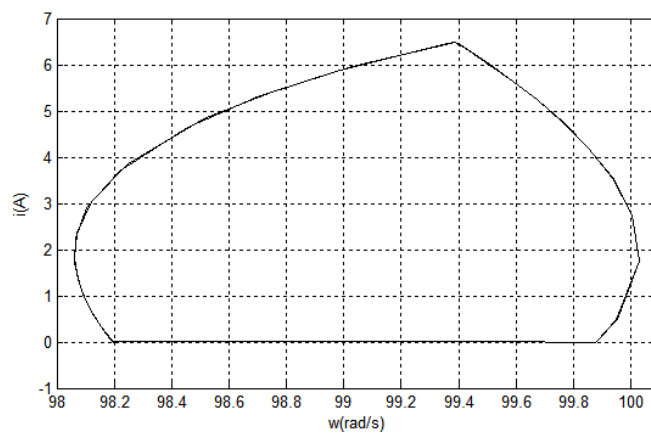


Figure 6.20: Phase portrait of motor speed and armature current at  $T_L=0.09$

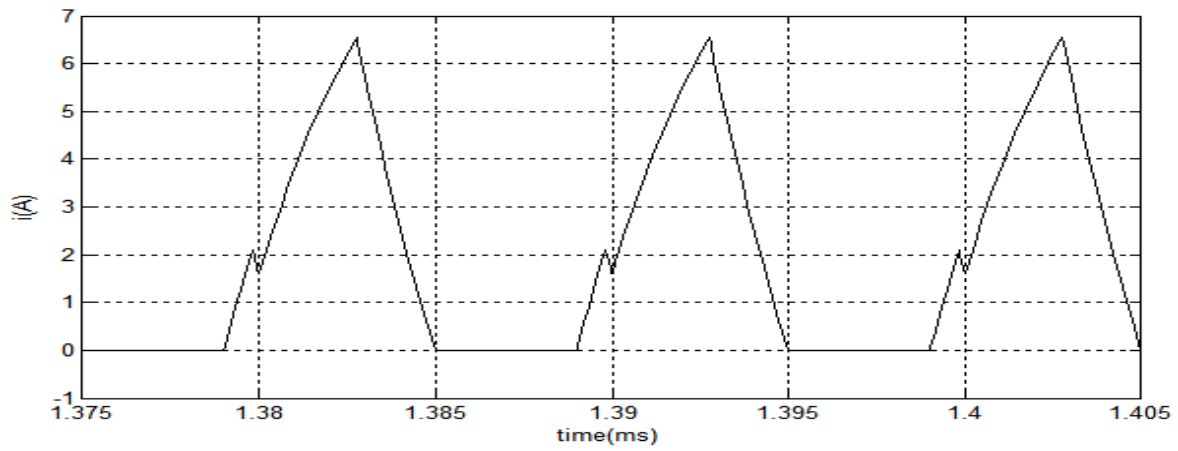


Figure 6.21: Time series plot of armature current at  $T_L = 0.10$  (Period-2)

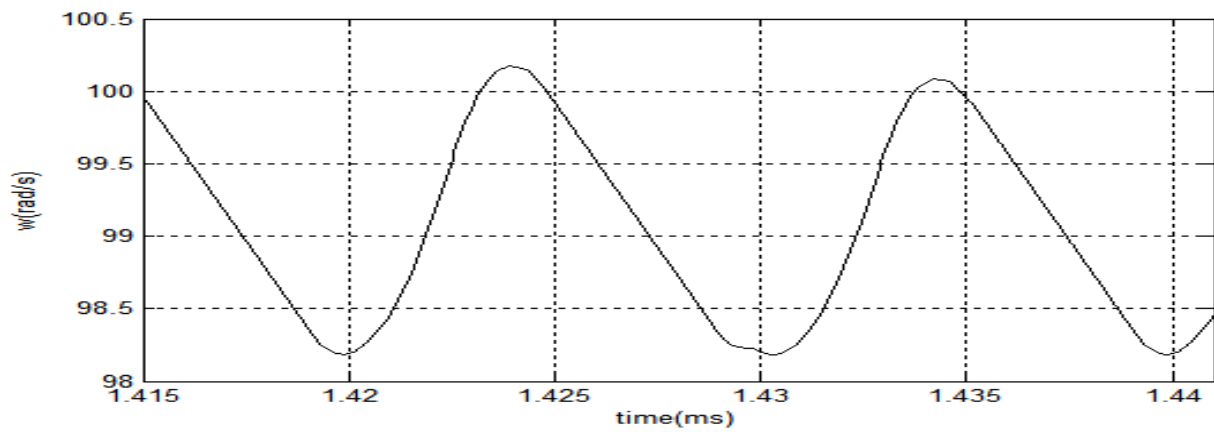


Figure 6.22: Time series plot of motor speed at  $T_L = 0.10$  (Period-2)

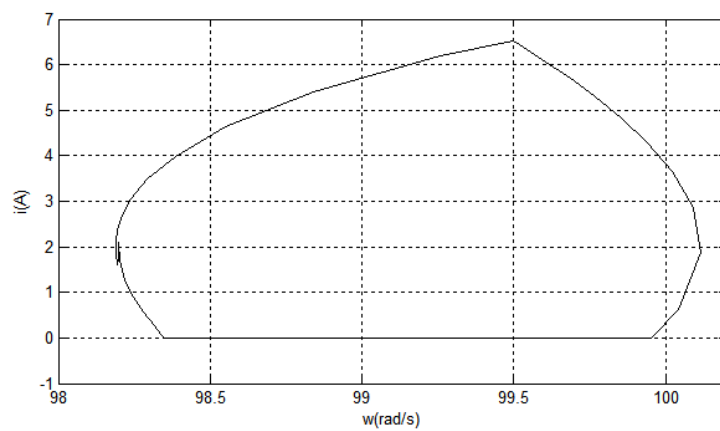


Figure 6.23: Phase portrait of motor speed and armature current  $T_L = 0.10$ (Period-2)



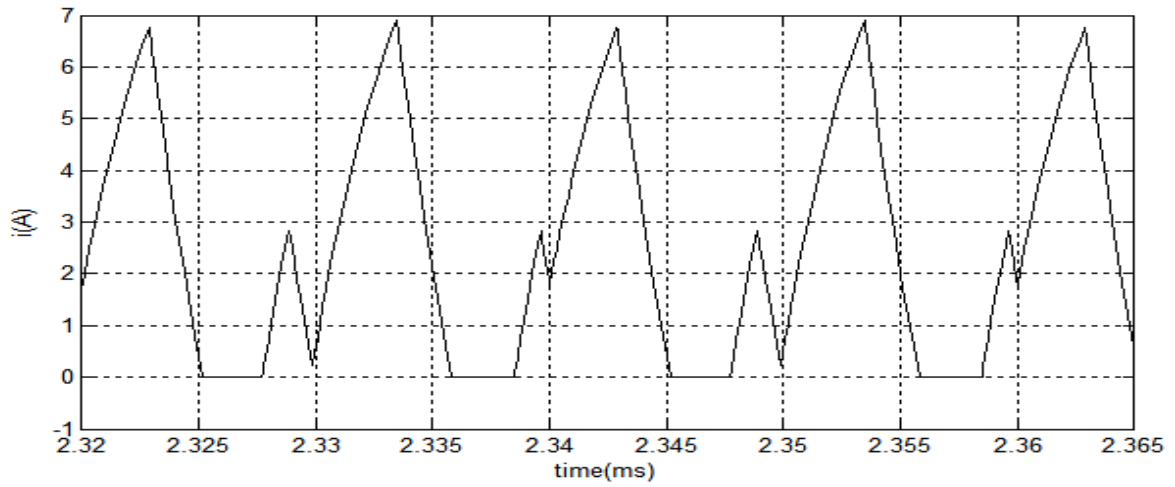


Figure 6.24: Time series plot of armature current at  $T_L = 0.12$

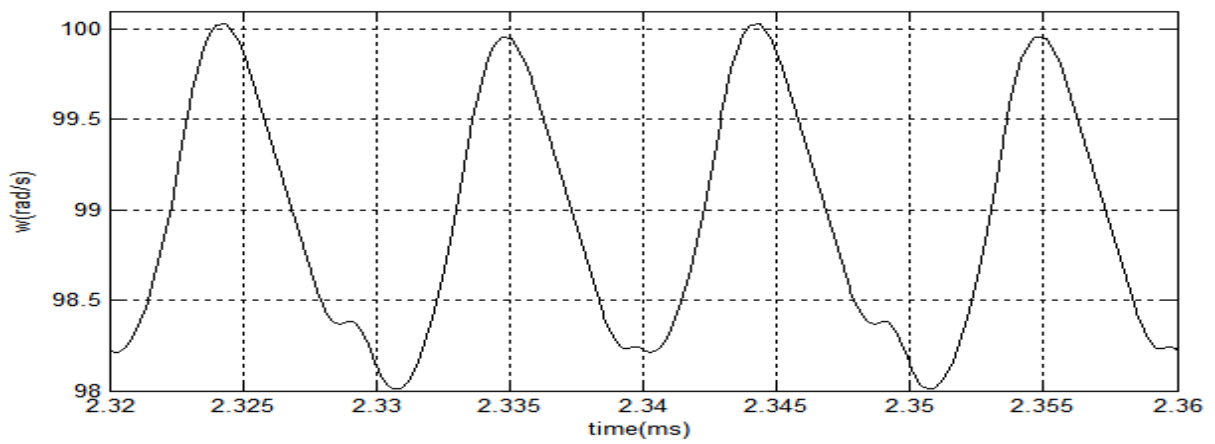


Figure 6.25: Time series plot of motor speed at  $T_L = 0.12$

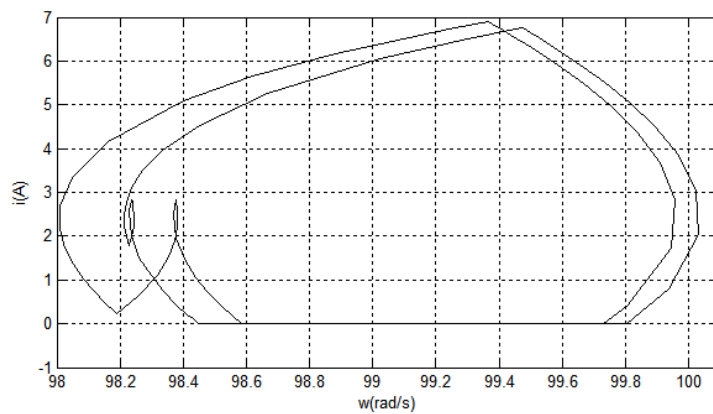


Figure 6.26: Phase portrait of motor speed and armature current  $T_L = 0.12$

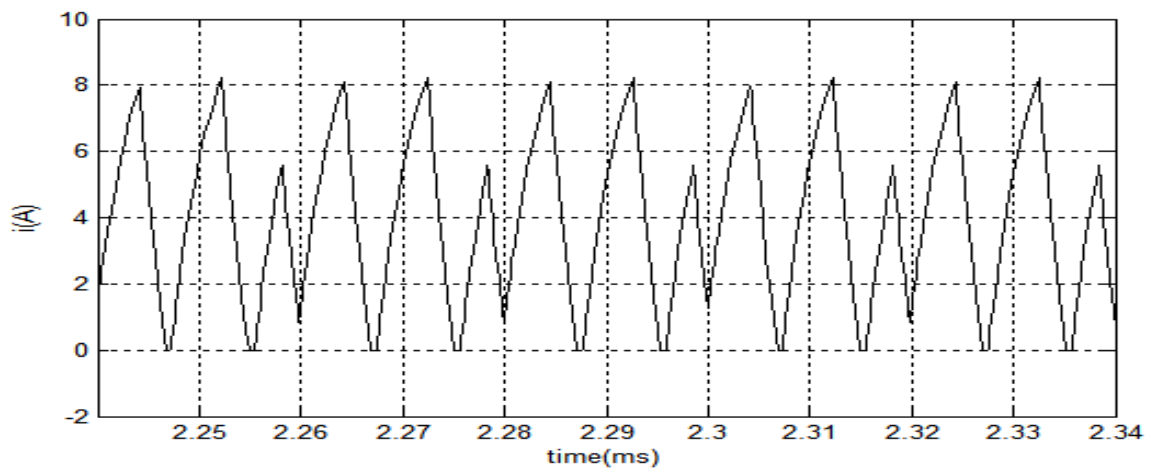


Figure 6.27: Time series plot of armature current at  $T_L = 0.20$

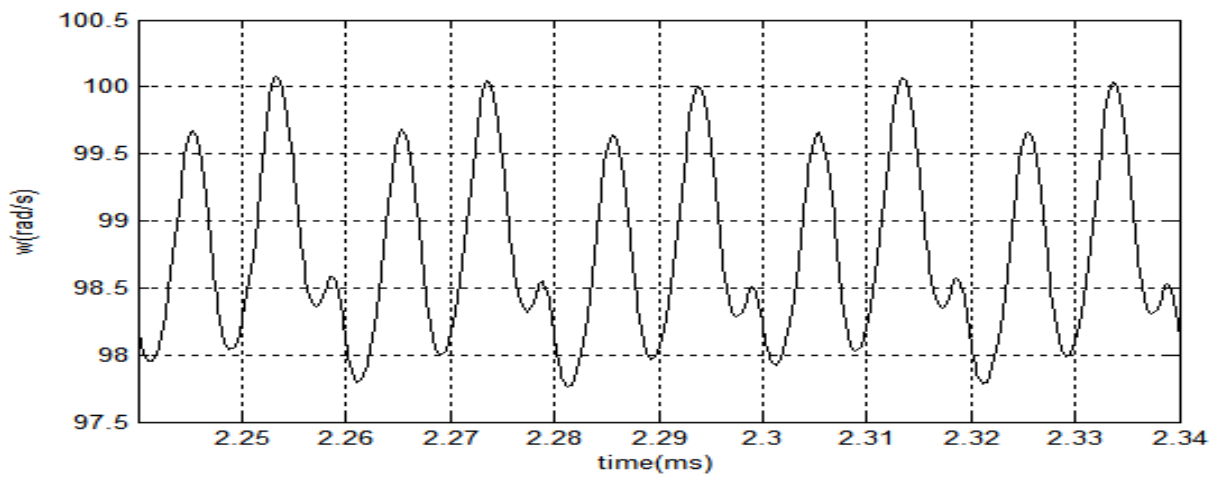


Figure 6.28: Time series plot of motor speed at  $T_L = 0.20$

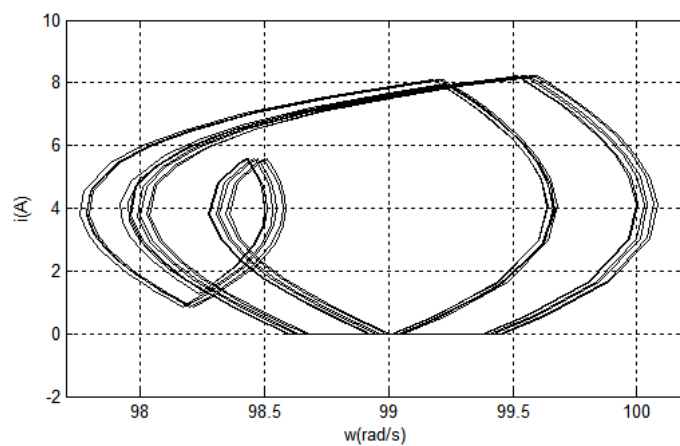


Figure 6.29: Phase portrait of motor speed and armature current at  $T_L = 0.20$

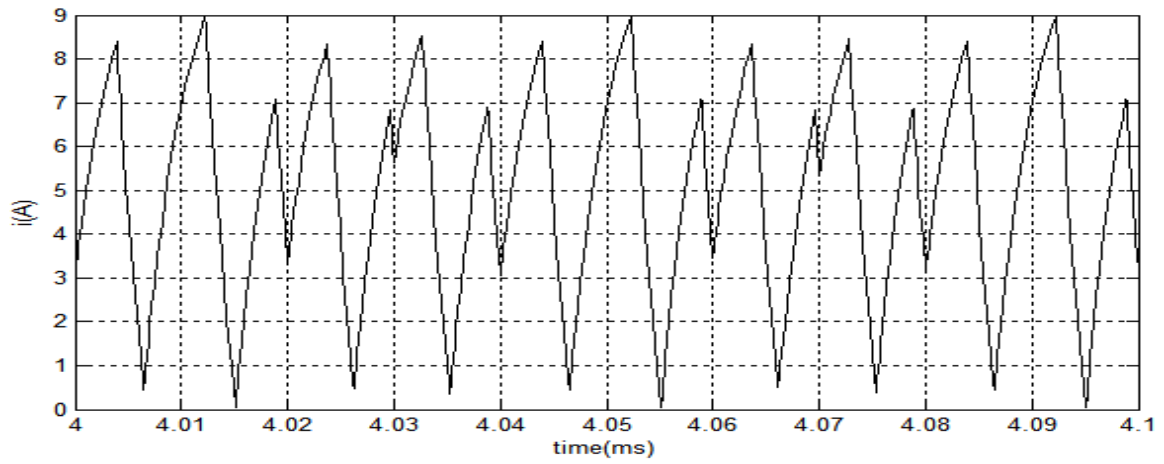


Figure 6.30: Time series plot of armature current at  $T_L = 0.25$

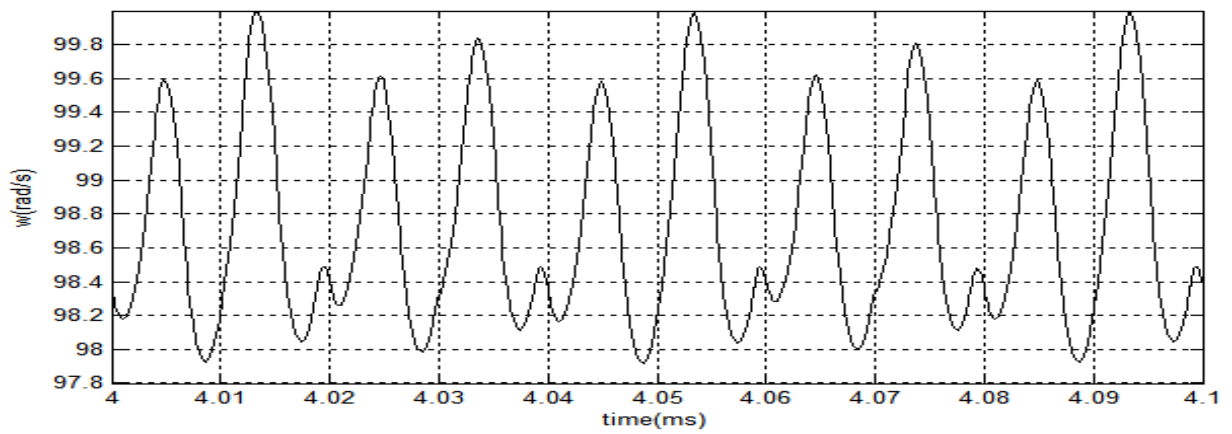


Figure 6.31: Time series plot of motor speed at  $T_L = 0.25$

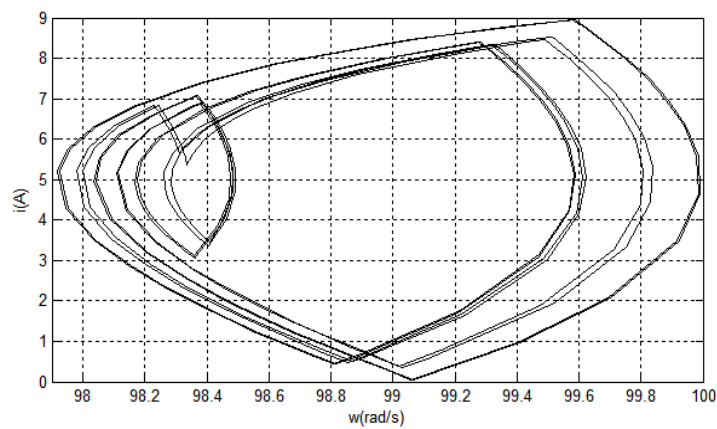


Figure 6.32: Phase portrait of motor speed and armature current  $T_L = 0.25$

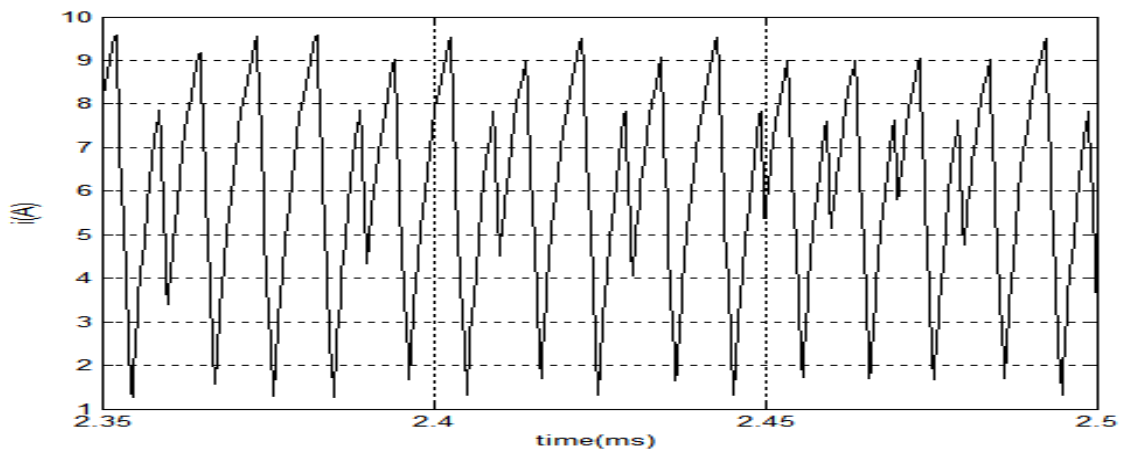


Figure 6.33: Chaotic time series plot of armature current at  $T_L = 0.30$

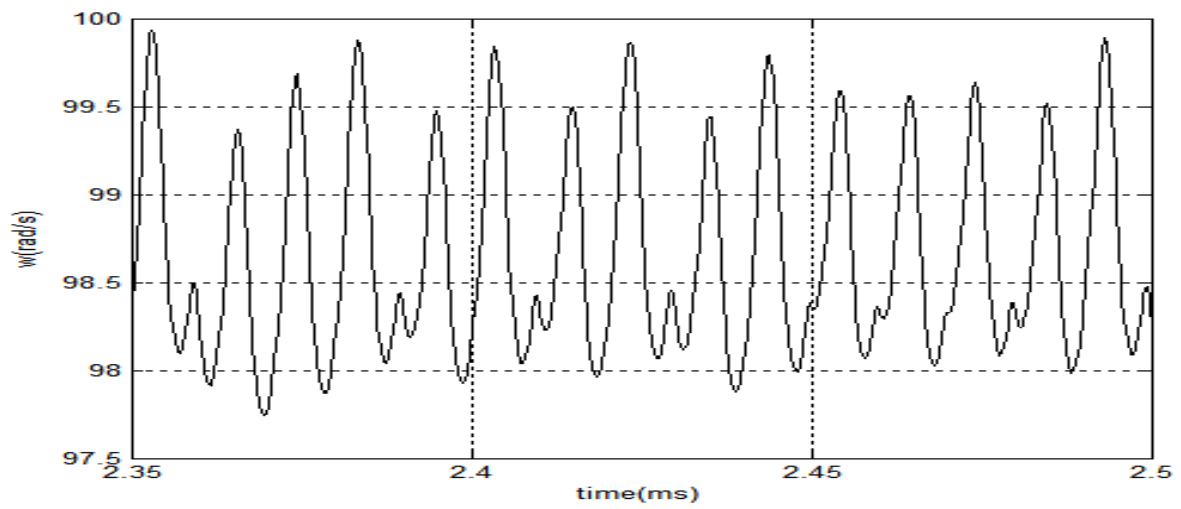


Figure 6.34 :Chaotic time series plot of motor speed at  $T_L = 0.30$

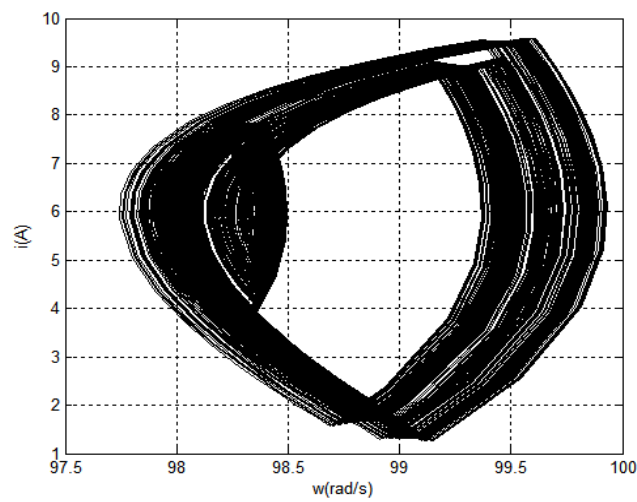


Figure 6.35: Phase portrait of motor speed and armature current (Chaotic trajectory)

#### 6.4 Observation of different Chaotic behavior of the DC Chopper Fed PMDC Drives for different switching frequencies ( $f_s$ )

The chaotic behavior of DC chopper fed PMDC drives is observed due to variation of the system parameters (like error amplifier gain( $g$ ) and Load Torque( $T_L$ )) but this behavior is slightly or considerably changed when switching frequency( $f_s$ ) is different.

The chaotic behavior is realized on PMDC motor drive at  $g=1.2$  and keeping Load Torque( $T_L$ )= $0.3\text{Nm}$  and switching frequency( $f_s$ )= $100\text{Hz}$ . Now if  $g$  and Load Torque( $T_L$ ) be the same and switching frequency( $f_s$ ) is varied then the behavior of that particular drives is changed.

Table 6.2: Condition of system at different switching frequency( $f_s$ )

Switching frequency( $f_s$ )	Condition
100Hz	Chaotic
150Hz	Chaotic
200Hz	Chaotic
250Hz	Period-2
300Hz	Period-2
350Hz	Period-2
400Hz	Period-1
450Hz	Period-2
500Hz	Period-1

It is clearly observed from the above figure that when the switching frequency( $f_s$ ) is varied the dynamic behavior the dc drive is changed. Chaotic behavior is observed from switching frequency( $f_s$ ) 100Hz to 200Hz (figure 6.36-6.38). Further variation of switching frequency( $f_s$ ) from 250Hz to 350Hz (figure 6.39-6.41) and 450Hz (figure 6.43) leads to period doubling.

The nominal orbit or Period-1 is observed at switching frequency( $f_s$ ) 400Hz (figure 6.42) and 500Hz (figure 6.44).

Table 6.3: Occurrence of Chaos at different switching frequency( $f_s$ ) and error amplifier gain( $g$ )

Switching frequency( $f_s$ )	Error amplifier gain( $g$ )
100Hz	1.2
150Hz	1.2
200 Hz	1.2
250 Hz	1.5
300 Hz	1.6
350 Hz	2.1
400 Hz	2.8
450 Hz	3.2
500 Hz	4.1

The Chaotic boundary is calculated for different switching frequency( $f_s$ ) using the table no.6.3. The chaotic and Non-Chaotic region is separated by the boundary in figure.6.45.

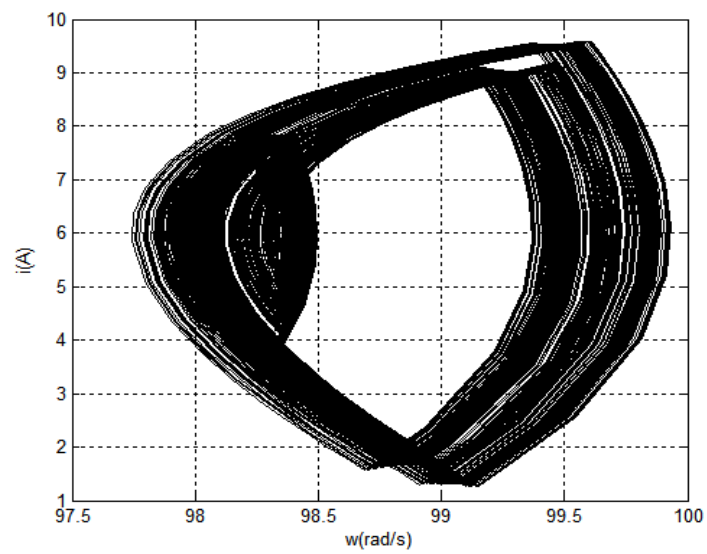


Figure 6.36: Phase portrait of motor speed and armature current (Chaotic trajectory) at  $f_s=100\text{Hz}$

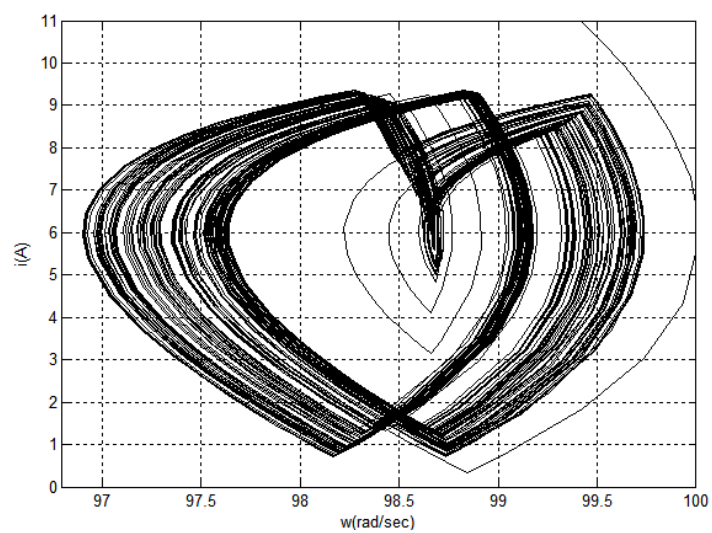


Figure 6.37: Phase portrait of motor speed and armature current (Chaotic trajectory) at  $f_s=150\text{Hz}$

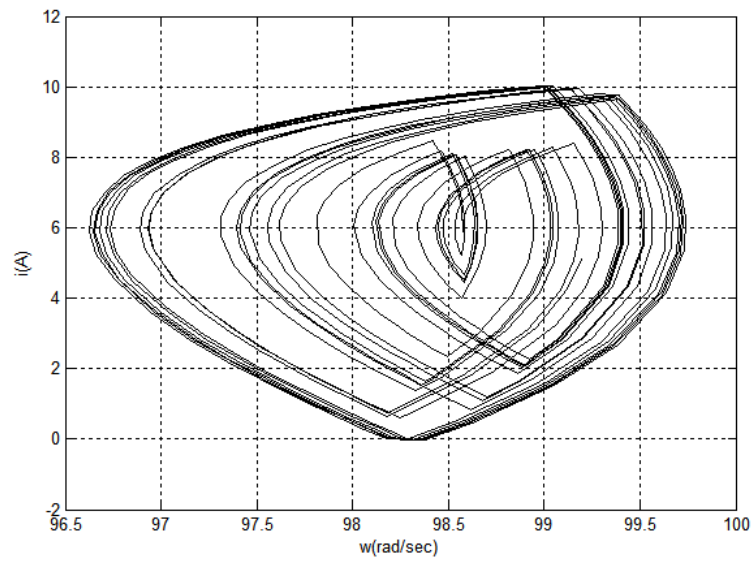


Figure 6.38: Phase portrait of motor speed and armature current (Chaotic trajectory) at  $f_s=200\text{Hz}$

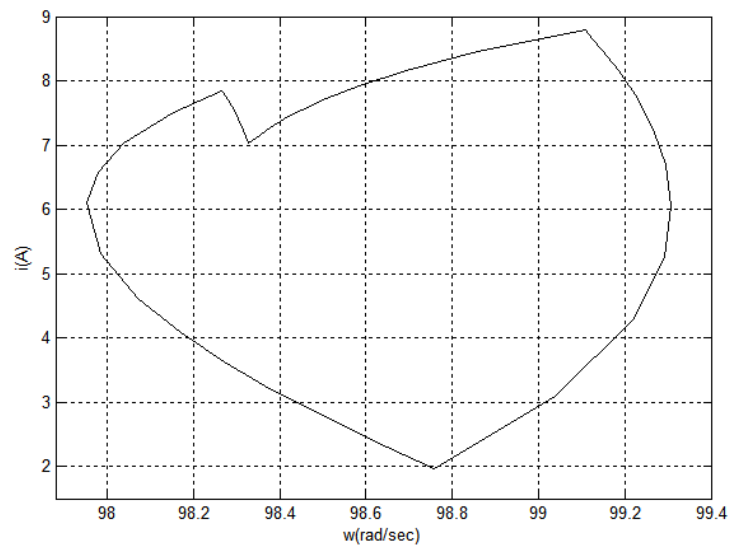


Figure 6.39: Phase portrait of motor speed and armature current (period-2) at  $f_s=250\text{Hz}$



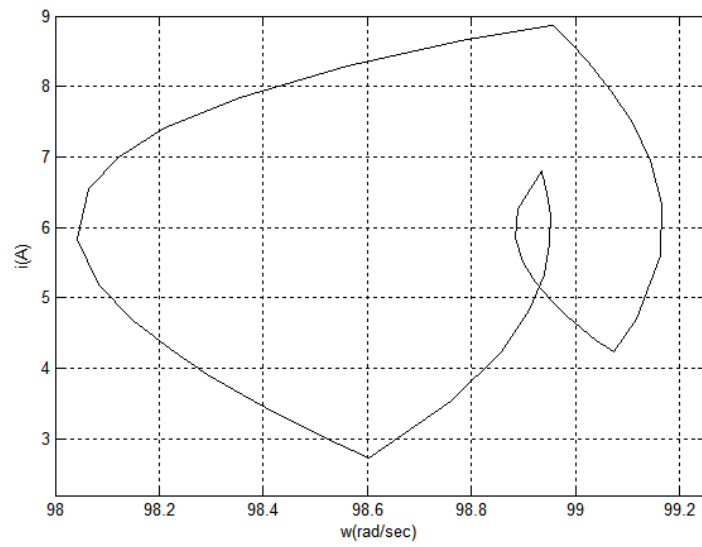


Figure 6.40: Phase portrait of motor speed and armature current (period-2) at  $f_s=300\text{Hz}$

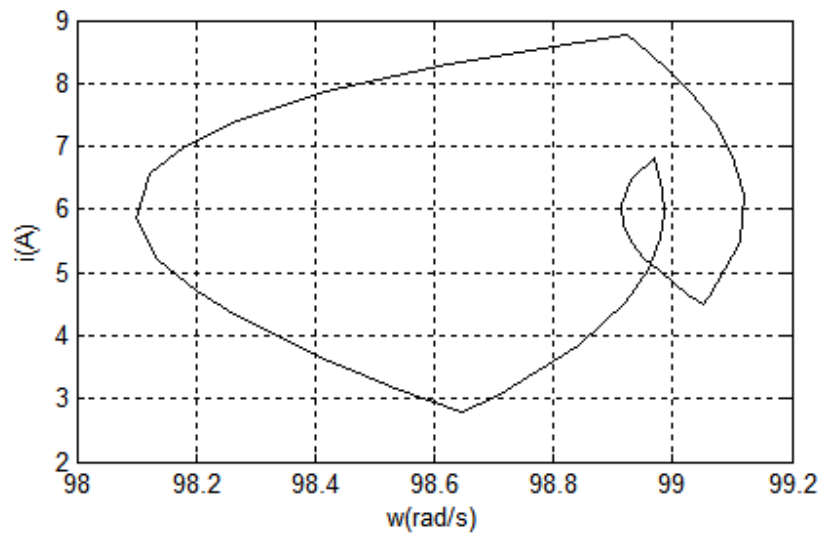


Figure 6. 41: Phase portrait of motor speed and armature current (period-2) at  $f_s=350\text{Hz}$

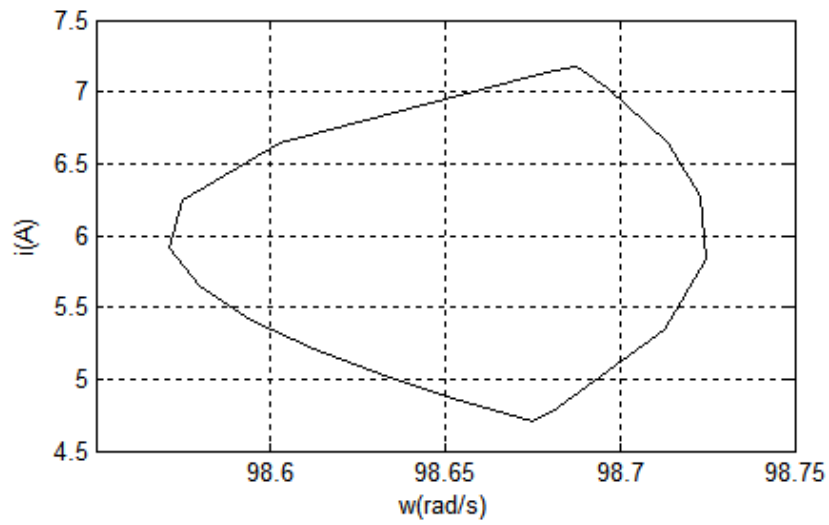


Figure 6.42: Phase portrait of motor speed and armature current (period-2) at  $f_s=400\text{Hz}$

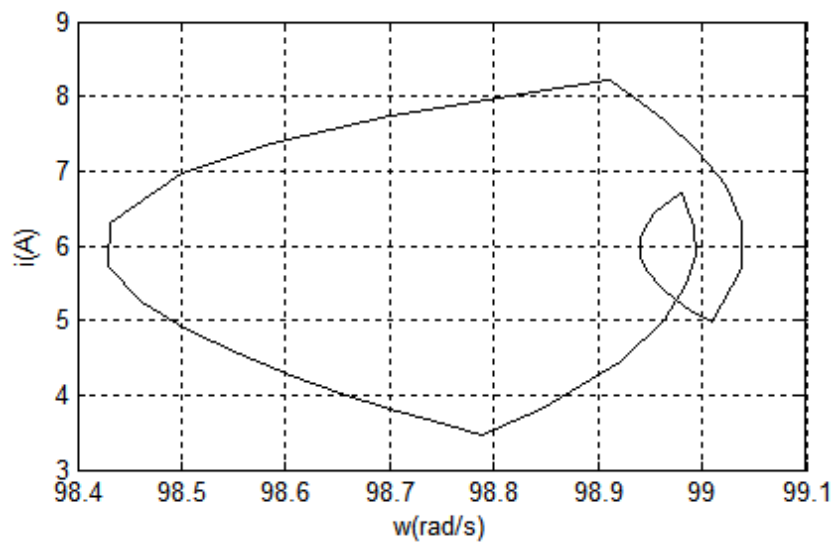


Figure 6.43: Phase portrait of motor speed and armature current (period-2) at  $f_s=450\text{Hz}$

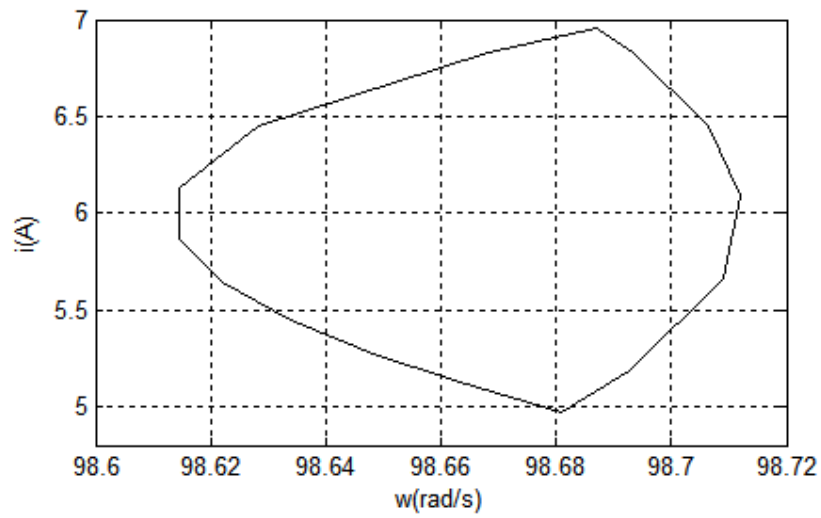


Figure 6.44: Phase portrait of motor speed and armature current (period-1) at  $f_s=500\text{Hz}$

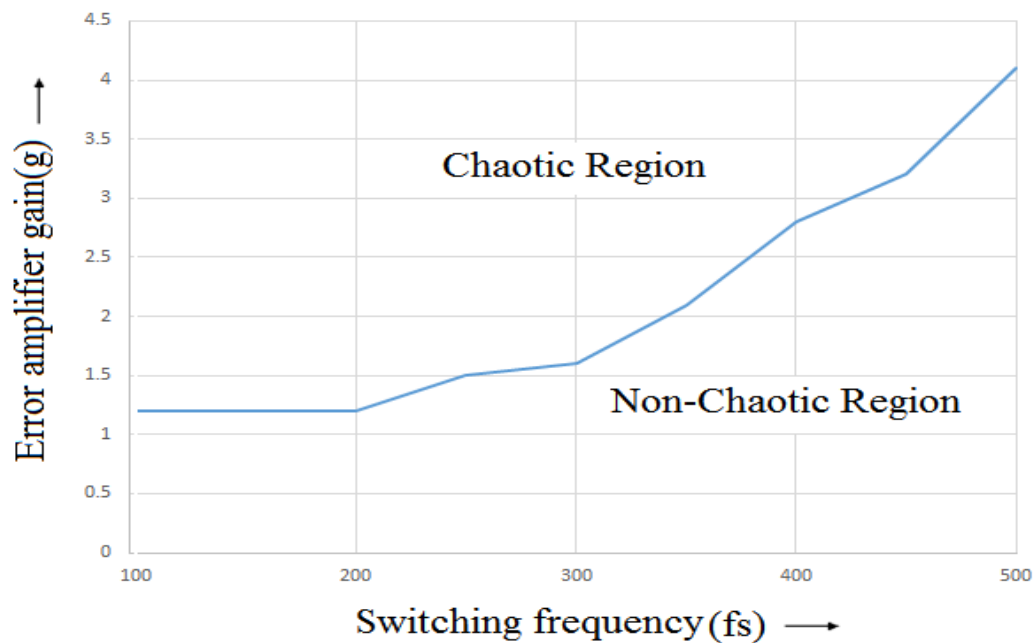


Figure 6.45: Error amplifier gain( $g$ ) against Switching frequency( $f_s$ ) to identify Chaotic and Non-Chaotic region

From the above figure 6.45, it is said that if the error amplifier gain( $g$ ) be  $y$  and switching frequency( $f_s$ ) be  $x$  then they are related to each other in a simple relationship given below

*Condition-1:*

$$\text{If } y \geq 4e-14x^6 - 6e-11x^5 + 4e-08x^4 - 2e-05x^3 + 0.0029x^2 - 0.2689x + 10.967$$

Then the system turns out to be a Chaotic one.

*Condition-2:*

$$\text{If } y < 4e-14x^6 - 6e-11x^5 + 4e-08x^4 - 2e-05x^3 + 0.0029x^2 - 0.2689x + 10.967$$

Then the system becomes non-Chaotic .

### **6.5. Observation of switching signal (PWM) during route to Chaos:**

The DC motor drives is an inherently nonlinear system. But the nonlinear behavior like Chaos is found when simple closed loop control scheme is applied with error amplifier gain( $g$ ). It is realized that the Chaotic behavior occurs in the system when the switching signal (PWM) is changed as a variation of amplifier gain ( $g$ ).

In this method, the output speed  $\omega(t)$  in the form of an analogue voltage from a tacho-generator is compared with the reference speed  $\omega_{ref}$  to obtain the speed error signal  $e(t) = \omega(t) - \omega_{ref}$ . The speed error is then multiplied by the gain of the operational amplifier to obtain the control signal  $V_c(t) = g \times (\omega(t) - \omega_{ref})$ . The PWM signal is obtained by comparing a high frequency saw tooth signal  $V_r(t)$  with the control signal.

When the saw tooth signal  $V_r(t)$  is greater than the control signal  $V_c(t)$ , the PWM waveform goes high, the switch closes and the diode is reverse biased. But when the saw tooth signal  $V_r(t)$  is lower than the control signal  $V_c(t)$ , the PWM signal goes low, the switch opens and the diode is forward biased. The PWM duty cycle ( $d$ ) is varied continuously to ensure that the actual speed  $\omega(t)$  tracks the reference speed  $\omega_{ref}$ .

The switching signal (PWM) is formed through the interaction of the control signal ( $V_c$ ) and ramp signal ( $V_r$ ). In figure.6.46 when the proportional gain ( $g$ ) parameter set to 0.2, the duty cycle of control signal (PWM) looks similar and repetitive through the time period. At this condition period-1 trajectory of armature current  $i_a(t)$  and motor speed  $\omega(t)$  is observed.

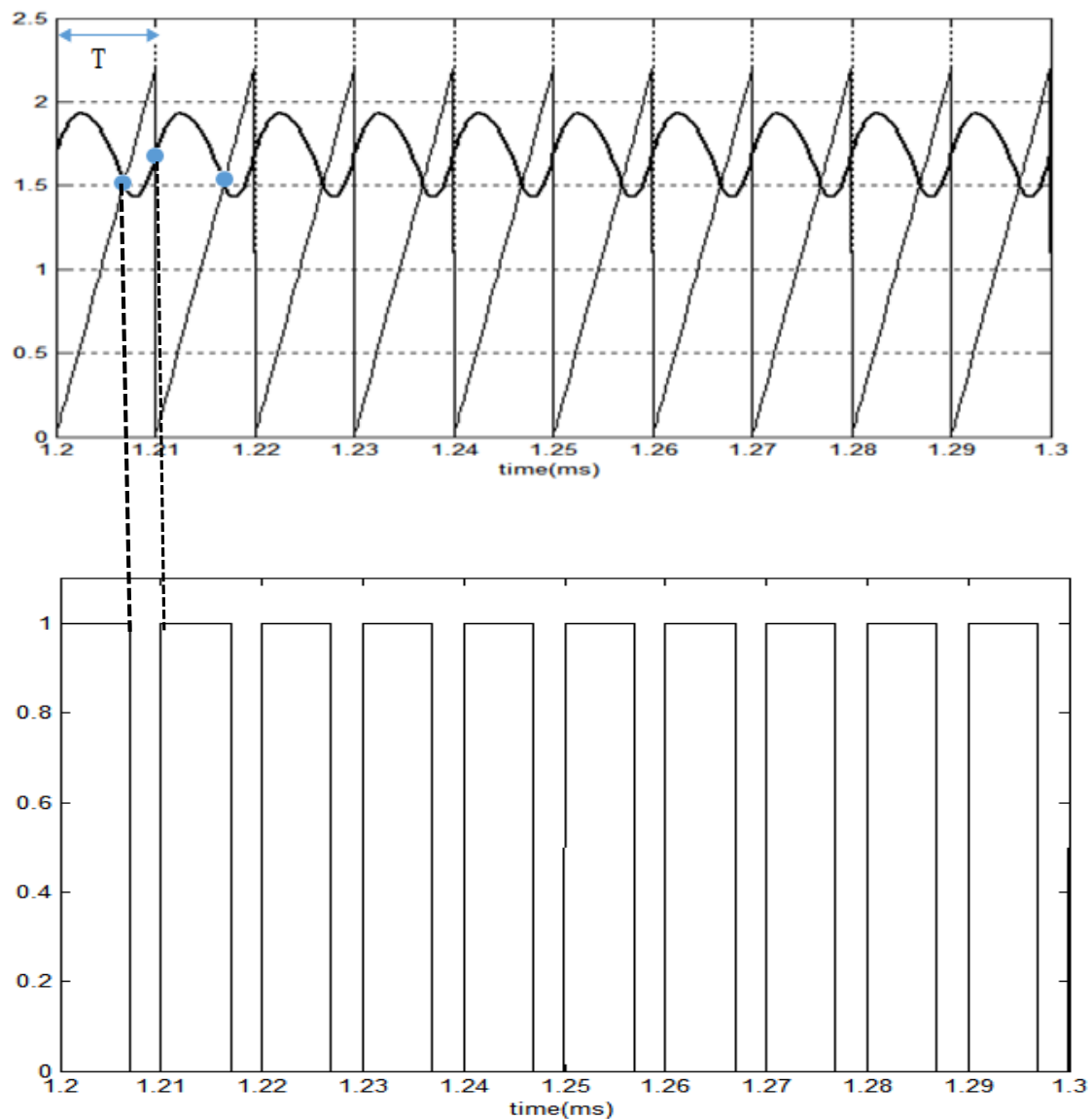


Figure 6.46. Interaction of the control and ramp signal at 100 Hz,  $T_L=0.3\text{Nm}$ ,  $g=0.2$

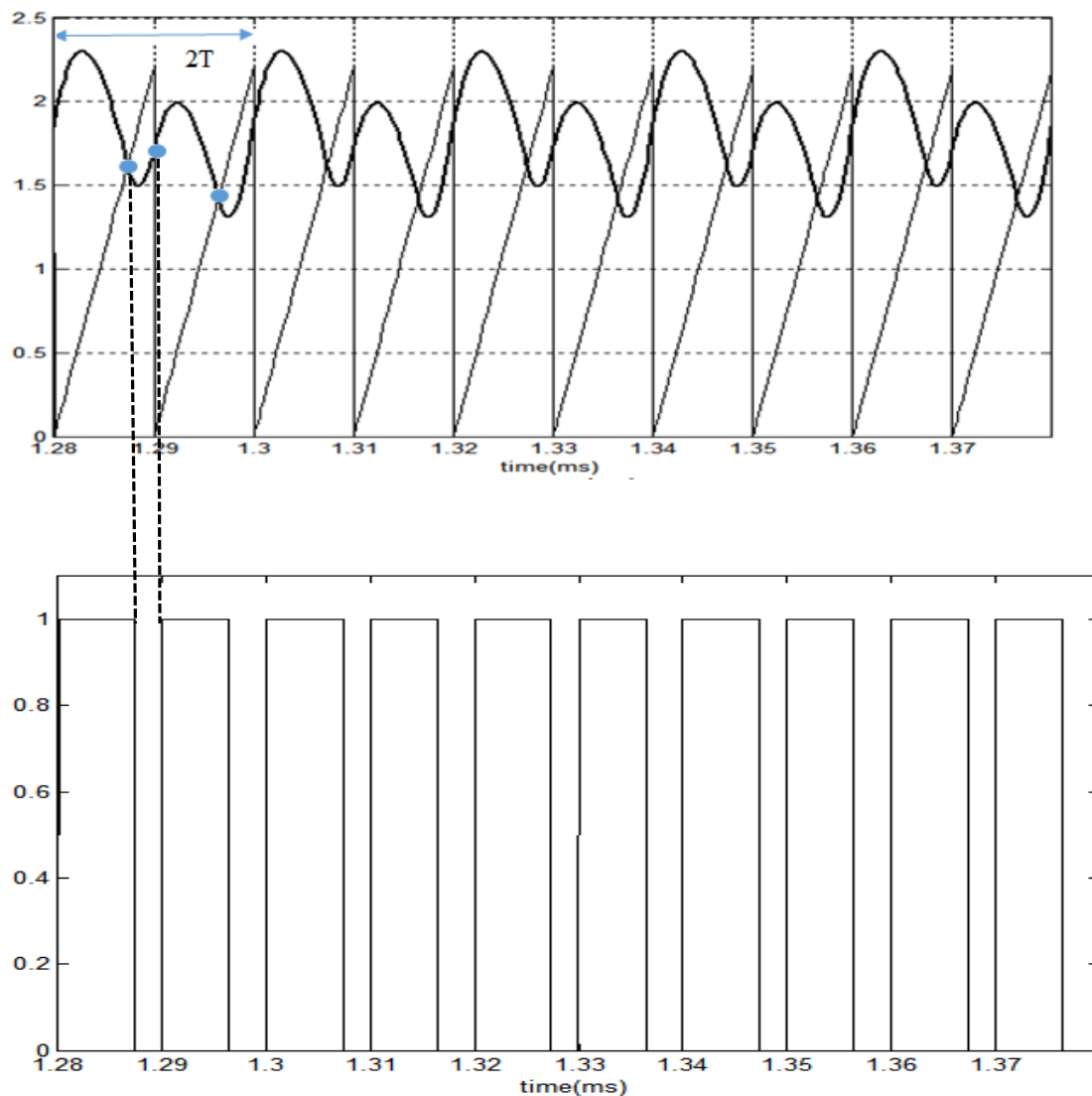


Figure 6.47. Interaction of the control and ramp signal at 100 Hz,  $T_L=0.3\text{Nm}$ ,  $g=0.3$

In figure.6.47 the interaction of the control signal ( $V_c$ ) and ramp signal ( $V_r$ ) crosses twice in one cycle but it repeats after two cycle of ramp signal ( $V_r$ ). As a result the period-2 trajectory of armature current  $i_a(t)$  and motor speed  $\omega(t)$  is observed at proportional gain ( $g$ ) parameter become 0.3

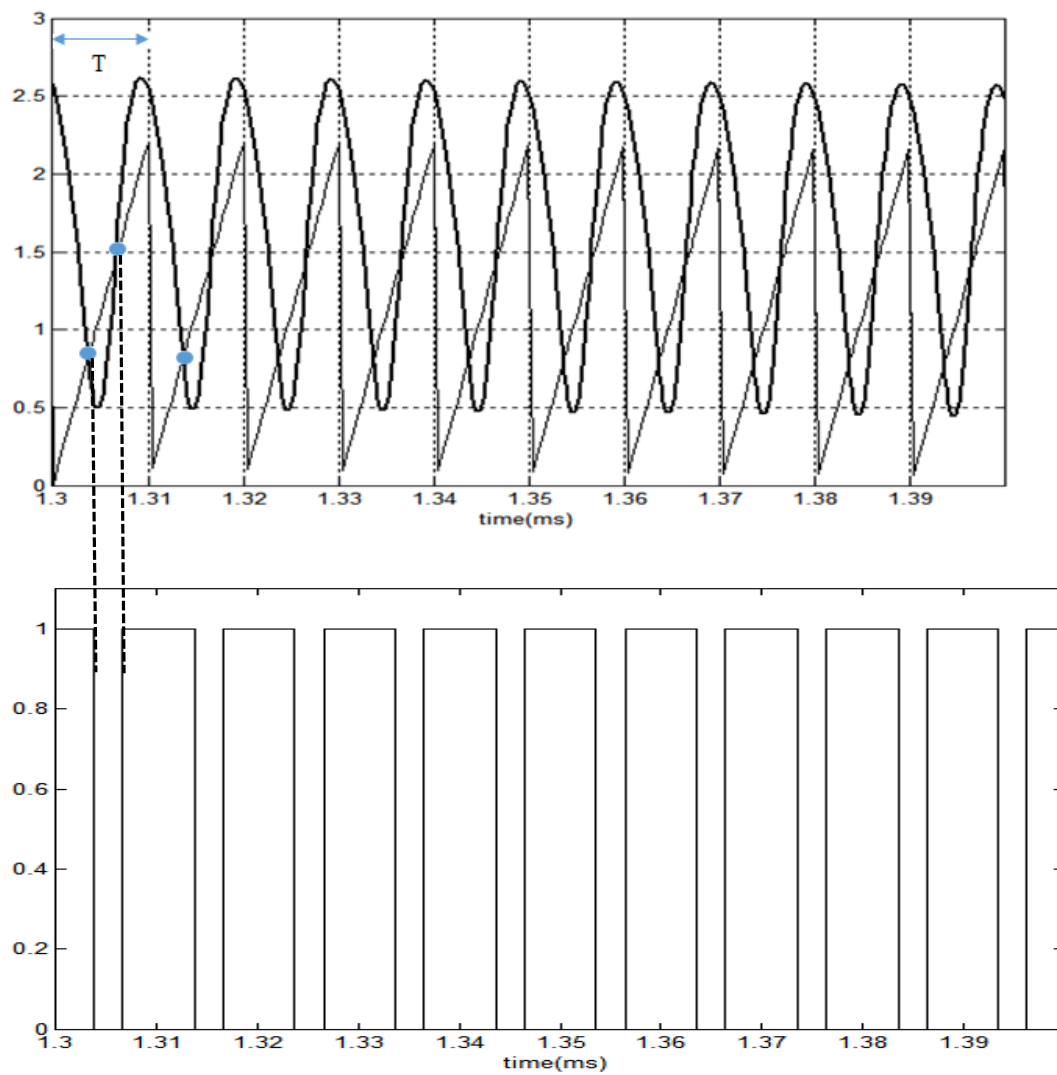


Figure 6.48. Interaction of the control and ramp signal at 100 Hz,  $T_L=0.3Nm$ ,  $g=0.9$

The interaction of the control signal ( $V_c$ ) and ramp signal ( $V_r$ ) crosses twice in one cycle and it repeats after a cycle of ramp signal ( $V_r$ ) in figure 6.48. As a result the period-1 trajectory of armature current  $i_a(t)$  and motor speed  $\omega(t)$  is observed at proportional gain ( $g$ ) parameter become 0.9

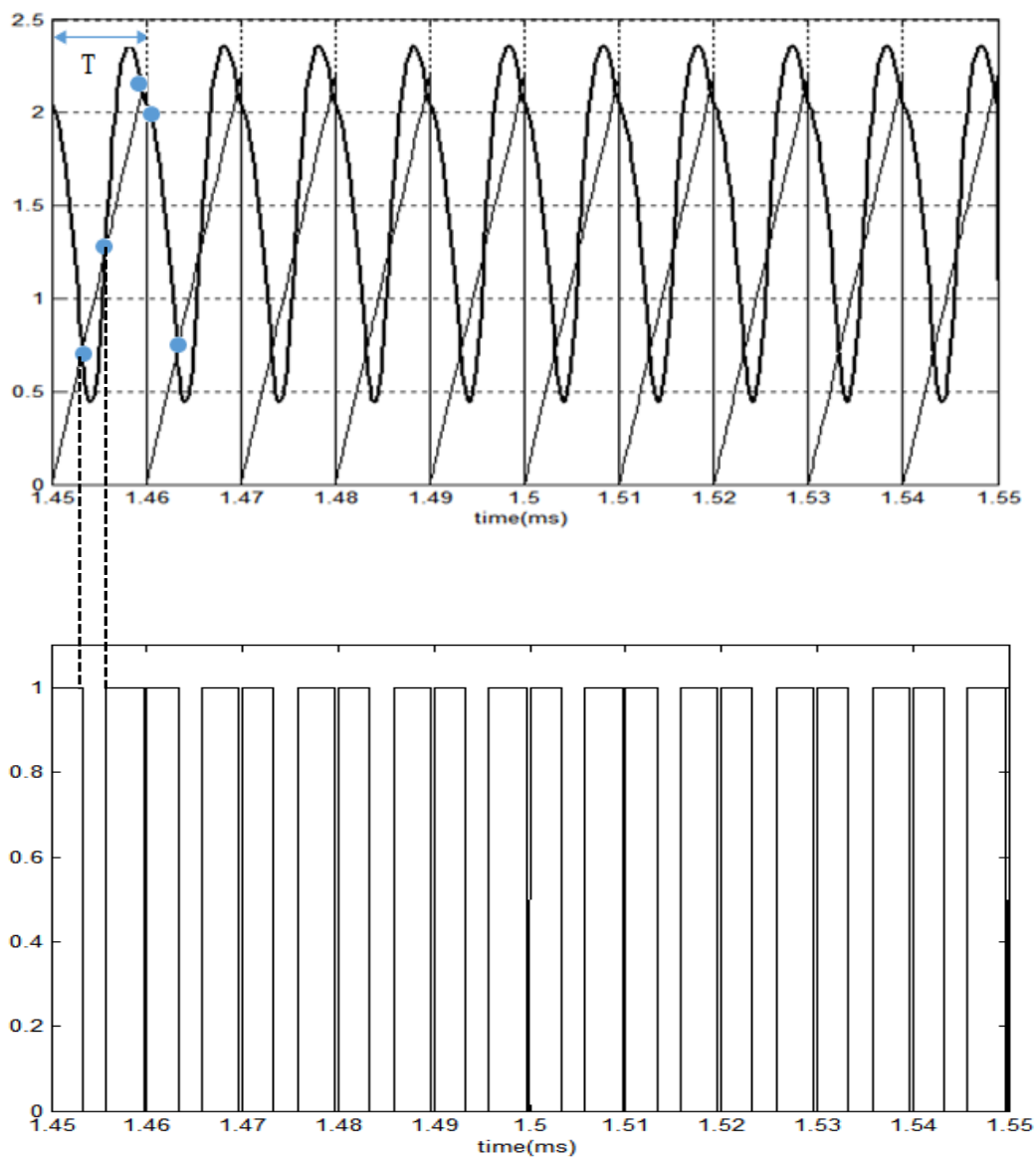


Figure 6.49. Interaction of the control and ramp signal at 100 Hz,  $T_L=0.3\text{Nm}$ ,  $g=1.0$

The interaction of the control signal ( $V_c$ ) and ramp signal ( $V_r$ ) crosses thrice in one cycle and it repeats after a cycle of ramp signal ( $V_r$ ) in figure 6.48. As a result the period-1 trajectory of armature current  $i_a(t)$  and motor speed  $\omega(t)$  is observed at proportional gain ( $g$ ) parameter is 1.



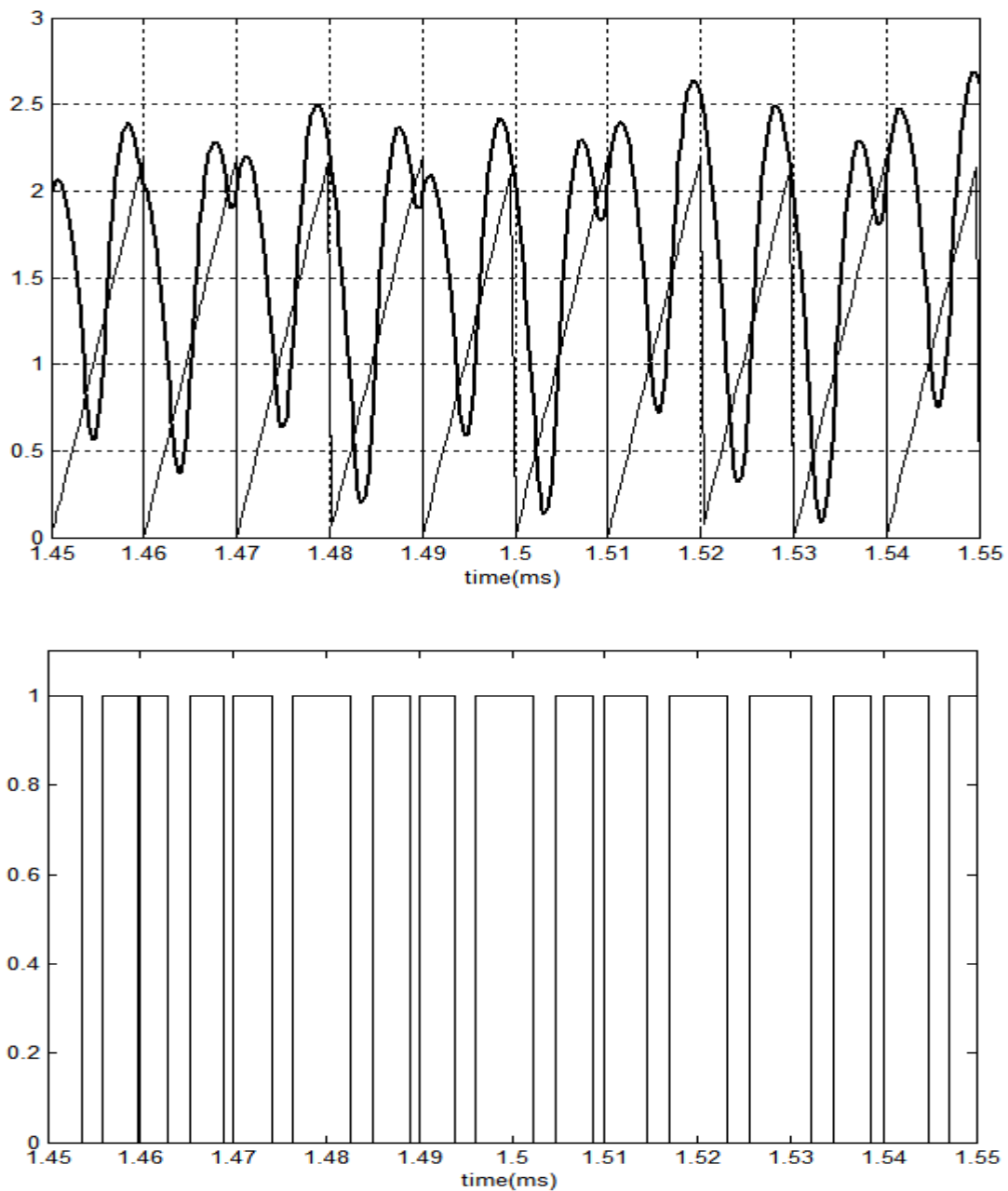


Figure 6.50. Control and ramp signal at 100 Hz,  $T_L=0.3\text{Nm}$ ,  $g=1.2$

The interaction of the control signal ( $V_c$ ) and ramp signal ( $V_r$ ) crosses differently for different cycle and it does not repeat after a cycle of ramp signal ( $V_r$ ) in figure 6.48. As a result the trajectory of armature current  $i_a(t)$  and motor speed  $\omega(t)$  becomes Chaotic, at proportional gain ( $g$ ) parameter is 1.2.

### 6.6. Special Observation on impact of Chaos in PMDC motor Drives:

It is realized that the average power and the standard deviation of the power wave become less when the system is in Chaotic zone.

So the Chaotic condition makes the fluctuation of average power consumption a lesser.

**Case -1:**  $f_s=100\text{Hz}$ , comparison between chaotic and non-chaotic power waveform

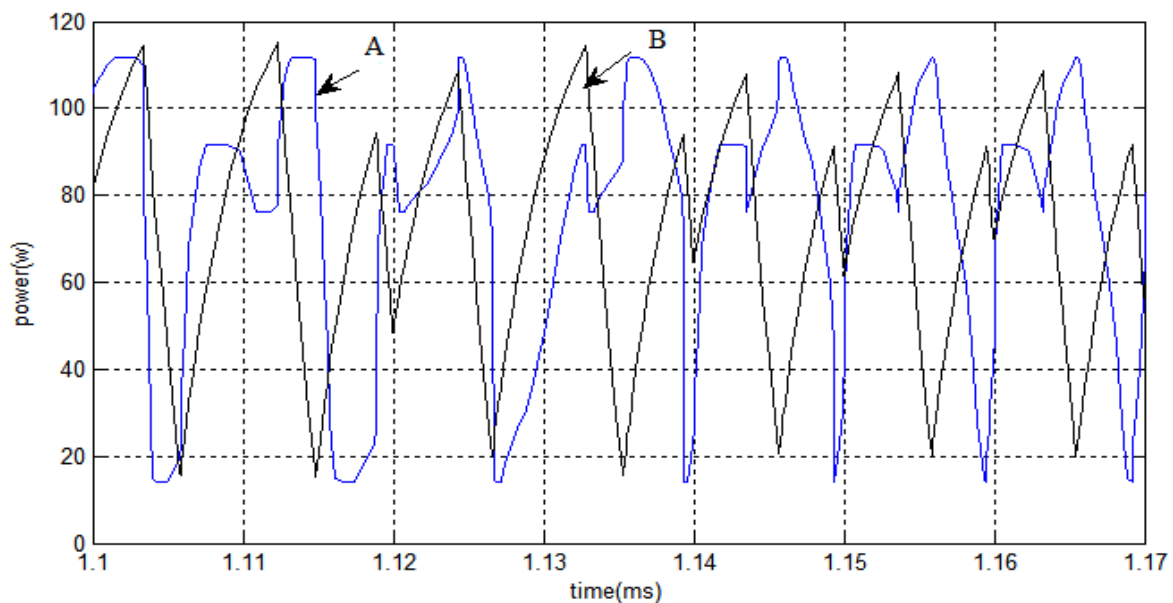


Figure 6.51: Non chaotic and chaotic power waveforms. Where A is chaotic wave and B is non-chaotic wave.

Average power at chaotic condition = 71.55887 W and Standard deviation = 29.5689 ( $g=1.2$ );

Average power at non-chaotic condition = 73.80809 W and Standard deviation = 30.73599 ( $g=1$ );

**Case -2:**  $f_s=150\text{Hz}$ , comparison between chaotic and non-chaotic power waveform

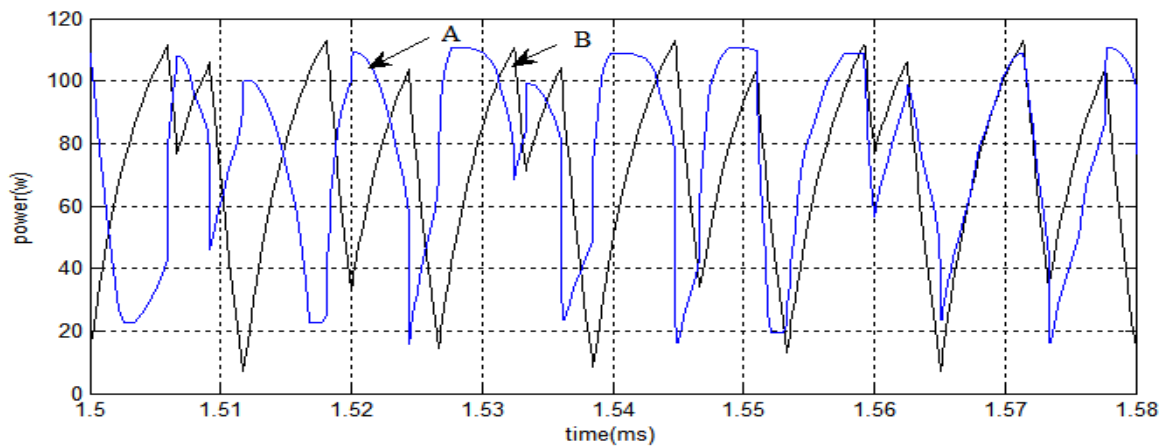


Figure 6.52: Non chaotic and chaotic power waveforms. Where A is chaotic wave and B is non-chaotic wave.

Average power at chaotic condition = 71.69843W and Standard deviation = 30.15689 ( $g=1.2$ );

Average power at non-chaotic condition = 73.64423W and Standard deviation = 32.31095 ( $g=1$ );

**Case-3:**  $f_s=200\text{Hz}$ , comparison between chaotic and non-chaotic power waveform

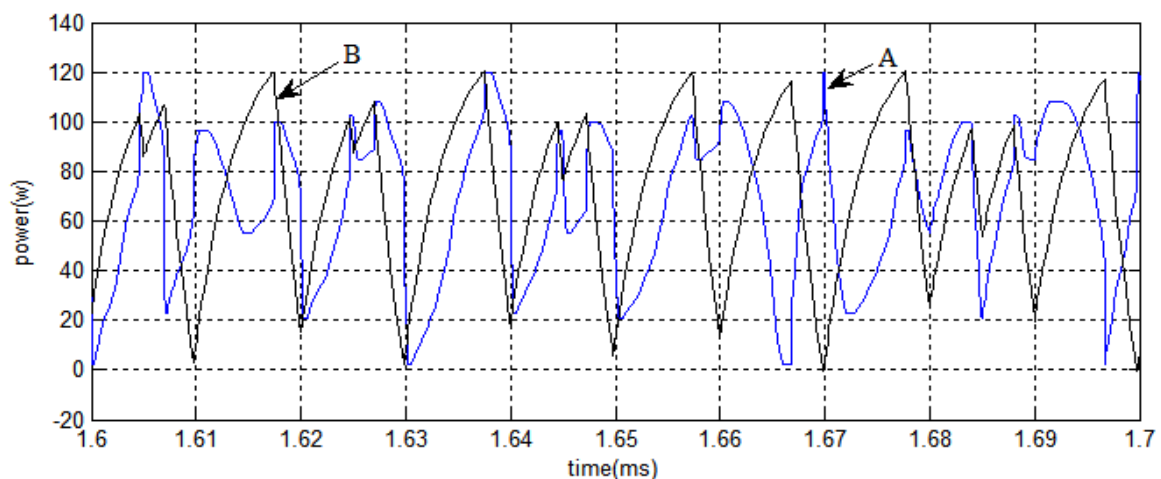


Figure 6.53: Non chaotic and chaotic power waveforms. Where A is chaotic wave and B is non-chaotic wave.

Average power at chaotic condition = 68.35 W and Standard deviation = 31.32491; ( $g=1.2$ )

Average power at non-chaotic condition = 73.56 W and Standard deviation = 29.2568; ( $g=1$ )

**Case-4:**  $f_s=250\text{Hz}$ , comparison between chaotic and non-chaotic power waveform

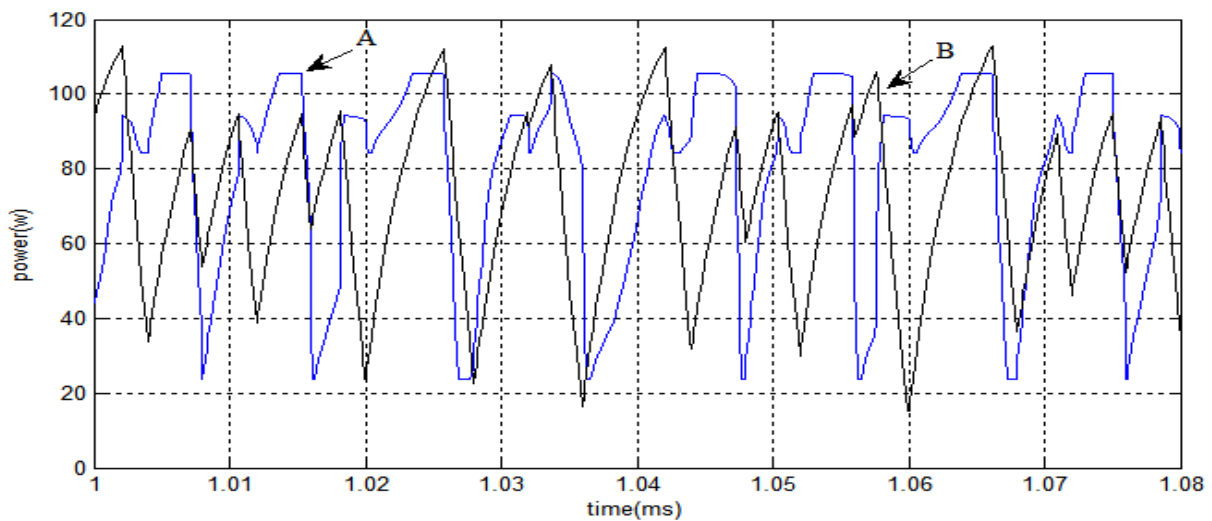


Figure 6.54: Non chaotic and chaotic power waveforms. Where A is chaotic wave and B is non-chaotic wave.

Average power at chaotic condition = 72.952 W and Standard deviation = 25.9128; ( $g=1.5$ );

Average power at non-chaotic condition = 78.77 W and Standard deviation = 28.1131; ( $g=1.2$ );

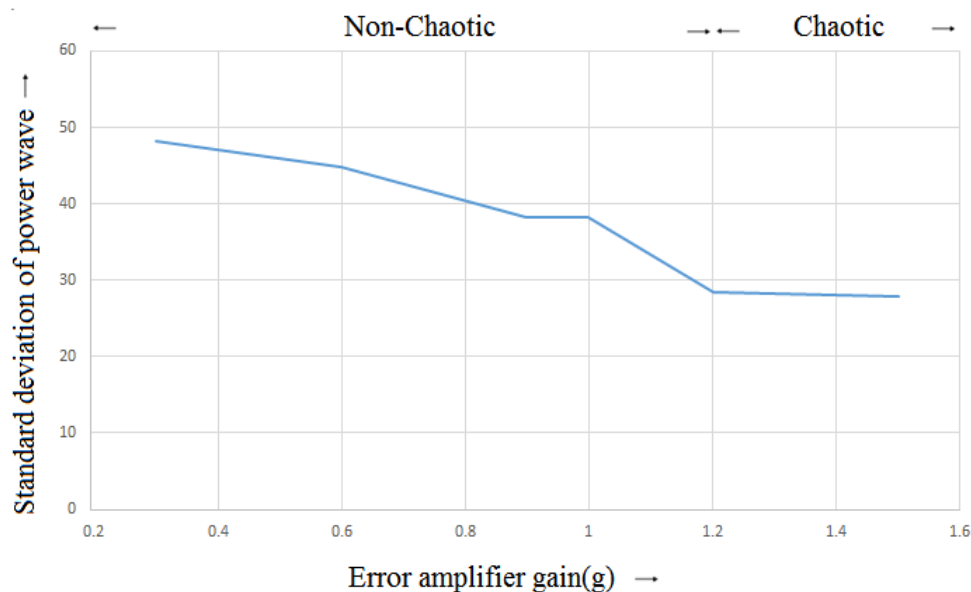


Figure 6.55: Standard deviation of power wave in Chaotic and non-Chaotic conditions

### 6.7 Summery:

In this chapter the nonlinear behavior (Chaos) of DC Chopper Fed PMDC Drives have been investigated with employing the Proportional Controller. Time series (Observe the state variables) and Phase portraits method are used to detect the chaos. The drive exhibits a period doubling route to chaos for variation of error amplifier gain( $g$ ) at constant Load torque ( $T_L$ ) and switching frequency ( $f_s$ ). It is also observed different Chaotic behavior of the DC Chopper Fed PMDC Drives for variation of Load torque ( $T_L$ ) at constant error amplifier gain( $g$ ) and switching frequency ( $f_s$ ). The dynamic behavior of the PMDC Drives is also changed with the variation of switching frequency( $f_s$ ). The chaotic and non-chaotic region is separated by the boundary which is obtained at error amplifier gain( $g$ ) against switching frequency( $f_s$ ). The interaction of the control signal( $V_c$ ) and ramp signal( $V_r$ ) exhibit different switching signal (PWM) during route to Chaos. A special observation is realized that the average value and the standard deviation of the power wave fluctuations become less when the system is in Chaotic zone. This phenomenon has been investigated at different switching frequency( $f_s$ ) to justify the realization.

# Chapter 7

## CONCLUSION AND FUTURE SCOPE OF WORK

## CONCLUSION AND FUTURE SCOPE OF WORK

### 7.1 Conclusion

In this thesis, the nonlinear phenomena in some commonly used electrical drives like the PMDC drives are analyzed. The period-1 orbit is changes as some system parameters (error amplifier gain( $g$ ), Load torque( $T_L$ ) and switching frequency( $f_s$ )) are varied. Further variation of the system parameters leads to a Chaotic attractor. Time series (Observe the state variables) and Phase portraits methods are used to detect the Chaos in this study. In this work the nonlinear analysis of a PMDC Motor Drives system is performed with the background mathematical assistance and MATLAB.

In this thesis the nonlinear behavior (Chaos) of DC Chopper Fed PMDC Drives have been investigated with employing the Proportional Controller. The drive exhibits a period doubling route to chaos for variation of error amplifier gain( $g$ ) at constant Load torque ( $T_L$ ) and switching frequency ( $f_s$ ). It is also observed different Chaotic behavior of the DC Chopper Fed PMDC Drives for variation of Load torque ( $T_L$ ) at constant error amplifier gain( $g$ ) and switching frequency ( $f_s$ ).

This thesis represents the first observation on the impact of switching frequency( $f_s$ ) in the nonlinear analysis of electrical drive systems. It is reported that the dynamic behavior of the PMDC Drives is also changed with the variation of switching frequency( $f_s$ ). The chaotic and non-chaotic region is separated by the boundary which is obtained at error amplifier gain( $g$ ) against switching frequency( $f_s$ ). The interaction of the control signal( $V_c$ ) and ramp signal( $V_r$ ) exhibit different switching signal (PWM) during route to Chaos.

A special observation is realized that the average value and the standard deviation of the power wave fluctuations become less when the system is in Chaotic zone. This phenomenon has been investigated at different switching frequency( $f_s$ ) to justify the realization. This realization can make Chaos a worthy phenomenon in a PMDC Motor Drives system.

## 7.2 Future scope on this Work:

In this thesis, the nonlinear phenomena namely Chaos is observed and analyzed in a PMDC Motor Drives using MATLAB simulation software. Future scope in this area may include:

The experiment has been focused on a particular PMDC Motor drive system with only a speed feedback control loop but the proposed approach and derivation can readily be applied or extended to other DC and AC drive systems with more complicated and advanced control schemes that is using in a specific industrial and research purpose.

A thorough knowledge in setting the operational parameter limits of the drives is necessary for desired operation. For instance, at some range of the system parameters, the steady state behavior will be the nominal Period-1 orbit, while at some other ranges the steady state trajectory will be either of quasi Periodic or chaotic. That's why to observe Chaos in an Electrical system is an interesting study for an electrical engineer.

Chaos plays a very important role in our everyday life and lots of studies have been done to realize and control of Chaos in a system. The normal belief is that to avoid Chaos is always beneficial for the system but it has been realized in this study through the simulation that the Chaos can be worthy for the PMDC Motor Drives system. Hence, the future work is to realize this through practical experiment.

The investigation of Chaos on fractional watt motor drive systems with this topology can be made an important impact. The application of the Chaos can be beneficial in complex systems with more than one interacting electrical drives such as robotic arms, unmanned aerial vehicles etc.

There is a huge advancement in medical and aeronautical science and application of Chaos is on the verge.

.



# Chapter 8

## REFERENCES

## REFERENCES:

- [1] J. Baillieul, R. Brockett, and R. Washburn, "*Chaotic motion in nonlinear feedback systems*," *IEEE Transactions on circuits and system*, vol. 27, pp. 990 - 997, 1980.
- [2] D. C. Hamill and D. J. Jeffries, "*Subharmonics and chaos in a controlled switched-mode power converter*," *Circuits and Systems, IEEE Transactions on*, vol. 35, pp. 1059-1061, 1988.
- [3] J. H. B. Deane and D. C. Hamill, "*Analysis, simulation and experimental study of chaos in the buck converter*," in *Power Electronics Specialists Conference, 1990. PESC '90 Record., 21st Annual IEEE*, 1990, pp. 491-498.
- [4] D. C. Hamill, J. H. B. Deane, and D. J. Jefferies, "*Modeling of chaotic DC-DC converters by iterated nonlinear mappings*," *IEEE Transactions on Power Electronics*, vol. 7, pp. 25-36, 1992.
- [5] K. Chakrabarty, G. Poddar, and S. Banerjee, "*Bifurcation behavior of the buck converter*", *IEEE Transactions on Power Electronics*, Vol. 11, May 1996, pp.439-447
- [6] E. Fossas and G. Olivar, "*Study of chaos in the buck converter*", *IEEE Transactions on Circuits and Systems-I: Fundamental Theory and Applications*, Vol. 43, January 1996, pp.13-25
- [7] C. K. Tse, S. C. Fung, and M. W. Kwan, "*Experimental Confirmation of Chaos in a Current-Programmed Cuk Converter*", *IEEE transactions on circuits and systems-I: fundamental theory and applications*, vol. 43, no. I, july 1996, pp.605-608
- [8] S. Banerjee, "*Coexisting Attractors, Chaotic Saddles, and Fractal Basins in a Power Electronic Circuit*", *IEEE transactions on circuits and systems-I: fundamental theory and applications*, vol. 44, no. 9, september 1997, pp.847-849
- [9] M. Bernardo, F. Garofalo, L. Glielmo, and F. Vasca, "*Switchings, Bifurcations, and Chaos in DC/DC Converters*", *IEEE transactions on circuits and systems-I: fundamental theory and applications*, vol. 45, no. 2, FEBRUARY 1998, pp.133-141

- [10] G.Olival; E.Fossas and C. Batlle, “*Non-smooth Continuation Of Periodic Orbits In a Chaotic Buck Converter*”, IEEE transactions on circuits and systems-I: fundamental theory and applications, vol. 45, no. 2,1999, pp.206-209
- [11] Jonathan H. B. Deane, Peter Ashwin, David C. Hamill and David J. Jefferies, “*Calculation of the Periodic Spectral Components in a Chaotic DC-DC Converter*”, IEEE transactions on circuits and systems-I: fundamental theory and applications, vol. 46, NO. 11, NOVEMBER 1999, pp.1313-1319
- [12] A.Gupta, S.Banerjee and D.Kastha, “*Experimental Study of Bifurcations in the Current Controlled dc-dc Buck-Boost Converter*”, National Conference On Nonlinear Systems & Dynamics, NCNSD-2003, vol. 46, NO. 11, DECEMBER 28-30, 2003, pp.333-336
- [13] S. C. Wong, C. K. Tse and K. C. Tam, “*Intermittent Chaotic Operation In Switching Power Converters*”, International Journal of Bifurcation and Chaos, Vol. 14, No. 8 2004, pp.2971-2978
- [14] Y. Kuroe and S. Hayashi, "Analysis of bifurcation in power electronic induction motor drive systems," in *Power Electronics Specialists Conference, 1989. PESC '89 Record., 20th Annual IEEE*, 1989, pp. 923-930 vol.2.
- [15] I. Nagy, "Tolerance band based current control of induction machines highlighted with the theory of chaos," in *Power Electronics Congress, 1994. Technical Proceedings. CIEP '94., 3rd International*, 1994, pp. 155-160.
- [16] N. Hemati, "Strange attractors in brushless DC motors," *Circuits and Systems I: Fundamental Theory and Applications*, IEEE Transactions on, vol. 41, pp. 40-45, 1994.
- [17] K. T. Chau, J. H. Chen, C. C. Chan, J. K. H. Pong, and D. T. W. Chan, "Chaotic behavior in a simple DC drive," in *Power Electronics and Drive Systems, 1997. Proceedings., 1997 International Conference on*, 1997, vol.1, pp. 473-479.
- [18] K. T. Chau, J. H. Chen, C. C. Chan, and D. T. W. Chan, "Modeling of subharmonics and chaos in DC motor drives," in *Industrial Electronics, Control and Instrumentation, 1997. IECON 97. 23rd International Conference on*, 1997, vol.2,pp. 523-528.
- [19] K.T. Chau, J.H. Chen, C.C. Chan, "Dynamic Bifurcation in De Drives," *Power Engineering Review on*, 1997, *IEEE*, vol. 22, pp. 1330-1336,
- [20] J. H. Chen, K. T. Chau, C. C. Chan, and Q. Jiang, "Subharmonics and Chaos in Switched Reluctance Motor Drives," *Power Engineering Review, IEEE*, vol. 22, pp. 57-57, 2002

- [21] Z. Suto, I. Nagy, and E. Masada, "Period adding route to chaos in a hysteresis current controlled AC drive," in *Advanced Motion Control, 2000. Proceedings. 6th International Workshop on*, 2000, pp. 299-304.
- [22] J. H. Chen, K. T. Chau and C. C. Chan, "Analysis of Chaos in Current-Mode-Controlled DC Drive Systems," *IEEE Transactions On Industrial Electronics*, vol. 47, no. 1, February 2000, pp. 67-76.
- [23] L. Zhong, P. Jin Bae, J. Young Hoon, Z. Bo, and C. Guanrong, "Bifurcations and chaos in a permanent-magnet synchronous motor," *Circuits and Systems I: Fundamental Theory and Applications, IEEE Transactions on*, vol. 49, pp. 383-387, 2002.
- [24] T. Tang, M. Yang, H. Li and D. Shen, "A New Discovery and Analysis on Chaos and Bifurcation in DC Motor Drive System with Full-bridge Converter," *Circuits and Systems I: Fundamental Theory and Applications, IEEE Transactions on*, 2006, vol. 40, pp. 1383-1388,
- [25] B. Basak, S. Parui, "Bifurcation and Chaos in Current Mode Controlled DC Drives In Continuous and Discontinuous Conduction Mode of Operation," *IEEE Transactions on Power Electronics and Drives*, 2009, pp. 4244-4247.
- [26] Dong Dai, Xikui Maa, Bo Zhang, Chi K. Tse, "Hopf bifurcation and chaos from torus breakdown in voltage-mode controlled DC drive systems", *ELSEVIER, Chaos, Solitons & Fractals*, 06 June 2011, vol. 44.
- [27] J. H. CHEN, K. T. CHAU and C. C. CHAN, "Chaos in voltage-mode controlled DC drive systems," *Taylor & Francis Transaction on International Journal of Electronics*, 09 Nov 2010, vol. 86, no. 7, pp. 857- 874
- [28] N. Okafor, B. Zahawi, D. Giaouris and S. Banerjee, "Chaos, Coexisting Attractors, and Fractal Basin Boundaries in DC Drives with Full-Bridge Converter", *IEEE Transactions on Power Electronics and Drives*, 2010, pp. 129-132.
- [29] S. Kundu, U. Kar, and K. Chakrabarty, "Co-existence of multiple attractors in the PWM controlled DC drives," *In The European Physical Journal Special Topics*, 2013, pp. 699-709.
- [30] P. Stumpf, A. Lőrincz and I. Nagy, "Analysis and Compensation of Chaotic Response in DC Motor Drive" *IEEE Transactions on Power Electronics and Drives*, 2011, pp. 83-88.
- [31] C. Kratochvil, M. Houfek, J. Kolacny, Roman Kriz, L. Houfek, J. Krejsa, "Chaos in drive systems" *Applied and Computational Mechanics -1*, 2007, pp. 121 - 126.
- [32] KT Chau, S. Ye, Y. Gao, J.H. Chen, "Application of chaotic-motion motors to industrial mixing processes" *IEEE Industry Applications Society*, vol. 15, No. 3, 2004, p. 1874-1880

- [33] S. Ye and K. T. Chau, "Chaoization of DC Motors for Industrial Mixing" IEEE Transactions On Industrial Electronics, Vol. 54, No. 4, August 2007, pp. 2024 – 2032
- [34] K. Chakrabarty and U. Kar, "Bifurcation and control of chaos in Induction motor drives" IEEE Transactions On Industrial Electronics, Vol.10, No. 4, August 2011, pp. 324 – 332
- [35] M. Babaei, J. Nazarzadeh, and J. Faiz, "Nonlinear Feedback Control of Chaos in Synchronous Reluctance Motor Drive Systems" IEEE Transactions On Industrial Electronics, Vol.15, No. 1, Nov. 2008, pp. 1704 – 1710
- [36] J. H. Chen, K. T. Chau, C. C. Chan and Quan Jiang, "Subharmonics and Chaos in Switched Reluctance Motor Drives" IEEE Transactions On Energy Conversion, Vol. 17, NO. 1, March 2002, pp. 73 – 78
- [37] R. Lina, L. Fucai, J. Yafei, "Active Disturbance Rejection Control for Chaotic Permanent Magnet Synchronous Generator for Wind Power System" Chines Control Conference, Vol. 57, NO. 4, July 2012, pp. 6878 – 6882
- [38] M. Feki, B. Robert, H.H.C.Iu, "A Proportional Plus Extended Time-Delayed Feedback Controller for a PWM Inverter" 35<sup>th</sup> Annual IEEE Power Electronics Specialists Conference, April 2004, pp. 3317 – 3312
- [39] B. Robert, M. Feki, H.H.C.Iu, "Control Of a PWM Inverter Using Proportional Plus Extended Time-delayed Feedback" International Journal of Bifurcation and Chaos, Vol. 16, No. 1, 2006, pp. 113–128
- [40] K. Chakrabarty and U. Kar, "Control of Bifurcation of PWM Controlled DC Drives" IEEE International Conference on Power Electronics, Drives and Energy Systems, Vol.6, No. 5, December 2012, 2012, pp. 978 – 982
- [41] B.G.M. Robert, "On Electronic Saturation Influence on Chaos in a PWM Inverter" IEEE International Conference on Power Electronics, Drives and Energy Systems, Vol. 2, No. 3, August 2013, pp. 8379 – 8384
- [42] Yu. V. Kolokolov and A.V. Monovskaya, "Detection of Initiation of a Bifurcation Phenomenon in the Dynamics of a PWM Converter" Russian Electrical Engineering. Allerton Press, Inc., Vol. 84, No. 1, December 2013, pp. 38–43
- [43] G. L. Baker, J. P. Gollub, "Chaotic Dynamics an Introduction", Cambridge University Press, 1990.
- [44] S. H. Strogatz, *Nonlinear Dynamics and Chaos : With Applications to Physics, Biology, Chemistry, and Engineering*. New York, United States: Perseus Books Publishing, LLC, 1994.

- [45] M. A. El-Sharkawi, *Fundamentals of Electric Drives*: Brooks/Cole, 2000
- [46] A. Hughes, *Electric Motors and Drives*, Third ed.: Newnes, 2006.
- [47] J. R. Brannan and W. E. Boyce, *Differential Equations :An Introduction to Modern Methods and Applications*. Hoboken, NJ, United States: John Wiley&Sons,Inc, 2007
- [48] P. Roy, S. Ray and S. Bhattacharya, “ *Control of Chaos in Brushless DC Motor: Design of Adaptive Controller following Back-stepping Method,*” International Conference on Control, Instrumentation, Energy & Communication (CIEC), IEEE, Kolkata, 2014, pp. 91-95

### **Thesis Consulted:**

- [49] P. ROY, “*Chaos In Nonlinear Systems And Its Control*”, Electrical Engineering Department of Jadavpur University, May, 2013
- [50] N. C. Okafor, “ *Analysis and control of nonlinear phenomena in electrical drives*”, School of Electrical, Electronic and Computer Engineering Newcastle University United Kingdom, September 2012